Aus dem Fachbereich Medizin

der Johann Wolfgang Goethe Universität

Frankfurt am Main

betreut am

Zentrum der Inneren Medizin

Medizinische Klinik 2

(Hämatologie, Onkologie, Hämostaseologie, Rheumatologie, Infektiologie)

Direktor: Prof. Dr. Hubert Serve

Minimal residual disease detection of the fusion protein DEK/CAN in t(6;9)(p23;q34) positive Acute Myeloid Leukemia and identification of target genes and key pathways for leukemogenesis

Dissertation

zur Erlangung des Doktorgrades der theoretischen Medizin

des Fachbereichs Medizin

der Johann Wolfgang Goethe-Universität

Frankfurt am Main

vorgelegt von

Selina Ferrara

aus Bühl

Frankfurt am Main, 2022

Dekan: Prof. Dr. Stefan Zeuzem

Referent: PD Dr. Martin Ruthardt

Korreferent: Prof. Dr. Peter Bader

Tag der mündlichen Prüfung: 31.10.2022

Table of contents

List of figures

List of tables

Abbreviations

-	Negative
%	Percent
+	Positive
°C	Celsius
µg	Microgram
µl	Micro liter
µM	Micro molar
AAFP	AML-associated fusion protein
ABL1	Abelson murine leukemia viral oncogene homolog 1
ALL	Acute lymphoblastic leukemia
Allo-HSCT	Allogeneic hematopoietic stem cell transplantation
AML	Acute myeloid leukemia
APL	Acute promyelocytic leukemia
ARF4 (d14)	ADP-ribosylation factor 4
ASXL1	Additional sex combs like 1
ASXL1	Additional sex combs-like 1
ATF2	Activating transcription factor 2
ATRA	All trans retinoic acid
BCA	Bicinchoninic acid
BCL2	B-cell lymphoma 2
Bp	Base pairs
CASP4	Caspase 4
CASP8	Caspase 8
CD	Cluster of differentiation

cDNA	complementary DNA
CEBPA	CCAAT/enhancer-binding protein alpha
CFU-S assay	Colony Forming Unit Spleen Assay
c-KIT	Stem cell factor receptor
CLL	Chronic lymphoblastic leukemia
CLP	Common lymphoid progenitor
CML	Chronic myeloid leukemia
CMP	Common myeloid progenitor
CO2	Carbon dioxide
CRM1	Chromosomal maintenance 1
CSF	Colony stimulating factor
CSF1R	Colony stimulating factor 1 receptor
CT	Cycle of threshold
Da	Dalton
ddH2O	Double-destilled water
DEPC	Diethylpyrocarbonate
DMEM	Dulbecco's Modified Eagle Medium
DMSO	Dimethyl sulfoxide
DNA	Deoxyribonucleic acid
DNase	Deoxyribonuclease
DNMT3A	DNA-methyltransferase 3A
dNTP	Deoxynucleosid-triphosphate
dUTP	Deoxyuridine-triphosphatase
EDTA	Ethylenediaminetetraacetate
ELN	European Leukemia Net

FAB classification	French-American-British classification
FCS	Fetal calf serum
FLT3	Fms-like tyrosine kinase-3
g	Gram
G-CSF	Granulocyte colony-stimulating factor
GM-CSF	Granulocyte-macrophage colony-stimulating factor
GMP	Granulocyte-monocyte progenitor
HDAC	Histone deacetylase
HIF1α	Hypoxia inducible factor, alpha subunit
HLA	Human Leukocyte Antigen
HSC	Hematopoietic stem cells
IDH1 and IDH2	Isocitrate dehydrogenase 1 and 2
IL-3	Interleukin 3
IL-6	Interleukin 6
ITD	Internal tandem duplication
JAK2	Janus Kinase 2
kDa	Kilodalton
LMO2	LIM domain only 2
LSC	Leukemic stem cell
LT-HSC	Long-term hematopoietic stem cells
M	Molar
MBTD1	Malignant brain tumor domain containing 1
MDS	Myelodysplastic syndrome
MEP	Megacaryotic and erythroid progenitor
mg	Milligram

MgCl2	Magnesium chloride
ml	Milliliter
mM	Milli Molar
MPP	Multipotent progenitor
MRD	Minimal residual disease
mRNA	messenger RNA
NaCl	Sodium chloride
NDRG1	N-myc downstream regulated gene 1
NES	Leucine-rich nuclear export signals
ng	Nano gram
NGS	Next generation sequencing
nM	Nano Molar
NOD/SCID	Nonobese diabetic/severe combined immunodeficient
NPC	Nuclear pore complex
NPM1	Nucleolar phosphoprotein B23
NUP214	Nucleoporin 214
OD	Optical density
PCR	Polymerase chain reaction
Pen/Strep	Penicillin/Streptomycin
PIM1	Proviral integration site 1
PML	Promyelocytic leukemia gene
PTP4A3	Protein tyrosine phosphatase 4a3
PTPRC	Protein tyrosine phosphatase receptor type C
qPCR	Real-time quantitative PCR
RARE	Retinoic acid respond element

RARα	Retinoic acid receptor alpha
RIN	RNA Integrity Number
RNA	Ribonucleic acid
RNase	Ribonuclease
RPM	Rounds per minute
RPMI	Roswell Park Memorial Institute-Medium
RT	Reverse Transcriptase
RUNX1	Runt-related transcription factor 1, AML1
RUNX1T1	RUNX1 Partner Transcriptional Co-Repressor 1, ETO
RXR	Retinoid X receptor
SCF	Stem cell factor
sec	Seconds
SEER	Surveillance Epidemiology and End Results
SH-2 domain	Sarcoma Virus-homology domain 2
SHP1/SHP2	Src-homology region 2 domain-containing phosphatases 1/2
SL-IC	SCID leukemia-initiating cell
SMEK2	SMEK homolog 2
STAT3/STAT5	Signal Transducer and Activator of Transcription 3 and 5
ST-HSC	Short-term hematopoietic stem cells
t(6;9)	Translocation of chromosome 6 and 9
TCR β	T-cell receptor β
TRIM25	Tripartite motif-containing 25
Tris	Tris(hydroxymethyl)aminomethane
UNG	Uracil-N-glycosylase
WHO	The world health organization

Wt	Wildtype
XPO1	Exportin 1

Summary

Acute myeloid leukemia (AML) is a neoplastic disease of an early myeloid precursor cell in hematopoiesis. It leads to the accumulation of monoclonal cells in the bone marrow and the peripheral blood, showing a differentiation block and deregulated self-renewal. Frequently, the leukemic cells exhibit genetic aberrations with reciprocal chromosomal translocations. These translocations induce the formation of a fusion protein, that can lead to new cellular functions and a transformation into a leukemic cell. Common chromosomal translocation in AML are t(8;21) or t(15;17), which cause the formation of the fusion proteins AML1/ETO and PML/RARα and determine the leukemic phenotype of the AML.

The translocation t(6;9) leads to the formation of the fusion protein DEK/CAN and is of special interest, because of its association with mostly young patients and a very aggressive course of the disease. The fusion product induces leukemia in a small subset of hematopoietic stem cells, but its mechanism of leukemogenesis is greatly unknown.

The intention of this work was to characterize the DEK/CAN-induced AML on a molecular genetic level to gain a deeper understanding of the disease pathogenesis. Therefore, gene expression analysis with polymerase chain reaction (PCR) and microarray analysis was performed.

To detect DEK/CAN in different cell lines by PCR and real-time quantitative PCR (qPCR), specific primers and probes were designed, and a standardized workflow was established. Emphasis was placed on the optimization of RNA isolation, DNase treatment, cDNA synthesis with following PCR and qPCR, which enabled the detection of the fusion product DEK/CAN in the cell lines 32B, Phoenix and FKH-1. To quantify the fusion product DEK/CAN, the method of qPCR with absolute and relative quantification was used. Absolute quantification enabled the calculation of an exact copy number of the fusion transcript DEK/CAN with a detection limit of 50 copies/µl at a sensitivity of 10^{-6}, which is of importance in determining the minimal residual disease (MRD) of patients with DEK/CAN-positive AML. MRD detection by qPCR is a highly sensitive diagnostic method to identify leukemic cells, even in low cell counts. This enables a thorough evaluation of the treatment response and allows an early detection of changes in the MRD level as part of the remission control.

Additionally, a microarray gene expression analysis was performed to identify alterations in relevant target genes and associated signaling pathways in DEK/CAN-positive cells.

Because of DEK/CAN's potential to induce leukemia in a subset of hematopoietic stem cells, Sca^+/Lin^- cells of the bone marrow of C57Bl/6 mice were used and transfected with the gene products DEK/CAN and PML/RARα. Microarray analysis led to the identification of 16 different genes of interest, which demonstrated significant alterations of gene expression in DEK/CAN-positive cells. They were validated and quantified with TaqMan assay assisted qPCR. The elevated expression of the transcription factors TRIM25, HIF1α and ATF2, in DEK/CAN-positive cells, indicated an altered transcription factor activity and interaction with DNA in the nucleus. The localization of DEK/CAN in the nucleus emphasizes this assumption. Also, the upregulated expression of the nuclear export receptor XPO1 suggested changes in nuclear transport processes and impaired export activity in DEK/CAN-positive cells.

Furthermore, the results demonstrated changes of gene expression in genes that are involved in the JAK/STAT signaling pathway. PTPRC, the Protein Tyrosine Phosphatase Receptor Type C, functions as a direct inhibitor of JAKs (Janus Kinases) and STATs (Signal Transducers and Activators of Transcription) and their associated signaling pathway.

It was shown that the gene expression of PTPRC was significantly reduced in DEK/CAN-positive cells. This allowed the assumption, that the reduced expression of PTPRC led to a loss of inhibition and thus a consecutive hyperactivation of the JAK/STAT signaling pathway. This hypothesis was supported by an independent activation of PIM1, a target gene of STAT5 and the activation of LMO2, a direct target gene of JAK2. In addition, the transmembrane receptor CSF1R, which is directly involved in STAT activation, also showed an upregulation in gene expression.

The results of this work show an activation of the JAK/STAT signaling pathway in DEK/CAN-positive cells, which may be a key mechanism in DEK/CAN-induced leukemogenesis.

Considering treatment options in the future, the addition of targeted therapy, such as pan-JAK inhibitors, to the standard therapy, could be a chance to improve the overall survival rate and the prognosis of t(6;9)-positive AML.

Zusammenfassung

Die akute myeloische Leukämie (AML) ist eine neoplastische Erkrankung unreifer myeloischer Vorläuferzellen der Hämatopoese. Es kommt zur Anhäufung monoklonaler Zellen im Knochenmark und im peripheren Blut, welche eine Differenzierungsblockade und deregulierte Selbsterneuerung aufweisen. Häufig werden in den leukämischen Zellen genetische Veränderungen mit reziproken chromosomalen Translokationen festgestellt. Diese führen zur Bildung von Fusionsproteinen und können durch Veränderung zellulärer Eigenschaften eine Transformation in eine leukämische Zelle induzieren. Verbreitete chromosomale Translokationen in der AML sind t(8;21) oder t(15;17), welche zur Bildung der Fusionsproteine AML1/ETO und PML/RARα führen und den leukämischen Phänotyp der AML bestimmen.

Die Translokation t(6;9) führt zur Bildung des Fusionsproteins DEK/CAN und ist von besonderer Relevanz, da sie häufig junge Patienten betrifft und aufgrund eines aggressiven Krankheitsverlaufes mit einer schlechten Prognose assoziiert ist. Es konnte nachgewiesen werden, dass das Fusionsprotein DEK/CAN eine Leukämie induzieren kann, jedoch ist der Mechanismus der Leukämogenese weitestgehend ungeklärt.

Ziel dieser Arbeit war es, die DEK/CAN-induzierte AML auf molekulargenetischer Ebene zu charakterisieren, um ein tieferes Verständnis für die Krankheitsentstehung zu erlangen. Hierfür wurden Genexpressionsanalysen mittels Polymerase-Kettenreaktion (PCR) und Microarray Analysen durchgeführt. Um DEK/CAN in verschiedenen Zelllinien mittels PCR und Real-time quantitative PCR (qPCR) nachweisen zu können wurden spezielle Primer und Sonden angefertigt, sowie ein standardisierter Arbeitsablauf etabliert. Im Fokus stand eine Optimierung von RNA Isolation, DNase Behandlung, cDNA Synthese mit anschließender PCR und qPCR, wodurch das Fusionsprotein DEK/CAN in den Zelllinien 32B, Phoenix und FKH-1 nachgewiesen werden konnte. Zur Quantifizierung des Genproduktes DEK/CAN wurde die Methode der qPCR mit absoluter und relativer Quantifizierung angewandt. Mit der absoluten Quantifizierung war es möglich eine exakte Kopienzahl des Fusionsproduktes DEK/CAN, mit einer minimalen Nachweisgrenze von 50 Kopien/µl, bei einer Sensitivität von 10^{-6}, zu erfassen, was zur Bestimmung der minimalen Resterkrankung (MRD) bei Patienten mit DEK/CAN-positiver AML bedeutsam ist. Die MRD-Analyse mittels qPCR ist eine der sensitivsten diagnostischen Methoden um Leukämiezellen auch in geringer Kopienzahl detektieren zu können. Somit wird ermöglicht,

das Therapieansprechen einzuschätzen und im Rahmen der Remissionskontrolle frühzeitig auf Veränderungen der Krankheitslast reagieren zu können.

Des Weiteren wurde eine Microarray Genexpressionsanalyse durchgeführt, um alterierte relevante Zielgene und assoziierte Signalwege in DEK/CAN-positiven Zellen zu identifizieren. Da bereits gezeigt werden konnte, dass DEK/CAN eine leukämische Transformation in unreifen hämatopoetischen Stammzellen induziert, wurden Sca^{+}/Lin^{-} Zellen aus dem Knochenmark von C57B1/6 Mäusen entnommen, und retroviral mit den Genprodukten DEK/CAN und PML/RARα transfiziert. Aus der Microarray Analyse konnten insgesamt 16 verschiedene Zielgene identifiziert werden, welche signifikante Expressionsunterschiede in DEK/CAN-positiven Zellen aufwiesen. Diese wurden anschließend mittels TaqMan-assistierter qPCR validiert und quantifiziert. Eine erhöhte Genexpression der Transkriptionsfaktoren TRIM25, HIF1α and ATF2 deuteten darauf hin, dass DEK/CAN eine direkte Interaktion mit DNA und eine veränderte Aktivität von Transkriptionsfaktoren veranlassen könnte. Da DEK/CAN eine nukleäre Lokalisation aufweist, wäre ein Wirken des Fusionsproteins im Zellkern wahrscheinlich. Zudem zeigte sich in DEK/CAN-positiven Zellen eine erhöhte Expression des nukleären Exportrezeptors XPO1, was auf veränderte nukleäre Transportprozesse hindeuten könnte.

Auffallend waren zudem mehrere Gene mit alterierter Genexpression, welche in den JAK/STAT Signalweg involviert sind. PTPRC, das Protein Tyrosin Phosphatase Rezeptor Typ C, fungiert als direkter Inhibitor von JAKs (Janus Kinasen) und STATs (Signal Transducers and Activators of Transcription) und deren assoziierten Signalweges. Es konnte gezeigt werden, dass die Genexpression von PTPRC in DEK/CAN-positiven Zellen signifikant reduziert war. Dies führte zu der Annahme, dass die verringerte PTPRC Expression zu einer aufgehobenen Inhibition und damit zu einer konsekutiven Hyperaktivität des JAK/STAT Signalweges führte. Diese Hypothese konnte durch eine gesteigerte Genexpression von PIM1, einem wesentlichen Zielgen von STAT5, sowie LMO2, einem direkten Zielgen von JAK2, untermauert werden. Auch zeigte sich eine gesteigerte Genexpression des Transmembranrezeptors CSF1R, der eine direkte STAT Aktivierung induziert. Die Ergebnisse dieser Arbeit zeigen, dass es in DEK/CAN-positiven Zellen zu einer Aktivierung des JAK/STAT Signalweges kommt, welcher eine relevante Rolle in der DEK/CAN-induzierten Leukämogenese spielen könnte. Die Ergänzung der Standardtherapie um eine zielgerichtete Therapie wie mit pan-JAK Inhibitoren, könnte zu einer Verbesserung der Überlebensrate und Prognose der t(6;9)-positiven AML beitragen.

1 Introduction

1.1 Hematopoiesis

The human body produces billions of leukocytes, erythrocytes, and thrombocytes per day, to replace the blood cells that were damaged by normal cellular processes, diseases or trauma. This highly regulated creation and replenishment of the blood system is called hematopoiesis (Jagannathan-Bogdan und Zon 2013). It is essential to comprehend the mechanism of hematopoiesis to gain further understanding of hematological diseases, such as leukemias or myeloproliferative disorders.

In early stages of the prenatal development, hematopoiesis of the embryo takes place in the aorta–gonad–mesonephros region and the yolk sac. Around the 16th gestational week, further development is shifted to the spleen, fetal liver and bone marrow (Morrison und Scadden 2014, Charbord et al. 1996). After birth, the bone marrow becomes the main location of hematopoiesis.

All blood cells descend from pluripotent hematopoietic stem cells (HSC) in the bone marrow. HSCs have the capacity of self-renewal and can differentiate into all blood cell types. Before developing into functionally mature blood cells, HSCs undergo maturation steps, creating a hierarchical series of intermediate progenitors. The terminal differentiated cells have a restricted life span and undergo apoptosis after a given time (Passegué et al. 2003). HSCs can be divided in two subsets of HSCs, the long-term subset (LT-HSC), which is capable of indefinite self-renewal, and the short-term subset (ST-HSC) which is capable of self-renewal for a limited time (~ 8 weeks) before they differentiate into multipotent progenitors (MPPs) (Reya et al. 2001). MPPs don't have self-renewal abilities but still have a full lineage differentiation potential (Weissman und Shizuru 2008). The MPPs differentiate to common myeloid progenitors (CMP) or common lymphoid progenitors (CLP) which determine either the myeloid or lymphoid lineage of blood cell development. The process of normal hematopoiesis is shown in Figure 1 (Passegué et al. 2003).

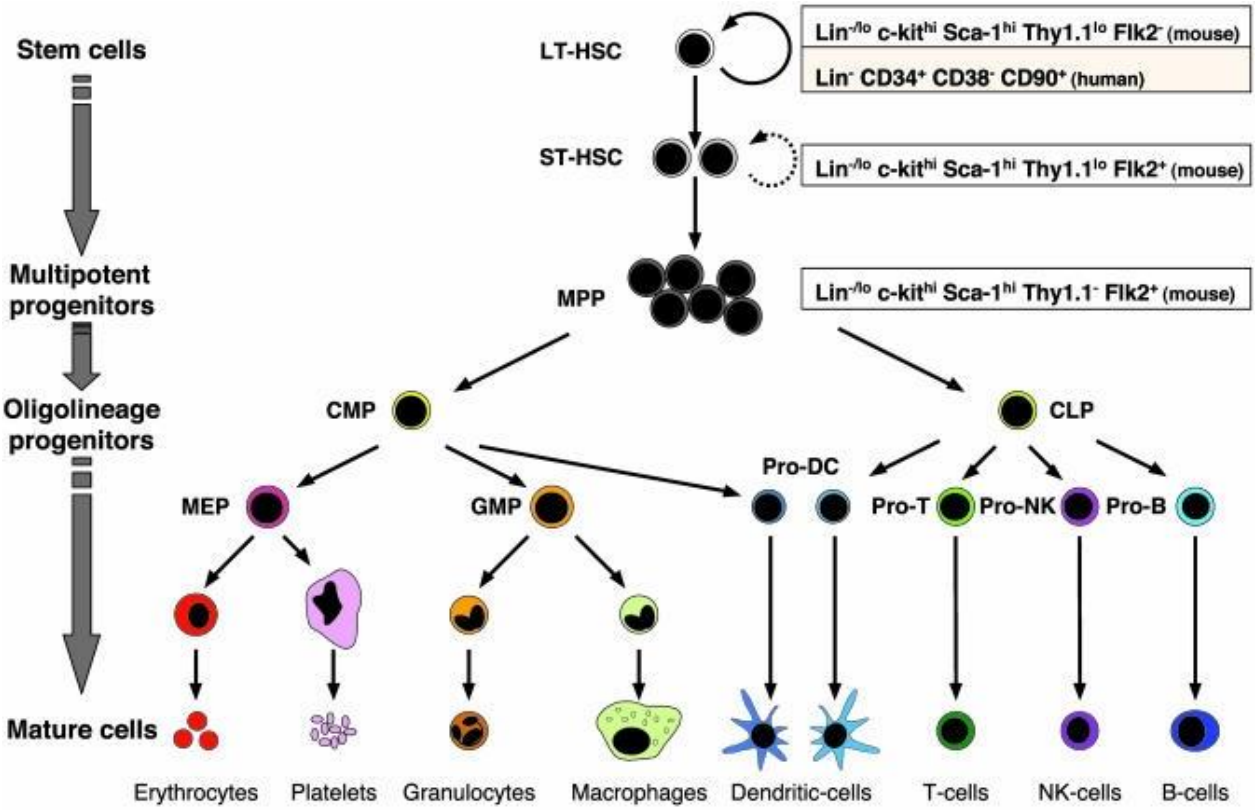

Figure 1: Hematopoietic differentiation
The hematopoietic differentiation originates in the hematopoietic stem cell (HSC). The HSC is divided in subsets of long- and short-term (LT-/ST) HSCs. The ST-HSCs develop into multipotent progenitors (MPPs), which do not share the self-renewing capacity of HSCs, but who can develop in both the myeloid and lymphoid lineage of hematopoiesis. MPPs differentiate in either common myeloid progenitors (CMP) or common lymphoid progenitors (CLPs). The CMPs build the myeloid lineage. The megacaryotic and erythroid progenitors (MEP) differentiate in mature erythrocytes or platelets and the granulocyte-monocyte progenitors (GMP) differentiate into granulocytes, macrophages and dendritic cells. The CLPs develop into T-, B- NK-, and dendritic cells (Passegué et al. 2003).

1.2 The hematopoietic stem cell

Totipotent stem cells are characterized by the capacity of self-renewal and differentiation in all types of tissue or somatic cells. When proliferating, there is always a daughter stem cell, which remains in its undifferentiated multipotent state. This daughter stem cell has been identified in hematopoiesis as the pluripotent hematopoietic stem cell, with a multilineage differentiation capacity for all the blood cells in hematopoiesis. The pioneers of revealing the existence of HSCs were Till and McCullogh in 1961. In an in vivo experiment, a Colony Forming Unit Spleen Assay (CFU-S assay), they demonstrated that single cells were able to generate multilineage descendants while preserving the multipotency of the parent cell. These cells were clonogenic bone marrow cells, which had the ability to generate myelo-erythroid colonies in the spleen of lethally irradiated

hosts. When retransplanting these clonogenic bone marrow cells in secondary lethally irradiated hosts, they were able to reconstitute all the hematopoietic cell lineages (TILL und MCCULLOCH 1961). These lasting, quiescent and multipotent HCS, capable of self-renewal, allow an indefinite formation of blood cells (Wang und Dick 2005).

Based on Till and McCulloch CFU-S assay, Ray Schofield formed first ideas of a nurturing environment of HSCs. Schofield discovered that isolated stem cells of the bone marrow were more capable to reconstitute hematopoiesis in irradiated animals than the multipotent progenitors, identified in the CFU-S assay. In 1978 he formulated the hypothesis of a stem cell niche, a specialized perivascular microenvironment in the bone marrow, preserving long-term self-renewal and prevention of maturation in stem cells (Schofield 1978). This microenvironment consists of mesenchymal stromal cells and endothelial cells (Morrison und Scadden 2014). The stromal cells synthesize and secrete growth factors, cytokines like the colony stimulating factor (CSF) or the stem cell factor (SCF), interferons, interleukins, and proteins of the extracellular matrix such as collagens, laminins and proteoglycans (Kronenwett et al. 2000).

HSCs can be mobilized to the peripheral blood. In vivo experiments have shown a stem cell mobilization after treatment with the cytokines granulocyte colony-stimulating factor (G-CSF) and granulocyte-macrophage colony-stimulating factor (GM-CSF) or after receiving myeloablative agents like chemotherapy, such as high-dose cyclophosphamide (Richman et al. 1976; Cline und Golde 1977; Dührsen 1988; Schwartzberg et al. 1992). This phenomenon has been advanced and applied in treatment of hematological diseases and is currently a standard procedure for autologous and allogenic stem cell transplantation. The hematopoietic stem cells get mobilized to the peripheral blood by stimulation of chemotherapy and G-CSF. They can then be collected by leukapheresis and serve as stem cell transplants in both autologous and allogenic stem cell transplantation (Sheridan et al. 1992; Schmitt et al. 2016).

1.3 Leukemia

The term leukemia was first introduced in 1847 by the German pathologist Rudolf Virchow in Berlin. He published a case report of a 50-year-old cook, Marie Straide, who was admitted to the Charité University Hospital of Berlin with peripheral edemas, splenomegaly, diarrhea, hematomas and nose bleedings. Her condition worsened rapidly, and she died within weeks. The autopsy

showed a milky substance in the blood vessels, comparable to pus. Further microscopic examination by Virchow revealed a very high cell count of leukocytes with concomitant anemia and thrombocytopenia. This finding led to the term leukemia (‘Leukämie’), coming from ‘leukos’, greek for ‘white’, indicating the macroscopic impression of white blood (Kampen 2012). This case report is a good clinical representation of the onset of leukemia in a patient. Currently, leukemia is described as a heterogenous hematopoietic disease, which demonstrates an uncontrolled proliferation of leucocytes. These proliferating cells are monoclonal, arising from a malignant transformation of a progenitor cell during hematopoiesis (Brown et al. 2012).

Leukemias can be divided into four groups, depending on the originating hematopoietic cell lineage, the clinical course of the disease and the affected leucocyte subtype. Leukemias can either be of lymphoblastic or myeloid origin and show an acute onset or chronic development of the disease. The four resulting groups of leukemia are the acute lymphoblastic or myeloid leukemia and the chronic lymphoblastic or myeloid leukemia.

Acute leukemia is characterized by a proliferation of undifferentiated monoclonal cells. These cells are referred to as blasts. In most cases, the disease progression is rapid and leads to death, if the patient remains untreated. Acute leukemias are subclassified into acute lymphoblastic leukemia (ALL) and acute myeloid leukemia (AML). ALL is the most frequent malignancy in children, whereas AML is predominant in adults and the elderly population (Newell und Cook 2021).

Chronic leukemias exhibit a clonal proliferation of pluripotent hematopoietic stem cells and typically have a chronic and slow course of the disease. Over time, chronic leukemias can develop an accelerated phase of blast proliferation and lead to an acute form of leukemia with blast crisis. Chronic leukemias are divided in chronic lymphoblastic leukemia (CLL) and chronic myeloid leukemia (CML) (Brown et al. 2012).

This work focusses on acute myeloid leukemia (AML). Therefore, the specification of acute lymphoblastic leukemia and chronic leukemias have not been taken into further account.

1.3.1 Epidemiology

The largest registry for cancer diseases in the United States of America, the Surveillance Epidemiology and End Results (SEER), defines an incidence for leukemia of 13,7 per 100.000 men and women per year, considering data from 2010 - 2014 (Howlader et al. 2014b). Thus, making

leukemia the ninth most common type of cancer in the United States of America. These trends are comparable with current data available for Germany (Nennecke et al. 2014).

When considering all the specific subtypes of leukemia, the data show a correlation to incidence and age distribution. Between 2005 and 2014, the incidence rate of leukemia has increased at an average rate of 0,3 % per year. A possible explanation for this finding, could be the increasing life expectancy of the population. In the same time period, the mortality has decreased at an average rate of 1 % per year.

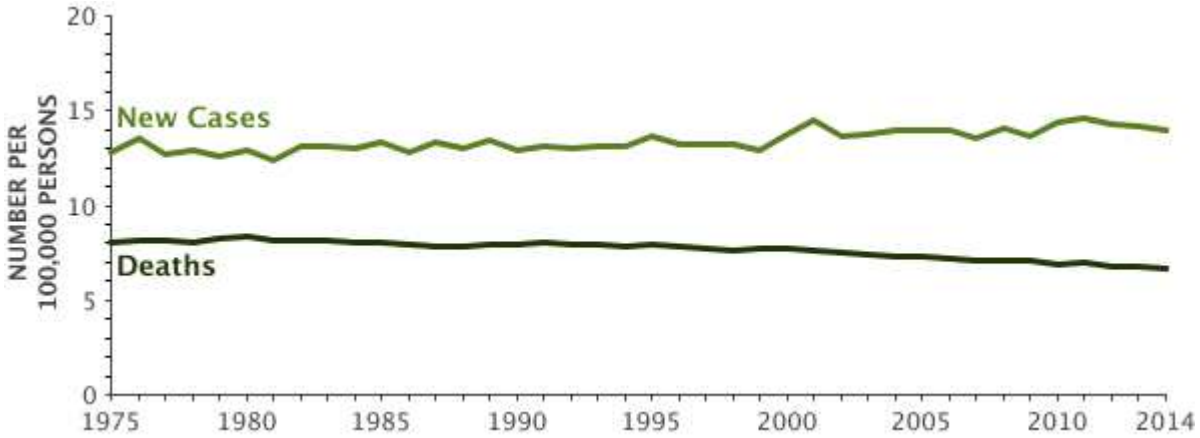

Figure 2: Incidence and mortality of leukemia
Incidence and mortality of leukemia from 1975-2014 in the US. All races and sexes are included. There are on average 13,7 of 100.000 new cases of leukemia (Howlader et al. 2014a).

The 5-year survival rate trend in patients with leukemia has shown a significant improvement over the past years. Table 1 shows the increased 5-year survival rate from 33 % in the year 1975 to 62,9 % in the year 2009, representing a distinct improvement of the prognosis of patients with leukemia. This development can be attributed to an expansion of therapeutic options, primarily the accomplishment of peripheral blood stem cell transplantation, and improved supportive care (Howlader et al. 2014a).

Year	1975	1980	1985	1990	1995	2000	2005	2009
5-Year Relative Survival	33.1 %	37.4 %	41.3 %	45.1 %	48.1 %	49.8 %	60.8 %	62.9 %

Table 1: Five-year relative survival in leukemia
The 5-Year Relative Survival increased to almost double in patients with leukemia (Howlader et al. 2014a).

1.3.1.1 Epidemiology of Acute Myeloid Leukemia (AML)

Focussing exclusively on the subtype of acute myeloid leukemia (AML), the incidence remains at 3,1 cases per 100.000 of the German population per year with a clear correlation to a higher age (Nennecke et al. 2014). The median age of initial diagnosis is 66 years, with 70 % of patients being older than 55 years (Howlader et al. 2014b). The incidence rises with age and is accompanied by a less favorable outcome. The five-year survival rate varies within individual risk groups. The Swedish Registry for AML revealed a 5-year-survival rate of 60 % of patients under the age of 30 years, a rate of 43 % of patients between the age of 45 and 54 years, a rate of 23 % of patients between the age of 55 to 64 years and decreasing survival rates in age populations above 65 years (Juliusson et al. 2012).

1.3.2 Acute Myeloid Leukemia (AML)

Acute myeloid leukemias are aggressive and rapidly progressive malignant blood cell disorders. An acquired malignant transformation arises from hematopoietic stem or precursor cells of the myeloid lineage and leads to the development of myeloblasts. These cells are characterized by an often uncontrolled proliferation, a pathological capacity of self-renewal and failure of differentiation into functional mature myeloid blood cells (Brown et al. 2012; Kouchkovsky und Abdul-Hay 2016). In the most cases, the blasts accumulate in the bone marrow and spread towards the peripheral blood, oppressing the normal-differentiated blood cells (Brown et al. 2012). This often causes bone marrow failure, resulting in pancytopenia and typical corresponding symptoms such as fatigue, dyspnoea, infections and hemorrhages (Shephard et al. 2016).

Without treatment, acute leukemias lead to bone marrow failure and mortality within a few months (Shallis et al. 2019). This explains the necessity of an immediate and aggressive treatment.

AML can occur as a secondary leukemia in patients with myelodysplastic syndrome or as an unwanted side effect of mutagenic therapy such as chemotherapy or radiation. DNA-damaging

mutations are an undesired effect of this type of therapy. Other risk factors for AML are the exposure to benzene, petroleum, pesticides, radioactive fallout (observed after the atomic bombing on Hiroshima and Nagasaki and the Tschernobyl accident), tobacco consumption, and the genetic alterations in trisomy 21 and Fanconi anemia (Kumar 2011). In the majority of cases, AML appears as a de novo, primary AML, in previously healthy individuals (Kouchkovsky und Abdul-Hay 2016).

1.3.2.1 AML classification

The classification of AML was established, considering morphological, cytogenetic and molecular criteria. An important diagnostic procedure is the bone marrow biopsy. The detection of more than 20 % of myeloblasts in the bone marrow confirms the diagnosis of acute myeloid leukemia (Döhner et al. 2010). After analysing cell morphology and cytochemistry of the leukemic cells, the leukemia can be classified within eight types (M0 to M7) of the French-American-British (FAB) Group classification system, suggested in 1976 (Table 2, Bennett et al. 1976). The table also contains cytogenetic features, which were added afterwards (Löwenberg et al. 1999).

Genetic alterations in leukemic blasts have an important impact on the prognosis of AML, influencing the management and treatment of the disease. Chromosomal aberrations can be detected in 50 – 60 % of AML patients. The associated chromosomal aberrations were subdivided in favourable, intermediate and adverse risk groups (Brown et al. 2012).

Type	Name	Morphology	Cytochemistry: peroxidase	Cytochemistry: esterase	Cytogenetics
M0	Acute myeloblastic leukemia, minimal differentiation	Immature blasts without or minimal differentiation	-	-	
M1	Acute myeloblastic leukemia, without maturation	Rarely granules	+	-	
M2	Acute myeloblastic leukemia, with granulocytic maturation	Azurophilic granules	+	-	t(8;21), t(6;9)

M3	Acute promyelocytic leukemia (APL)	Phosphorus-rich granules, Auer rods, faggot-cells	+	-	t(15;17)
M4	Acute myelomonocytic leukemia	Monocytic blasts	+	+	inv(16), t(16;16), del(16q)
M5	Acute monoblastic leukemia	Monoblasts, Promonocytes	-	+	del(11q), t(9;11), t(11;19)
M6	Acute erythroid leukemia	Immature erythroblasts	+	-	
M7	Acute megakaryoblastic leukemia	Immature blasts	-	+	t(1;22)

Table 2: French-American-British (FAB) – classification system of AML (Bennett et al. 1976, Vardiman et al. 2009, Löwenberg et al. 1999)

The World Health Organisation (WHO) modified the FAB classification by adding genetic characteristics, immunophenotype and clinical presentation, defining six subgroups (Table 3, Kouchkovsky und Abdul-Hay 2016). The classification was revised in 2016 in order to integrate the numerous advances made in AML research and guiding the management of the disease (Arber et al. 2016). Based on molecular characteristics, AML is subdivided in three risk groups in the 2017 European Leukemia Net (ELN) risk classification (Döhner et al. 2017).

Types	**Genetic abnormalites**
AML with recurrent genetic abnormalities	AML with t(8:21)(q22;q22); RUNX1/RUNX1T1
	AML with inv(16)(p13.1q22) or t(16;16)(p13.1;q22); CBFB/MYH11
	APL with PML/RARα
	AML with t(9;11)(p21.3;q23.3); MLLT3/KMT2A
	ML with t(6;9)(p23;q34.1); DEK/CAN
	AML with inv(3)(q21.3q26.2) or t(3;3)(q21.3;q26.2); GATA2, MECOM

	AML (megakaryoblastic) with t(1;22)(p13.3;q13.3); RBM15/MKL1
	AML with BCR/ABL1 (provisional entity)
	AML with mutated NPM1
	AML with biallelic mutations of CEBPA
	AML with mutated RUNX1 (provisional entity)
AML with myelodysplasia-related changes	
Therapy-related myeloid neoplasms	
AML, not otherwise specified	AML with minimal differentiation
	AML without maturation
	AML with maturation
	Acute myelomonocytic leukemia
	Acute monoblastic/monocytic leukemia
	Acute erythroid leukemia
	Pure erythroid leukemia
	Acute megakaryoblastic leukemia
	Acute basophilic leukemia
	Acute panmyelosis with myelofibrosis
Myeloid sarcoma	
Myeloid proliferations related to Down syndrome	Transient abnormal myelopoiesis
	ML associated with Down syndrome

Table 3: WHO classification of AML and related neoplasms (Kouchkovsky und Abdul-Hay 2016, Arber et al. 2016)

1.3.2.2 Characteristics of the leukemic cell

The different types of leukemia can vary in their appearances, but they have selected characteristics in common.

The leukemic phenotype is characterized by an elevated proliferation capacity, unlimited potential for self-renewal, increased cell survival, impaired differentiation and genomic instability (Passegué et al. 2003). Hematopoiesis normally regulates cell proliferation in dependence of mitogenic growth signals. Leukemic cells can gain independence of these growth signals. The cause for this new independence can be a genetic aberration, which often induces a manipulation of usual growth signaling pathways by giving rise to oncogenes or impairing other growth-related genes. They can stimulate cell proliferation in absence of any exogenous growth signals (Hanahan und Weinberg 2000).

Additionally, the block of differentiation in leukemic cells drives a continuous proliferation. The leukemic cells never reach a mature, differentiated, post-proliferative stage. Leukemic cells also gain independence of the mechanism of apoptosis, the controlled cell death. This leads to an increased cell survival and supports the uncontrolled proliferation of the leukemic cells (Zheng et al. 2004). The potential of self-renewal is a feature seen in hematopoietic stem cells. This similarity gave rise to the idea of the leukemic stem cell model.

1.3.2.3 The leukemic stem cell

The xenotransplantation of leukemic blasts from primary AML from a human individual into nonobese diabetic/severe combined immunodeficient (NOD/SCID) mice revealed that a small subgroup of leukemic cells was able to initiate and sustain the growth of leukemic clones. This subgroup was phenotypically identified as Thy1-, CD34+, CD38- cells and referred to as SCID leukemia-initiating cells (SL-ICs). The SL-ICs were able to differentiate into leukemic blasts, indicating that the development of leukemia is a multistep process, organized hierarchically. Serial injections of human AML leukemic cells showed engraftment in NOD/SCID mice to a second and third generation, indicating a high self-renewal capacity (Bonnet und Dick 1997).

These results introduced the leukemic stem cell model. This model implies that there is only a minority of leukemic cells, the leukemic stem cells (LSCs), which possess the ability to initiate and maintain the disease. They own the ability of self-renewal and cell differentiation, resembling

functions of HSC (Passegué et al. 2003; Zheng et al. 2004). The current hypothesis is, that HSC transform into LSC by genetic mutations and aberrations, such as gene fusion constructs, and initiate leukemogenesis. It was shown that the presence of AML-associated fusion proteins (AAFPs), such as PML/RARα, RUNX1/RUNX1T1 and DEK/CAN, induce leukemia in mice from a small subset of HSCs. The subset belongs to long-term HSCs and shows activation in STAT signaling. The genetically transformed HSC functions as a LSC and induces the leukemic transformation and conservation of the disease (Reya et al. 2001; Oancea et al. 2014).

1.3.2.4 Genetics in AML

Research over the past four decades has shown that genetic aberrations are of substantial importance in the pathogenesis of AML. The acquired somatic mutations and chromosomal translocations are heterogenous and give rise to various forms of AML with a mutual accumulation of immature, undifferentiated myeloid cells (Passegué et al. 2003; Papaemmanuil et al. 2016; Kouchkovsky und Abdul-Hay 2016). The current achievements in whole genome and next generation sequencing (NGS) have enabled a thorough picture of genetic aberrations in AML. The detected aberrations were subdivided in groups, describing the biological function of the affected and mutated gene. These groups contain genes involved in epigenetic modification, cell signaling, transcription factor function and the nucleophosmin (NPM1) shuttling protein, among others (Bullinger et al. 2017). The most frequent detected mutated epigenetic regulators are the DNA-methyltransferase 3A (DNMT3A), the additional sex combs-like 1 (ASXL1) as well as the isocitrate dehydrogenase 1 and 2 (IDH1 and IDH2) (Asada et al. 2019; Mondesir et al. 2016). Current data implies their occurrence in early steps of leukemogenesis with presence in the initial leukemic clone (Bullinger et al. 2017; Papaemmanuil et al. 2016). Recurrent detected mutated signaling genes are the fms-like tyrosine kinase-3 (FLT3) and the stem cell factor receptor c-KIT. The most common mutated transcription factor genes are the CCAAT/enhancer-binding protein alpha (CEBPA) and the runt-related transcription factor 1 (RUNX1). They can be mutated or also form a component in aberrant gene fusions, as described in the following chapter (Gaidzik et al. 2016; Ley et al. 2013a). Another important and frequent mutation is localized in the nucleolar phosphoprotein B23 (NPM1) gene. It is seen in around 30% of de novo AML and leads to a dysregulation of the nucleocytoplasmatic shuttling and localization of NPM1 and its interaction partners (Falini et al. 2005).

Most patients have more than one somatic mutation. Sequencing data analysis indicated an average of 13 somatic mutations detectable in one patient (Ley et al. 2013a; Bullinger et al. 2017).

Up until NGS allowed a more detailed approach in characterizing genetic alterations in AML, a model was used, that subdivided the detected genetic alterations in matters of their influence on the leukemic blast (Ishikawa et al. 2009). Class I mutations implied an activation of signalling pathways by mutated receptor tyrosine kinases such as FLT3 or mutated stem cell factor c-KIT (Ley et al. 2013b). The class II mutations were associated with alterations in cell differentiation by affecting transcription factors or the cell cycle. Significant mutations in this group are chromosomal aberrations. It was discussed if the presence of mutations in both groups are necessary to induce leukemogenesis, which could not be confirmed. Clinical data has shown that high risk genetic aberrations alone, such as the fusion product DEK/CAN, drive the AML with high risk for relapse, even in absence of FLT3 or other class I mutations (Ley et al. 2013b; Ishikawa et al. 2009). Figure 3 gives an overview of frequent co-occurring gene mutations in AML (Patel et al. 2012).

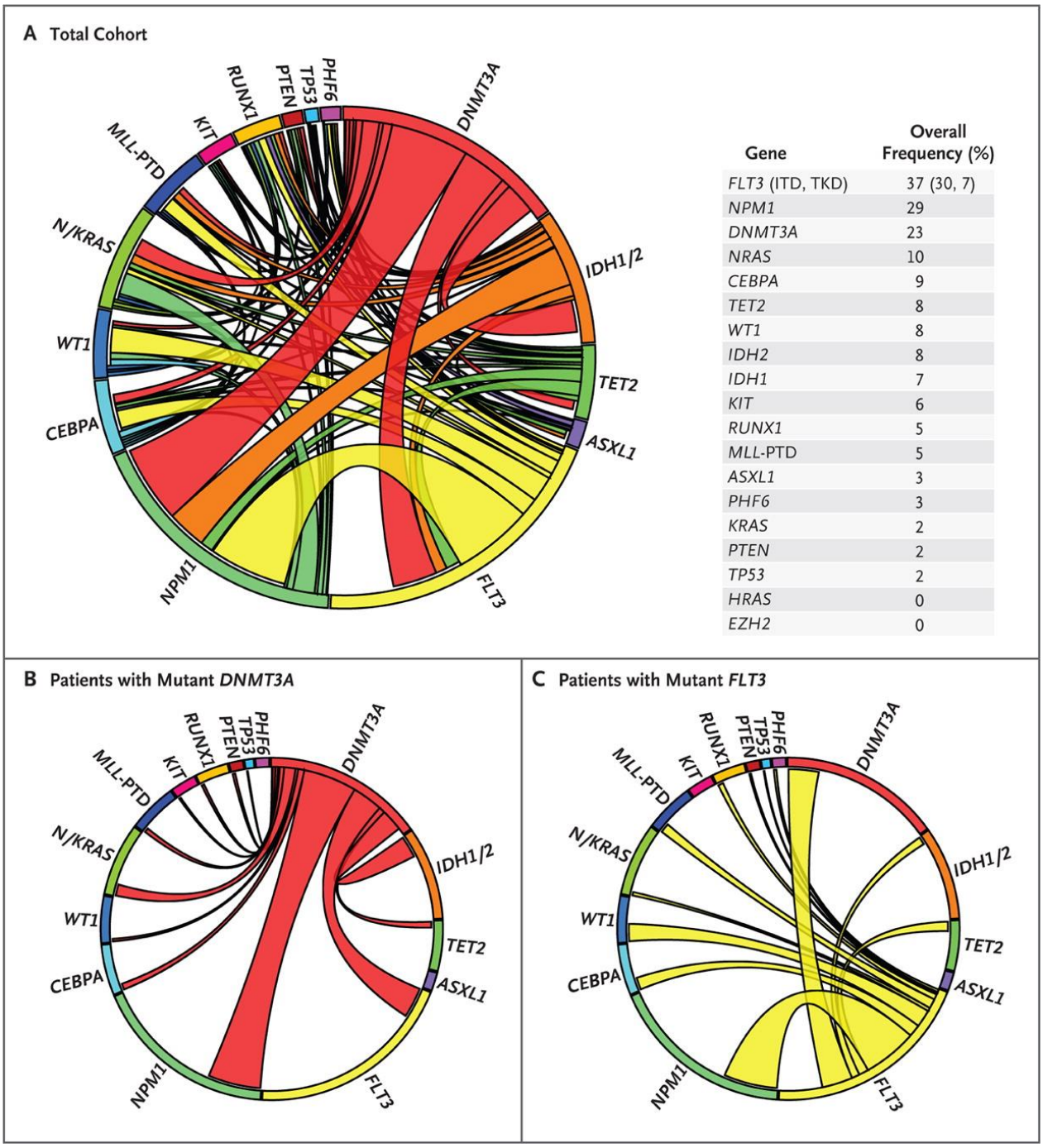

Gene	Overall Frequency (%)
FLT3 (ITD, TKD)	37 (30, 7)
NPM1	29
DNMT3A	23
NRAS	10
CEBPA	9
TET2	8
WT1	8
IDH2	8
IDH1	7
KIT	6
RUNX1	5
MLL-PTD	5
ASXL1	3
PHF6	3
KRAS	2
PTEN	2
TP53	2
HRAS	0
EZH2	0

Figure 3: Gene mutations in AML
This circos diagram gives an overview of frequent and pairwise gene mutations in AML. The arc length shows the frequency of a mutation and the width shows the percentage of patients who have a mutation in the second illustrated gene. **A** demonstrates the mutational frequency of a selected total patient cohort of newly diagnosed AML. **B** and **C** demonstrate the frequent co-occurring gene mutations in DNMT3A and FLT3-mutated patients (Patel et al. 2012).

1.3.2.5 AML-associated fusion proteins (AAFPs)

In 50 - 60 %, structural chromosomal aberrations, such as translocations, deletions or inversions, are detected in leukemic blasts in AML (Brown et al. 2012). The majority is associated with structural chromosomal translocations, causing a gene fusion with a resulting fusion product. The product then contains the 5' end of one gene and the 3' end of a different gene (Caligiuri et al. 1997). The fusion product leads to an aberrant gene transcription with the potential to induce a leukemic transformation in early hematopoiesis (Look 1997).

The WHO classification for AML (Table 3) recognizes seven recurrent important chromosomal balanced translocations and inversions and their variants. They are included because of their high significance in disease management and prognosis by prediction of remission rate, relapse and overall survival (Döhner et al. 2010). Recurrent fusion products in AML are listed in

Table **4** with PML/RARα, AML1/ETO, CBFβ/MYH11 and MLL fusions being the most frequent examples of AAFPs (Kumar 2011).

Translocations	Fusion protein	Frequency of occurrence (% of AML)
t(8;21)	AML1/ETO	10 %
t(15;17)	PML/RARα	10 %
inv(16)	CBFβ/MYH11	5 %
der(11q23)	MLL-fusions	4 %
t(9;22)	BCR/ABL1	2 %
t(6;9)	DEK/CAN	<1 %
t(1;22)	OTT/MAL	<1 %
t(8;16)	MOZ/CBP	<1 %
t(7;11)	NUP98/HOXA9	<1 %
t(12;22)	MN1/TEL	<1 %
inv(3)	RPN1/EVI1	<1 %
t(16;21)	FUS/ERG	<1 %

Table 4: Acute myeloid leukemia-associated fusion proteins (Kumar 2011)
This table shows the frequency of occurrence of different AAFPs. PML/RARα, AML1/ETO, CBFβ/MYH11 and MLL fusions are the most common AAFPs.

1.3.2.5.1 AML-associated fusion proteins and transcriptional function

In most cases, one of the components of a fusion protein in AML encodes a transcription factor, which has various regulation functions in hematopoiesis. Aberrant transcriptional regulation and control can be an influential factor in oncogenesis (Lewin 1991). The fusion product may activate the transcription factor, altering its former function but keeping its DNA-binding motifs. This way, the fusion product can interact with the transcriptional networks, for example the corepressor complex, to influence the regulation of hematopoiesis. Through interaction with a corepressor to a locus of active transcription, the fusion protein changes the expression of target genes, which can be crucial for myeloid development and a base point for leukemic transformation (Kumar 2011). The influence on transcription factors enables alterations in very early stages of hematopoiesis, often forming the top of regulatory signaling cascades and leading to relevant changes in cell development and differentiation. The target genes on the end of the altered signaling pathway are mostly unidentified (Look 1997). A good example for such a fusion product is AML1/ETO. It is the most common chromosomal aberration in AML. The acute myeloid leukemia 1 (AML1, also named RUNX1) gene encodes a transcription factor, which influences several genes that are important in hematopoietic differentiation. Relevant target genes are the t-cell receptor β (TCR β), the growth promoting cytokines interleukin 3 (IL-3) and granulocyte-macrophage colony-stimulating factor (GM-CSF), and granulocyte proteins (Licht 2001). ETO, also named RUNX1T1, is also a transcription factor, which represses target genes by interaction with corepressors (Erickson et al. 1992). The AML1/ETO translocation fuses the DNA binding site of RUNX1 with nearly the entire ETO gene, giving the fusion product the RUNX1-associated transcriptional activation combined with gene repressive features.

1.3.2.5.2 PML/RARα

PML-RARα is a chromosomal aberration, inducing the leukemic phenotype of acute promyelocytic leukemia (APL), M3 of the FAB classification, occurring in 5 - 10 % of AMLs (Avvisati et al. 1992).

The reciprocal chromosomal translocation induces a gene fusion of the promyelocytic leukemia gene (PML) on chromosome 15 and the retinoic acid receptor alpha (RARα) on chromosome 17. RARα belongs to the family of nuclear receptors, regulating genes which are important for the

maturation of promyelocytes. RARα functions in dependence of its ligand, all trans retinoic acid (ATRA). In absence of ATRA, RARα binds the nuclear retinoid X receptor (RXR). The heterodimer RARα/RXR then binds to specific DNA sequences, the so-called retinoic acid respond elements (RARE), and inhibits transcription of its target genes by recruiting corepressor complexes, such as histone deacetylases (HDACs) (Martens et al. 2010; Licht 2006). In presence of ATRA, the transcription of the target genes is activated, inducing and regulating myelocytic cell differentiation. The PML/RARα fusion leads to an altered RAR behaviour. It blocks the transcription of the target genes with inhibition of downstream signaling, and consequently blocks hematopoietic differentiation (Thé et al. 1991; Martens et al. 2010; Licht 2006). PML/RARα loses its sensitivity to physiological ATRA concentrations, but reacts to high dosages of ATRA, which became an essential agent in APL treatment (Martens et al. 2010; Coombs et al. 2015). This highly interesting finding has promoted research in many other AAFPs (Kumar 2011).

1.3.2.6 Therapeutic strategies in AML

Treatment of AML, excluding acute promyelocytic leukemia (APL), consists of an intensive chemotherapy regimen which is divided in four main steps: induction, consolidation 1, consolidation 2 and either an allogeneic hematopoietic stem cell transplantation (allo-HSCT) or a third phase of consolidation. The most commonly used cytostatic agents are anthracyclines, such as daunorubicine, idarubicine and mitoxantrone as well as cytarabine and etoposide (Kumar 2011). Allo-HSCT is indicated if no complete remission is attained after the induction chemotherapy and in patients with high-risk genetic abnormalities based on the ELN risk stratification.

Focus of current research is to find and add targeted therapies, dependent on the presence of specific genetic mutations to the standard chemotherapy. These new therapeutic approaches contain IDH1/2 (isocitrate dehydrogenase 1 and 2)-inhibitors, BCL2 (B-cell lymphoma 2)-inhibitors or FLT3-ITD specific agents (Stein et al. 2019; Perl et al. 2019). In particular, elderly or multimorbid patients can benefit from low-dose chemotherapy in combination with targeted therapy such as the BCL-2 inhibitor Venetoclax (DiNardo et al. 2018; DiNardo et al. 2019).

Additionally, patients often require intensive supportive treatment such as antiemetics, blood transfusions, antiviral- antifungal and antibacterial drugs.

1.3.2.7 Minimal residual disease (MRD)

The term minimal residual disease (MRD) defines a small remaining cell count of leukemic blasts in a patient during or after treatment. These remaining cells are usually not detectable by the standard microscopic examination and can result in a relapse of the disease. MRD detection is done on a molecular level by polymerase chain reaction (PCR) or by flow cytometry. If the AML is characterized by a genetic aberration, for example a gene fusion transcript, molecular techniques such as real-time quantitative PCR can be used to detect cells who contain the genetic aberration. It serves as a template for remission control by PCR. Monitoring the disease by measuring the MRD level is an important prognostic factor in acute leukemia and has a high value in remission control after intensive treatment and after allogeneic stem cell transplantation. Additionally, a multiparameter flow cytometry is very useful to identify an aberrant AML immunophenotype (Kern et al. 2003; Ravandi et al. 2018).

1.4 The t(6;9)-positive AML

The chromosomal reciprocal translocation t(6;9), with the resulting fusion protein DEK/CAN, belongs to the acute myeloid leukemia-associated fusion proteins. Its appearance is very rare with a detection in about 1 % of patients with AML (Slovak et al. 2006). Affected patients are usually of young age with a median age of 23 years when first diagnosed. Both sexes are equally involved (Chi et al. 2008). The prognosis is usually poor with a 5-year survival rate of 28 % in children and 9 % in adults (Slovak et al. 2006). The median survival is one year after being diagnosed (Chi et al. 2008). This classifies the t(6;9)-positive AML as a high-risk subgroup with unfavourable outcome and poor prognosis (Brown et al. 2012). The t(6;9)-positive AML is listed as a separate entity within the group of AML with recurrent genetic abnormalities of the WHO classification since 2008 and associated with the adverse risk group of the 2017 ELN risk classification system (Vardiman et al. 2009; Döhner et al. 2017). DEK/CAN has also been detected in the myelodysplastic syndrome (MDS) (Chi et al. 2008).

The t(6;9) positive AML is associated with a high frequency of internal tandem duplications in the receptor tyrosine kinase FLT3 (FLT3-ITD mutations), which is found in 9 of 10 patients, contributing to a poor prognosis (Thiede et al. 2002).

1.4.1 Cytology and immunohistochemistry of t(6;9)-positive AML

Most patients with a t(6;9)-positive AML classify as the M2 or M4 subtype according to the French-American-British classification (AML-FAB). Cytology of the bone marrow is characterized by hypercellularity with various hematopoietic cell populations, dysplasias and increased basophils (Pearson et al. 1985). The blasts can contain Auer bodies in the cytosol. Immunohistochemistry shows positivity for the cluster of differentiation (CD) 9, CD13, CD33, CD38, CD117 and the Human Leukocyte Antigen - isotype DR (HLA-DR). The blasts facultatively express CD34 and the terminal deoxynucleotidyl transferase (Oyarzo et al. 2004).

1.4.2 Therapeutic approach of t(6;9)-positive AML

Patients with t(6;9)-positive AML are treated analogue to the described chemotherapy regimen in chapter 1.3.2.6 A recent study has revealed a benefit for DEK/CAN-positive patients, undergoing direct allo-HSCT, independent of the achievement of a first complete remission after induction chemotherapy. Patients with first complete remission showed higher 5-year relapse-free and overall survival when treated with early allo-HSCT compared to consolidation therapy. Concerning the adverse risk constellation in t(6;9)-positive AML, allo-HSCT is the only option to achieve complete remission for most patients. The presence of a FLT3-ITD mutation or other chromosomal aberrations did not have an impact on the overall survival (Kayser et al. 2019).

1.4.3 The structure of DEK-CAN

The chromosomal aberration t(6;9) was first detected in large cytogenetic studies in patients with AML in 1976. The chromosomal translocation leads to a fusion of the 5'- end of the DEK gene on chromosome 6 to the 3'-end of the CAN gene, also known as nucleoporin 214 kDa (NUP214) gene, on chromosome 9. The created fusion transcript DEK/CAN is controlled by the DEK promoter (Soekarman et al. 1992). The breakpoints are set in introns of the corresponding genes (Lindern et al. 1992). The transcript encodes the fusion protein DEK-CAN with a molecular mass of 165 kD (Soekarman et al. 1992; Lindern et al. 1992). DEK-CAN consists of 8 N-terminal exons of DEK and 19 C-terminal exons of CAN. A reciprocal fusion transcript CAN/DEK has not been detected in t(6;9)-positive patients (Oyarzo et al. 2004).

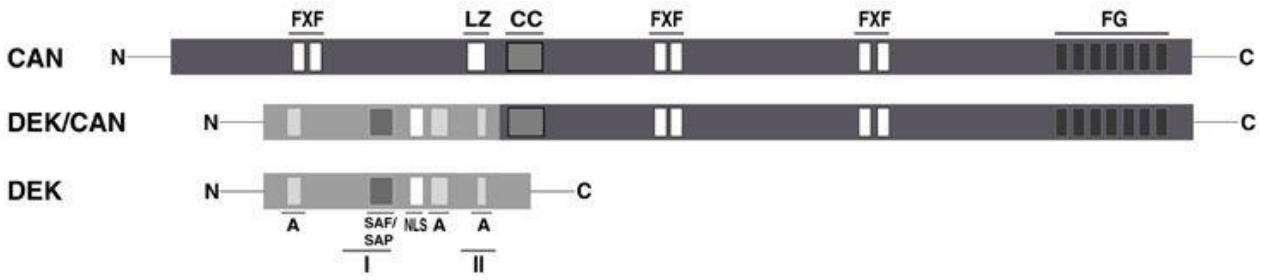

Figure 4: The schematic structure of CAN, DEK and their fusion product DEK/CAN
CAN contains 36 exons and the following structures. FXF: repeat motifs; FG: repeat motifs; LZ: leucine zipper; CC: coiled-coil. DEK contains 9 exons. It includes acidic regions (A), two DNA binding domains (I and II) and a nuclear localisation signal (NLS). The fusion product DEK/CAN contains the exons 17-36 of CAN and the exons 1-8 of DEK (Oancea et al. 2010).

1.4.4 Current state of research

Previous work has shown that DEK/CAN has leukemogenic potential and induces leukemia from a small subpopulation of HSCs. This subset of cells has the phenotype $Sca1^+$, $cKit^+$, Lin^-, Flk2 which corresponds to the characterization of LT-HSCs. In the ST-HSCs, DEK/CAN is not able to induce leukemia, but it leads to a higher proliferation activity. Additionally, DEK/CAN increases the colony number in CFU-S assays, proposing a positive influence on the self-renewal potential of HSCs. It was postulated that DEK/CAN-positive leukemia is induced in LT-HSCs and maintained by HSCs and committed progenitors. This led to the idea, that DEK/CAN-positive leukemia progresses from both leukemia-initiating and leukemia-maintaining cells. These findings were gained in a transduction/transplantation model of DEK/CAN-positive leukemia in sub-lethally irradiated mice. A transgenic animal model is not established for DEK/CAN (Oancea et al. 2010).

Further studies revealed an elevated activation of the Janus Kinase 2 (JAK2) and Signal Transducer and Activator of Transcription 3 and 5 (STAT3/STAT5) proteins in DEK/CAN-positive AML, presuming they might play a significant role in DEK/CAN-induced leukemogenesis (Oancea et al. 2014). The activation status of STAT3 and STAT5 was higher in both PML/RARα- and DEK/CAN-positive cells, compared with a negative control.

JAK2, the activator of the STAT signaling pathway, as shown in Figure 5, showed an elevated activation in DEK/CAN-positive cells, but not in PML/RARα-positive cells (Oancea et al. 2014).

These findings demonstrate that the mechanism of DEK/CAN-induced leukemic transformation is still greatly unknown. To gain further understanding, the counterparts DEK and CAN should be looked at individually.

1.4.5 DEK

The DEK protein was first discovered in the t(6;9) (p23;q34)-positive AML as a part of the fusion product DEK/CAN. Shortly after, there was found an association of autoantibodies to the DEK protein with juvenile rheumatoid arthritis, systemic lupus erythematosus and sarcoidosis (Sierakowska et al. 1993; Dong et al. 1998). Later on, DEK was described as an oncoprotein in various solid cancers such as melanoma, hepatocellular carcinoma and breast cancer (Khodadoust et al. 2009; Le Yu et al. 2016; Liu et al. 2012). Nowadays, it is known that DEK is located in the nucleus and expressed ubiquitously in all eukaryotic cells (Capitano und Broxmeyer 2017).

1.4.5.1 Structure of DEK

The DEK gene on chromosome 6 encodes a nuclear phosphoprotein with a molecular mass of 43 kDa. DEK contains DNA-binding sites, numerous acidic domains (aspartate/glutamate rich) and a nuclear localisation signal.

DEK can interact with DNA by its SAP-box (scaffold attachment factor-A/B; acinus; Pias) and a DNA-binding site at the carboxy-terminus of the protein. The DNA-binding of DEK is more dependent of the structure than of the sequence of the DNA. DEK has a high affinity to cruciform and superhelical DNA. It induces the formation of positive supercoils into circular DNA (Böhm et al. 2005). Most of the DEK protein is associated with chromatin and in ~ 10% with RNA (Kappes et al. 2001). By interacting with chromatin, DEK may be able to influence epigenetic and transcriptional gene regulation. The exact mechanism and role of DEK in this context is still unknown. All structures of DEK are preserved in the DEK/CAN fusion product.

1.4.5.2 Regulation of DEK

DEK can be influenced by phosphorylation, acetylation and poly-ADP-ribosylation (Kappes et al. 2004; Cleary et al. 2005; Kappes et al. 2008). Phosphorylation can regulate the DNA-binding

activity of DEK. It was shown that the affinity to DNA is lower in the phosphorylated state of DEK. The DEK protein remains associated to chromatin even in the phosphorylated state by dimerization with unphosphorylated DEK. These modifications may be significant in the regulation of DEK and its task in the cell (Kappes et al. 2004).

1.4.5.3 Role of DEK in differentiation and hematopoiesis

Narrowing down the role of DEK is challenging, as its various functions are very complex.

Beyond its ability to bind DNA and chromatin and thus influencing epigenetic and transcriptional regulations of cells, it impacts cellular functions such as proliferation and differentiation. It shows a high expression in hematopoietic, proliferating cells. The DEK expression declines in differentiated and mature cells (Ageberg et al. 2006).

Furthermore, by its location in the nucleus, DEK is involved in nuclear processes, such as transcription, DNA replication and DNA repair. Knock-down models for DEK demonstrated an increased DNA damage with DNA strand brakes and a higher reaction to exogenous stress (Kavanaugh et al. 2011).

It has been demonstrated that DEK can also be secreted by macrophages and neutrophils and act as an extracellular stimulator for proinflammatory cascades. Additionally, it has been demonstrated that extracellular DEK regulates hematopoiesis by activating the chemokine receptor CXCR2 signaling. The proliferation of hematopoietic stem cells was induced, whereas the proliferation of hematopoietic precursor cells was reduced (Capitano et al. 2019). This confirms DEKs function in maintenance of HSCs.

1.4.6 CAN

The function of the human protein CAN, located on chromosome 9, was discovered in 1993 as a member of the nuclear pore complex (NPC) by immune electron microscopy. It functions as a nucleoporin and consequently got the alternative name nucleoporin 214 (NUP214). The nucleoporin CAN is located on the cytoplasmatic site of the NPC and contains phenylalanine-glycine-repeats (FG-repeats) in its structure, which are important for the nuclear transport function of the NPC (Kraemer et al. 1994). Additionally, CAN influences the cell cycle, mitosis and gene

expression. The deletion of CAN or DEK/CAN in mouse embryos causes cell cycle arrest in the G2 phase with limited nuclear transport of mRNA and proteins (van Deursen et al. 1996; Chatel und Fahrenkrog 2012).

1.4.6.1 The nuclear pore complex (NPC)

The nuclear pore complex is a large multiprotein compound, containing a nuclear and a cytoplasmic membrane. It consists of a core scaffold, eight stokes which form a cylindrical nuclear channel and peripheral filaments from the core to the nucleus and the cytoplasm. The complete structure encloses around 456 protein molecules and approximately 30 nucleoporines with recurring FG-repeats. The FG-molecules are unfolded and flexible in their conformation and manage to act as an important barrier in nuclear transport processes (Alber et al. 2007; Rout et al. 2000; Lim et al. 2006).

The NPC is essential in the transport of molecules between the nucleus and the cytoplasm of eukaryotic cells. It restricts nuclear permeability of molecules > 40 kDa and controls nucleocytoplasmic transport. The nucleocytoplasmic transport is regulated by transport receptors of the karyopherin-beta-protein family. Karyopherin-beta proteins can function as importins and exportins. The most important nuclear exportin is chromosomal maintenance 1 (CRM1), also called exportin 1 (XPO1). It can recognize proteins with leucine-rich nuclear export signals (NES) and subsequently letting them exit the nucleus towards the cytoplasm. This enables a nucleocytoplasmic transport of different molecules, proteins and mRNA (Fukuda et al. 1997; Mendes und Fahrenkrog 2019).

1.4.6.2 CAN as fusion partner in other LAFP

There have been different chromosomal reciprocal translocations involving the CAN gene described in AML and ALL. The gene fusion DEK/CAN has only been detected in AML. Other translocations containing the CAN gene are SET/CAN, also called SET/NUP214, which arises by a deletion in chromosome 9. The deletion leads to a fusion to the nuclear proto-oncogene SET, which has mainly been detected in T-ALL. Another fusion involves the tyrosine kinase ABL1 (abelson murine leukemia viral oncogene homolog 1) in T- and B-ALL. It is the second most common fusion with ABL1 in leukemia. Like the chromosomal translocation BCR/ABL1, the in

this case episomal fusion leads to an uncontrolled activation of the ABL1 kinase (Keersmaecker et al. 2008). All the CAN fusions share a rather bad prognosis (Graux et al. 2004; Mendes und Fahrenkrog 2019).

1.5 The JAK/STAT signaling pathway

The JAK/STAT signaling pathway is substantial in the hematopoietic system and involved in various mechanisms such as cell proliferation, differentiation, apoptosis and immunologic responses (Pencik et al. 2016). Clonal mutations of JAK2 have been identified and correlated with myeloproliferative disorders such as polycythemia vera (James et al. 2005).

The JAK/STAT signaling pathway transfers extracellular signals into the nucleus and activates the transcription of target genes. The extracellular ligand binds to an enzyme-linked receptor in the cell membrane, which is associated with the Janus Kinase JAK and secondly to Signal Transducers and Activators of Transcription, called STATs. JAK functions as a tyrosine kinase and includes four members of the JAK family, JAK 1, JAK2, JAK3 and the non-receptor tyrosine-protein kinase 2 (TYK2) (Wilks et al. 1991; Velazquez et al. 2011). JAK gets activated by ligand-induced dimerization of the cell surface receptor. The conformational change leads to a high proximity of JAKs and induces transphosphorylation as well as phosphorylation of tyrosine residues of the receptor, which then serve as a binding site for Sarcoma Virus-homology domain 2 (SH-2 domains) (Greenlund et al. 1994). All STATs contain a SH-2 domain and can bind to the phosphorylated tyrosines (Haan et al. 2000; Heim et al. 1995). JAK then phosphorylates a tyrosine of STAT which leads to a dissociation of STAT from the receptor. The SH-2 domain of a second STAT binds to the phosphorylated tyrosine and creates a dimer of two STAT molecules. These dimers are then active and translocate into the nucleus, secondly binding promotors of target genes and activating gene transcription. (Levy und Darnell 2002).

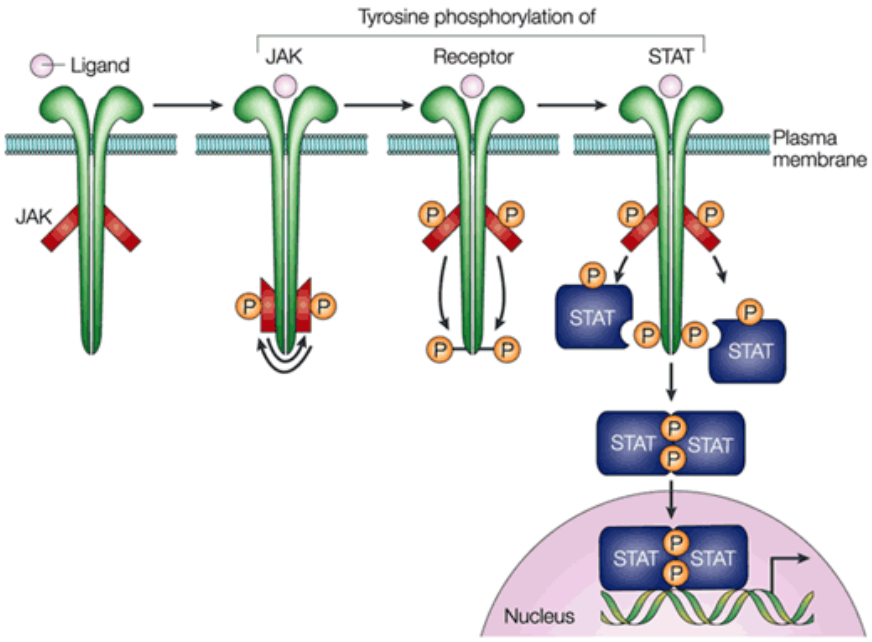

Figure 5: The JAK/STAT signaling pathway
An extracellular ligand binds to the JAK-associated transmembrane receptor, which leads to a dimerization of the receptor. This induces the transphosphorylation and phosphorylation of tyrosine residues by Janus kinases (JAKs). The phosphorylation attracts the binding of signal transducers and activators of transcription (STATs). The following phosphorylation of STATs by JAK induces a STAT dimerization and a succeeding translocation to the nucleus to activate gene transcription (Levy und Darnell 2002)

There are seven different STAT proteins described, STAT1, 2, 3, 4, 5A, 5B and 6. They are all important in the regulation of gene expression in many cellular functions (Copeland et al. 1995; Horvath 2000). Apart from the SH-2 domain and the tyrosine phosphorylation site for STAT activation and dimerization, the structure of STAT contains a DNA-binding domain, a transactivation domain (TAD) as well as coiled coil domains for protein interaction (Levy und Darnell 2002).

The JAK/STAT signaling cascade has multiple positive and negative regulation mechanisms. One of the main mechanisms relies on a balance of phosphorylation by ligand-activation and dephosphorylation by tyrosine phosphatases. Positive regulators are, for example, interferons, IL-6, IL-4 and G-CSF as extracellular activators. Important negative regulators are tyrosine phosphatases that dephosphorylate and thereby inactivate JAK. Mentionable are the tyrosine phosphatases Src-homology region 2 domain-containing phosphatases 1 and 2 (SHP1 and SHP2) as well as the protein tyrosine phosphatase receptor type C (PTPRC), which encodes the Cluster of differentiation 45 (CD45). CD45 is also named leukocyte common antigen, because of its

expression in all hematopoietic cells. It plays a major role in regulating JAK and in B- and T-cell signaling. (Xu und Qu 2008; Irie-Sasaki et al. 2001; Porcu et al. 2012).

1.6 Dissertation hypothesis and aims

The t(6;9)-positive AML with the resulting fusion product DEK/CAN affects a young patient population, with a poor prognosis and a very aggressive course of the disease.

The translocation of the chromosomes 6 and 9 leads to the formation of a novel protein DEK/CAN, which induces leukemia in a subset of hematopoietic stem cells (HSC). The exact mechanism of DEK/CAN-induced leukemogenesis and the function of the fusion protein is greatly unknown.

Our goal was the characterization of the DEK/CAN-induced leukemia on a molecular level by identification and detection of the gene transcript and further gene expression analysis.

We aimed to establish a workflow to enable the detection and quantification of the fusion product by standard and real-time quantitative PCR (qPCR). This allows a molecular monitoring of the fusion transcript, which is relevant in testing the minimal residual disease (MRD) of leukemic cells before, during and after treatment in affected patients.

Secondly, we were interested in gene expression analysis in DEK/CAN-positive cells, to identify target genes that influence and enhance the development of DEK/CAN-induced leukemogenesis.

By characterizing DEK/CAN-positive AML on a molecular level, we want to gain further understanding of the DEK/CAN-induced leukemogenesis and find new targets that drive the disease and might gain relevance in the treatment of this particularly aggressive AML.

2 Materials

2.1 Instruments and equipment

Instruments and equipment	Manufacturer
Binocular microscope	Carl Zeiss, Oberkochen Germany
Bioanalyzer 2100	Agilent, Santa Clara, USA
Blotting apparatus	Invitrogen, Karlsruhe, Germany
Cell culture flasks and dishes	Greiner, Heidelberg, Germany
Cell culture incubator	Thermo Fisher HERAEUS, Baltimore, USA
Cell scraper	Corning, Wiesbaden, Germany
Cell strainer (40 µm)	Becton Dickinson, Heidelberg, Germany
Centrifuge Megafuge 1.0 with Rotor BS4402/A	Heraeus, Hanau, Germany
Centrifuge Rotina 48 RS Table top	Hettich, Tuttlingen, Germany
Centrifuge Rotina 420R Benchtop	Hettich, Tuttlingen, Germany
Centrifuge Rotanta 460 Benchtop	Hettich, Tuttlingen, Germany
Centrifuge Sorvall RC-5B refrigerated superspeed	Hettich, Tuttlingen, Germany
Centrifuge Table top 5415C	Eppendorf, Hamburg, Germany
Cryotubes	Nalgene, Rochester, NY , USA
Cytofunnel	Shandon, Pittsburgh, USA

Gel electrophoresis system	BioRad, Munich, Germany
Freezer – 20 °C	Liebherr, Germany
Freezer – 80 °C	Heraeus, Hanau, Germany
Fridge 4 °C	Liebherr, Germany
Liquid nitrogen container	Nunc, Wiebaden, Germany
Nitrocellulose membrane (0.45 µm)	Bio-Rad Laboratories, Munich, Germany
Odyssey Fc-Imaging System	Li-Cor Bioscience, Lincoln USA
PCR Mastercycler pro, Vapo protect	Eppendorf, Hamburg, Germany
PCR Cycler, Real-Time-PCR-System, SureTect	Thermo Scientific, Waltham, USA
Pipettboy	Brandt, Lemgo, Germany
RNase-free tubes and microfuge tubes	Thermo Fisher Scientific, Waltham, USA
Spectrophotometer NanoDrop	Thermo Fisher Scientific, Waltham, USA
Spectrophotometer Gene Quant II	Pharmacia Biotech, Freiburg, Germany
Steril bank, Laminar flow Sterile bank Class II Nuaire	Zapf Instruments, Sarsted Germany
Laminar Flow; Sterile bank Class II	W.H.Mahl, Trendelburg –Langenthal, Germany
Steril filter 0,22 / 0,45 µM	Millipore, Eschborn, Germany

2.2 Chemicals

Agarose	Sigma-Aldrich, Munich, Germany
Bromophenol blue	Sigma, Steinheim, Germany
Calcium chloride	Sigma, Steinheim, Germany
Chloroform	Fluka, Deisenhofen, Germany
ddH_2O	Sigma, Steinheim, Germany
DEPC	Sigma, Steinheim, Germany
dGTP/dATP/dTTP/dCTP-Nucleotides	Roche, Basel, Switzerland
DMSO	Sigma, Steinheim, Germany
DNA marker	New England Biolabs, Frankfurt, Germany
Ethanol	Merck, Darmstadt, Germany
Formaldehyde	Merck, Darmstadt, Germany
Glycogen, RNase-free	Sigma, Steinheim, Germany
Glycine	Merck, Darmstadt, Germany
HD Green, DNA dye	Intas, Göttingen, Germany
Isopropanol	Fluka, Deisenhofen, Germany
Luminol	Fluka, Deisenhofen, Germany
Medium Cell culture RPMI	Gibco-BRL, Invitrogen München Germany
Methylene blue	Sigma, Steinheim, Germany

NaCl	Merck, Darmstadt, Germany
PBS	PAA, Cölbe, Deutschland
RNA-Bee	AMS Biotechnology, Abingdon, UK
SDS	Sigma, Steinheim, Germany
Sodium carbonate	Sigma, Steinheim, Germany
Sodium acetate	Fluka, Deisenhofen, Germany
Sodium citrate	Roth, Karlsruhe, Germany

2.3 Special reagents and materials

2.3.1 PCR reagents

dNTPs	Bioline, Luckenwalde, Germany
MgCl2	Bioline, Luckenwalde, Germany
PCR Buffer	Bioline, Luckenwalde, Germany
PfuTurbo polymerase	Stratagene, La Jolla, USA
Primers	Sigma, Steinheim, Germany
Taq DNA polymerase	Bioline, Luckenwalde, Germany

2.3.2 TaqMan qPCR primer and probes

TaqMan Universal PCR Master Mix	Applied Biosystems, Thermo Fisher scientific, Waltham, USA
TaqMan Gene Expression Assays, primer and probes	Applied Biosystems, Thermo Fisher scientific, Waltham, USA

2.3.3 Enzymes

Klenow-Fragment DNA-polymerase I	New England Biolabs, Frankfurt, Germany
Restriction endonucleases	New England Biolabs, Frankfurt, Germany
RNase Inhibitor	Promega, Mannheim, Germany
RNase-free DNase I	Thermo Fisher Scientific, Waltham, USA
RNase-free DNase RQ1	Promega, Mannheim, Germany
T4 DNA ligase	New England Biolabs, Frankfurt, Germany
Taq-DNA-polymerase	Biosystems, Weiterstadt, Germany

2.3.4 Kits

Tetro cDNA Synthesis Kit	Bioline, Luckenwalde, Germany

2.3.5 Plasmids and vectors

2.3.5.1 Used vectors

Vector	**Construct**	**Promotor**	**Reporter**	**Promotor**	**Resistance**

Pinco-HA-empty	HA	5'LTR	GFP	CMV	Amp
Pinco-HA-DC	HA-DEK/CAN	5'LTR	GFP	CMV	Amp
Pinco-PR	PML/RARα	5'LTR	GFP	CMV	Amp
Paco-HA-empty	HA	5'LTR	CD2	CMV	Amp
Paco-HA-DC	HA-DEK/CAN	5'LTR	CD2	CMV	Amp
Paco-PR	PML/RARα	5'LTR	CD2	CMV	Amp

2.3.5.2 Cloned vectors

The production of plasmids for HA-DEK/CAN is described in Oancea et al. 2010. The plasmid production of HA-PML/RARα is described in Zheng et al. 2004.

2.3.6 Primer

Primer	**Sequence 5' – 3'**
DEK/CAN forward	GCCAAAAGAGAAAAACCTAAA
DEK/CAN reverse	GCAAGGATTTGGTGTGAGAT
GAPDH forward	GAAGGTGAAGGTCGGAGTC
GAPDH reverse	GAAGATGGTGATGGGATTTC

Primer and probes of TaqMan qPCR assay see in 3.11.3.

3 Methods

3.1 Working with eukaryotic cell lines /cell biology techniques

3.1.1 General cell culture conditions

Working with eukaryotic cell lines, the usage of sterile instruments in a sterile work bench is essential. This contains sterile buffers, medium, pipettes and centrifuge tubes. The cells were cultivated in culture flasks in a humidified atmosphere at 37°C with 5 % CO_2. The cell medium was renewed every two to three days.

3.1.2 Used cell lines

All cells, except for ecotropic Phoenix, were acquired from the "Deutsche Sammlung von Mikroorganismen und Zellkulturen GmbH" (DSMZ, German Collection of Microorganisms and Cell Cultures). Ecotropic Phoenix cells were obtained from Nolan lab, Stanford, USA.

Cell line	Characteristics	Medium
U937	Established from a pleural effusion of a 37-year old male patient with generalized histiocytic lymphoma, promonocytic characteristics	RPMI 1640, 10 % FCS, 1 % L-Glutamine, 1 % Pen/Strep
U937-HA-DEK/CAN	U937 with stable expressed HA-DEK/CAN	RPMI 1640, 10 % FCS, 1 % L-Glutamine, 1 % Pen/Strep
Phoenix Ecotropic	Modified 293T cells (transformed human embryonal kidney cell line) functioning as packaging cell line. Express the viral structural genes gag, pol and env	DMEM, 10 % FCS, 1 % L-Glutamine, 1 % Pen/Strep
32D	Established from bone marrow of C3H/HeJ mice. IL3 dependent murine cell line	RPMI 1640, 10 % FCS, 1 % L-Glutamine, 1 %Pen/Strep, 10 ng/ml IL-3

FKH-1	Established from the peripheral blood of a 61-year-old man with Philadelphia chromosome negative CML with trilineage myelodysplasia at refractory leukemic transformation into AML M4; carries t(6;9)(p23;q34) leading to DEK/NUP214 (DEK/CAN) fusion gene.	RPMI 1640, 20 % FCS, 1 % L-Glutamine, 1 % Pen/Strep
Sca^{+}/Lin^{-}	Mouse BM cells	DMEM 10% FBS inactive, 1% L-Glutamine, 1 % Pen/Strep, 20 ng/ml mIL-3, 20 ng/ml mIL-6, 100 ng/ml mSCF

Table 5: Used cell lines

3.1.3 Cell counting

In order to count the cultivated cells, the cells were dissolved in a 1:5 dilution with 0,4 % trypan blue in 0,9 % NaCl. A high cell density required higher dilutions. The unstained cells were considered non-viable cells and were not included in the cell count.

With the standardised Neubauer cell count chamber, the total cell count was calculated as follows:

$$\text{Cell concentration} = \frac{(\text{Total cell count x dilution factor})}{\text{Number of counted Neubauer chambers}}$$

3.1.4 Storage, freezing and thawing of eukaryotic cells

Storage of eukaryotic cells was held in liquid nitrogen. Thawing was carefully performed in a water bath at 37°C. The cryotube content was diluted with 10 ml of fresh medium and centrifuged for 5 minutes at 1200 rpm. Discarding the supernatant, this step was repeated twice, to ensure thorough washing of the cells. After the last washing step, the cell pellet was resuspended in medium and placed in a tissue culture plate or bottle.

The minimum cell count for freezing cells was 7 x 10^6 cells/µl. The cell medium mixture was centrifuged at 1200 rpm for 10 minutes to divide the cells from the medium. The cell pellet was carefully resuspended in 0,5 ml of freezing solution I and transferred to a cryotube. In a next step,

0,5 ml of freezing solution II were added to the cell solution and mixed by inversion. The cryotubes were frozen in filled Isopropanol containers over night at – 80 °C. The last step was the transfer of the cryotubes into liquid nitrogen for storage.

Freezing solution I:

68 % RPMI 1640

30 % FCS

1 % Pen / Strep

1 % L-Glutamin

Freezing solution II:

80 % RIPA-1640

20 % DMSO

3.1.5 Subculturing of eukaryotic cells

The cell cultures were checked by microscope and subcultured regularly to maintain their logarithmic growth curve. The confluence of the cells indicated the right time to split cells. A confluence of approximately 80 % required subculturing to maintain the logarithmic growth curve. Attached cell lines required trypsinization. Therefore, the culture medium was carefully removed and the attached cells were washed twice with PBS. Using a pipette, 0,25 % trypsin EDTA was then dripped onto the cells, moving the flask gently to ensure trypsin contact with all the cells. They were incubated for 2 – 5 minutes at 37 °C until the cells detached from the culture flask. Adding medium inactivated the trypsin and a cell dilution was now possible.

Suspension cells were diluted with fresh medium and transferred to a new culture flask. The dilution factor changed depending on the cell type and growth velocity.

3.2 RNA isolation with RNA-Bee

To isolate total RNA from eukaryotic cells, the monophasic solution RNA-Bee (Amsbio, Germany), containing phenol and guanidine thiocyanate was used. The cells were prepared by

centrifugation at 1200 rpm for 8 minutes to split them from the culture medium. After discarding the supernatant, the cells were washed with PBS and lysed in 1 – 2 ml RNA-Bee. All the following steps were performed in an RNase-free environment with RNase free solution substances and materials. To the RNA-Bee mixture, 200 µl of chloroform was added and shaken thoroughly for 15 seconds. After an incubation of 3 minutes at room temperature, the cells were centrifuged at 12.000 rpm for 10 minutes at 4 °C. The generated upper aqueous phase contains the RNA and was transferred into a fresh 1,5 ml Eppendorf tube. The remaining solution can be used for protein and DNA isolation. Continuing with the aqueous phase, 1 µl of RNase-free glycogen and 500 µl isopropyl alcohol were added and mixed carefully with the pipet. After an incubation of 30 minutes at – 20 °C, the mixture was again centrifuged at 12.000 rpm for 10 minutes at 4 °C. In this step the RNA was precipitated, which is usually visible as a glycogen blue pellet on the bottom of the tube. After discarding the supernatant, 200 µl of 75 % ethanol in DEPC water was added to the pellet and centrifuged at 7500 rpm for 5 minutes at 4 °C. Removing the ethanol, only the RNA pellet remains, which was dried for around 15 minutes at room temperature. The pellet has then been lysed in 20 µl RNase free water and incubated for 10 minutes at 55 – 60 °C. The RNA could then be stored at -80 °C.

3.3 Protein isolation with RNA-Bee

After dissolving the cells in RNA-Bee and removing the RNA-containing supernatant, the remaining DNA was precipitated with 300 µl of 100 % ethanol. After an incubation of 3 minutes at room temperature and centrifugation at 2.000 rpm for 5 minutes at 4 °C, the phenol-ethanol-supernatant was removed with the pipet and transferred into a 2 ml Eppendorf tube for protein extraction. The total protein was first precipitated with 1,5 ml isopropanol with an incubation time of 10 minutes at room temperature. The precipitate was then centrifuged at 12.000 rpm for 10 minutes at 4 °C. Each extracted protein pellet was then washed three times with 2 ml 0,3 M guanidine hydrochloride in 95 % ethanol, incubated 20 minutes at room temperature and centrifuged at 7.500 rpm for 5 minutes at 4 °C. After the third round of centrifugation, 1,6 ml ethanol were added and mixed by vortexing. The mixture was then incubated for 20 minutes at room temperature and centrifuged at 7.500 rpm for 5 minutes at 4 °C. Removing the supernatant, the protein pellet remained and was dried at room temperature. The extracted protein was lysed in

1 % SDS. If the lysation remained incomplete, an incubation at 55 °C for 10 minutes or a sonification process was performed. The lysate was then stored at -20 °C.

3.4 Benzonase treatment of protein lysates

The protein lysates were treated with benzonase endonuclease to reduce their viscosity. First step was the preparation of the dilution buffer for benzonase, wich contains:

20 mM TrisHCL (pH = 8)

2 mM MgCl2

20 mM NaCl

50 % glycerol

190 µl of dilution buffer was added to 10 µl of benzonase. Then 5µl of diluted benzonase was added to each 100 µl of protein lysate and vortexed. After an incubation of 30 minutes on ice the samples were ready to be stored at -20 °C.

3.5 Measurement of protein concentration

The protein concentration can be determined by photometric measurements. The bicinchoninic acid (BCA) assay kit was used according to the manufacturer's instruction and quantified with a spectrophotometer at 595 nm. The standards for protein concentration were prepared with different concentrations of BCA (0.5 to 10 mg/ml).

3.6 Measurement of RNA concentration and purity

To determine the concentration and purity of RNA in a solution, spectrophotometric quantification is a well-established method. The RNA samples were evaluated by using the NanoDrop spectrophotometer (Thermo Fisher Scientific, USA). The absorption maximum of nuclear acids (DNA and RNA) is at 280 nm wavelength. The RNA concentration results in the measurement of the extinction at 260 nm with the formula:

$$c = OD260nm \times 50 \times f$$

c = RNA concentration in µg/ml

OD = optical density (an OD260nm of 1,0 equates to 40 µg/ml single-strand RNA)

f = dilution factor

Due to the absorption of aromatic sidechains, proteins have an absorption maximum at 280 nm wavelength. By determining the ratio of OD260nm/OD280nm, a potential protein contamination of the RNA can be excluded. A ratio between 1,8 and 2,0 indicated a valuable purity of the RNA.

3.7 Measurement of RNA quantity and quality

When quantifying RNA, spectrophotometric methods, as described above, are well-established and give a predictive value of the RNA's purity.

But especially when working with RNA for gene expression analysis, the RNA quality and integrity form the groundwork for any following result. Of particular interest is the messenger RNA (mRNA) sequence, which directly reflects corresponding gene expression. The mRNA is in a constant process of formation and degradation and therefore a very instable molecule. It is built by RNA-Polymerases, enables the protein translation in prokaryotic and eukaryotic cells and gets degraded by ribonucleases. (Fleige und Pfaffl 2006a)

Double-strand total RNA as well as single-strand mRNA, are both unsteady molecules that degrade easily by contamination. Degraded RNA would distort any information on detected gene expression activity. This explains the necessity for a particularly attentive quality control. The integrity, purity, concentration and size of the isolated total RNA were determined with the RNA-6000-Nano-LabChip-Kit using the Agilent-2100-Bioanalyzer (Agilent Technologies, USA). It is based on the technique of capillary electrophoresis, an electro kinetic separation method, which measures the size and concentration of twelve RNA samples on a chip format, at the same time. The chip format reduced separation time and sample consumption. The RNA was diluted to a concentration of 5 ng/µl to 500 ng/µl with RNase free water. The samples (1 µl) were pipetted on the chip well plate and moved over microfluidic glass channels, which are interconnected among the wells, in an electric field. The charged RNA was electrophoretically driven by a voltage gradient. The molecules got separated by size through sieving polymer coated capillaries.

Moreover, the micro channels contained dye molecules, which intercalated between RNA strands. These complexes got registered on a fluorescence detector and contained the information of the RNA fragment size and their migration time. The data was visualized in electrophoresis gel-like bands and electropherograms for each sample (instruction manual Agilent-2100-Bioanalyzer, Agilent Technologies, USA).

In addition, Agilent Technologies and Quantitom Bioinformatics developed an expert software which generates the RNA integrity number (RIN). The RIN is based on the entire electrophoretic trace of the RNA sample, which characterizes the integrity of total RNA samples from RIN 1 (complete degradation) to RIN 10 (no degradation). To secure high quality RNA, only samples with a RIN ≥ 8 were considered. The compared samples had to show identical RIN values. When fulfilling these criteria of RNA integrity, further steps in RNA analysis were made. Studies have shown that the performance and efficiency of PCR deteriorates when the RNA integrity is reduced (Fleige und Pfaffl 2006b).

The complete isolated RNA, that was used in this work, was analyzed with the Bioanalyzer technology to ensure a high integrity of the RNA.

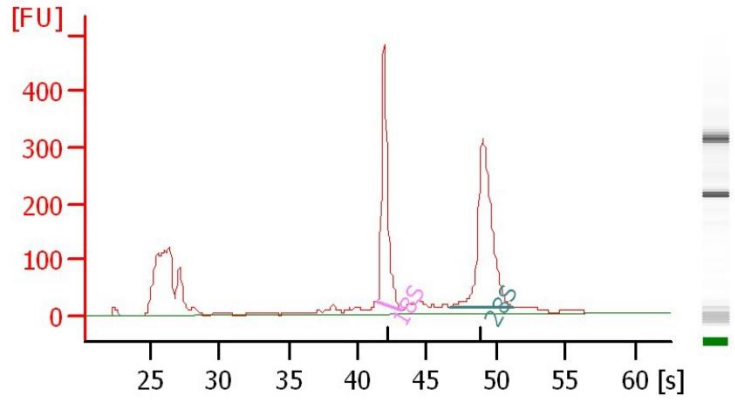

Figure 6: Electropherogram for RIN classification
This graph was preserved from 1 µl isolated, with DNase treated RNA of Phoenix Eco cells, transfected with the vector Paco-HA-DC. The following data was computed: RNA Area: 2,585.2, RNA concentration: 1,348 ng/µl, rRNA Ratio [28s / 18s]: 1.3, RNA Integrity Number (RIN): 9.3 [s] = seconds. The typical peaks show the 18S and 28S ribosomal fragments of eukaryotic RNA. The sample indicated satisfying RNA quality.

3.8 RNA treatment with Deoxyribonuclease (DNase)

The deoxyribonuclease (DNase) treatment of RNA samples formed an essential step in maintaining the RNA's integrity and removing any kind of genomic DNA contamination. This was very important in this work to ensure optimal RNA quality prior to real-time quantitative PCR. Acting as a second competitor, genomic DNA contamination can falsify PCR results (Huang et al. 1996). The RNase-free DNase is an endonuclease that degrades double- and single-stranded DNA. Phosphodiester bonds get hydrolyzed resulting in mono and oligo deoxyribonucleotides with 5'-phosphate and 3'-OH groups. The enzyme activity is dependent on calcium and is activated by magnesium ions which are contained in the DNase reaction buffer.

Two different DNase kits were used and evaluated in terms of their outcome. The first kit was the RNase-free DNase I from Thermo Fisher Scientific which was compared to the RQ1 RNase-free DNA kit from Promega. Furthermore, results were compared with or without DNase treatment. All steps were performed according to the corresponding guidelines with RNase free solution substances and materials.

The DNase digestion in both kits was set up as follows:

RNA in water	10 µg
10 x reaction buffer	1 µl
RNase-free DNase	1 u/µg RNA
*RNase Inhibitor	1 u/µg RNA
Nuclease-free water to a final volume of 50 µl	

* Both protocols were modified by adding 1 u/µg RNA of RNase Inhibitor (Promega, USA) to secure the RNA samples from degradation.

The samples were then incubated at 37 °C for 30 minutes for DNase digestion. Afterwards, a phenol-chloroform extraction was done to purify, wash and precipitate the RNA (chapter 3.2).

3.9 Reverse transcription

The enzymatic activity of reverse transcriptase was used to translate in vitro RNA into the complementary DNA (cDNA). Reverse transcriptases are RNA-dependent DNA-polymerases which can use either RNA or DNA sequences as a template. The cDNA synthesis starts with the enzymatic activity of the reverse transcriptase and continues with hydrolyzation of the RNA-DNA hybrid strand by the exoribonuclease activity of the reverse transcriptase. Afterwards, a double strand cDNA is generated, which can be used as a template for following PCR and real-time quantitative PCR reactions.

The cDNA synthesis was performed with the Tetro cDNA Synthesis Kit by Bioline. All steps were performed according to the corresponding guideline with RNase free solution substances and materials.

First step was the preparation of the following mixture on ice:

1 µg RNA	x µl
Random hexamer primers	1µl
DEPC-treated water	up to 10 µl

These samples were incubated for 5 minutes at 70 °C to denature the secondary structures of the RNA. Next, the samples were immediately chilled on ice and spun down shortly with a centrifuge. In the meantime, the priming premix was prepared on ice in an RNase free reaction tube.

Priming premix:

10 mM dNTP mix	1 µl
5x RT Buffer	4 µl
Ribosafe RNase Inhibitor	1 µl
Tetro Reverse Transcriptase (200 u/µl)	1 µl
DEPC-treated water	up to 10 µl

The priming premix was then added to the RNA samples and mixed gently by pipetting. They were incubated at 25 °C for 10 minutes and then at 45 °C for 30 – 60 minutes. This incubation enabled

efficient reverse transcription which got terminated by incubating the samples at 85 °C for 5 minutes. The newly generated cDNA samples were chilled on ice and stored at – 20 °C.

Additionally, every RNA sample was tested for genomic DNA contamination. This was performed by a parallel reaction preparation without the Tetro Reverse Transcriptase in the priming mix. This served as an internal control for the RNA's purity and consequently also its integrity.

3.10 Polymerase chain reaction (PCR)

The polymerase chain reaction, short PCR, is a fundamental technology to amplify specific DNA fragments. This DNA can then be detected, analyzed and sequenced. The reaction is cyclic and comprises three main steps: denaturation, annealing and elongation of the DNA.

The required oligonucleotide primers were designed to match their complementary defined DNA sequences. Each primer pair had to be tested in different conditions concerning the MgCl2 concentration and the annealing temperature in order to get the best result (Kramer und Coen 2001). The polymerase reaction was performed by the Mango-Taq polymerase with its corresponding reaction buffers.

For a 50µl preparation:

Taq polymerase	2,5 U
Reaction buffer	10x
MgCl2	25 – 50 mM
dNTPs	10 mM
Forward primer	10 µM
Reverse primer	10 µM
Template DNA	5 - 50 ng
ddH_2O	up to 50 µl

Double-destilled water (ddH_2O) was added up to a total sample volume of 50 µl. The reaction was initiated by denaturing the DNA at 95°C for 5 minutes, followed by 35 cycles of PCR reaction.

Program for Mastercycler pro (Eppendorf, Germany):

1) For DEK/CAN:

95 °C	4 minutes	
95 °C	45 seconds	x 35 cycles
48 °C	45 seconds	x 35 cycles
72 °C	45 seconds	x 35 cycles
72 °C	10 minutes	

2) For PML/RARα

95 °C	3 minutes	
95 °C	45 seconds	x 35 cycles
58 °C	1 minute	x 35 cycles
72 °C	45 seconds	x 35 cycles
72 °C	10 minutes	

3.11 Real-time quantitative PCR (qPCR)

The real-time quantitative PCR (qPCR) relies on the same principle as the standard PCR method, adding the possibility to quantify the produced molecules with a DNA-binding fluorescent dye. The detection of the fluorescence allows direct measurement of produced DNA molecules for each cycle. The qPCR is therefore also referred to as real-time PCR. It was used to acquire not only the general detection of a certain gene, but also the direct quantification of DNA which then correlates directly with gene expression. Also, it allows a broad result evaluation due to comparable values. At the end of each cycle the fluorescence was measured.

3.11.1 TaqMan quantitative PCR

Quantitative monitoring of gene expression was performed by the DNA Engine Opticon 2 System by Biorad, USA, with the TaqMan assay as the detection mechanism. The qPCR Master Mix No

ROX (Eurogentec, Belgium) was used for all experiments, which contained HotGoldStar DNA polymerase, MgCl2, Uracil-N-glycosylase, dNTPs with dUTP, and optimized buffer components. The Uracil-N-glycosylase (UNG) treatment was carried out to avoid the reamplification of carry-over PCR products. The qPCR Master Mix was used as per the manufacturer's instructions. The TaqMan PCR was always conducted in triplicates with positive and negative controls, following standard protocols using the Opticon 2 System.

For a 50 µl preparation:

2x reaction buffer	25 µl
Forward primer	100 – 900 nM
Reverse primer	100 – 900 nM
Probe	100 – 200 nM
Template DNA	5 – 50 ng
ddH_2O	up to 50 µl

Thermal cycle conditions:

50 °C	2 minutes	UNG step
95 °C	10 minutes	Polymerase activation / UNG inactivation
95 °C	15 seconds	40 cycles
60 °C	30 seconds	40 cycles
50 °C	forever	Hold

The program monitored the amplification for 40 cycles. Each cycle showed an increase in the fluorescence and was plotted on data graphs and tables. An important value for quantification is the cycle of threshold (CT). The CT value stands for the number of PCR cycles needed to reach a constant defined fluorescence level.

3.11.2 TaqMan assay

The TaqMan assay technique benefits from the 5'-3'-exonuclease activity of the Taq-Polymerase (Holland et al. 1991). In a TaqMan assay, a fluorogenic probe, complementary to the target

sequence, is added to the PCR reaction. This TaqMan probe consist of a 18-22 base pairs (bp) oligonucleotide probe which is tagged with a reporter fluorophore at the 5'-end and a quencher fluorophore at the 3'-end (Liu et al. 2006). The fluorescent dyes used in this study were FAM, for the reporter, and TAMRA for the quencher. Temperatures above 50 °C induce a hybridisation of primer pairs and probes to the target sequence. The fact, that the probe hybridizes directly to the template, increases the specificity of the detection. In an intact probe, the proximity of reporter to quencher oppresses the fluorescence. During PCR, the probe hybridizes with the template, between the forward and the reverse primer, and is hydrolyzed by the 5'-3'-exonuclease activity of the Taq-Polymerase. This releases the reporter molecule away from the quencher, increasing the fluorescence intensity of the reporter dye. This process is repeated in every cycle with increasing fluorescence intensity analogous to the quantity of the PCR product (Gangisetty und Reddy 2009). This implies, that large amounts of DNA show a fast detection of fluorescence and small amounts of DNA a slow fluorescent release.

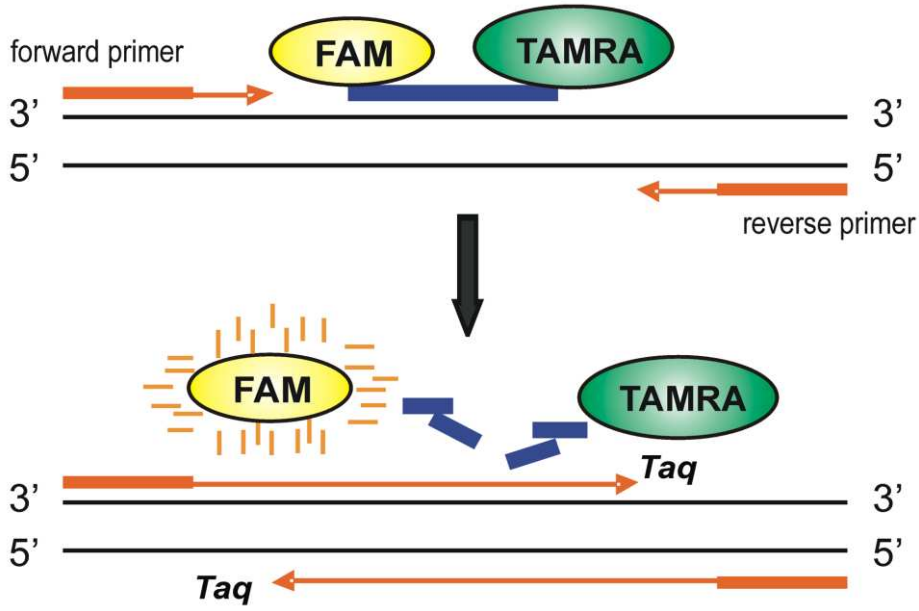

Figure 7: TaqMan chemistry
In an intact probe, the quencher suppresses the fluorescence emission of the reporter dye. While PCR, the Taq-Polymerase with its 5'-3'-exonuclease activity divides the probe and separates the quencher from the reporter dye. This induces an increase of fluorescence of the reporter. For every PCR cycle the fluorescence increases and can be detected in "real-time" (Gangisetty und Reddy 2009).

3.11.3 Design of primers and probes

Various primers and TaqMan probes were used for gene expression analysis in this study. The majority were predesigned TaqMan gene expression assays, offered by Applied Biosystems, Germany. The primers and TaqMan probes for the fusion protein DEK/CAN were designed based on a publication by Ostergaard et al. from 2004 and the primers and TaqMan probes for the fusion protein PML/RARα were designed based on a publication by Oancea et al. from 2014, both using Primer Express Software by Applied Biosystems. They were designed based on the DEK/CAN and PML/RARα sequences published in the NCBI nucleotide database.

Target	Primer/probe 5'→3'	
DEK/CAN	FP:	ATTACTGGCCAGTGCTAACTTG
	RP:	GATTGTTGGCTAGGGTGTTAAA
	Probe:	FAM-TTCCAGATGCTGATCCCACTCCA-TAMRA
PML/RARα	FP:	AGAGGATGAAGTGCTACGCCT
	RP:	TTCCGGGTCACCTTGTTGAT
	Probe:	FAM-TAGTGCCCAGCCCTCC-TAMRA

Table 6: Sequences of forward primer (FP), reverse primer (RP) and probe for DEK/CAN and PML/RARα in qPCR (Oancea et al. 2014; Ostergaard et al. 2004).

For an DEK/CAN validation assay, the following genes were used from the predesigned Applied Biosystems gene expression assays. The genes human and mouse GAPDH were used as house-keeping genes.

TRIM 25	Tripartite motif-containing 25
XPO1	Exportin 1
HIF1α	Hypoxia inducible factor, alpha subunit
ATF2	Activating transcription factor 2
PTPRC (CD45)	Protein tyrosin phosphatase

MBTD1	Malignant brain tumor domain containing 1
NDRG1	N-myc downstream regulated gene 1
SMEK2	SMEK homolog 2
CASP8	Caspase 8
ARF4 (p14)	ADP-ribosylation factor 4
CASP4	Caspase 4
ASXL1	Additional sex combs like 1
PTP4A3	Protein tyrosine phosphatase 4a3
PIM1	Proviral integration site 1
CSF1R	Colony stimulating factor 1 receptor
LMO2	LIM domain only 2

Table 7: Selected genes for TaqMan quantitative PCR validation and gene expression assay

3.11.4 Optimization of qPCR

Before initiating the actual experiments with DEK/CAN, the primer and probe concentrations and PCR program elongation time had to be optimized. A series of experiments with alternate primer and probe concentrations for the endogenous reference gene GAPDH and the fusion protein DEK/CAN was performed. Used cell material was cDNA from Phoenix (Phx) Eco cells, which contained the constructs Paco-HA-empty and Paco-DC as well as the Plasmid Pinco-HA-DC-GWB.

Primer concentration	Probe concentration
100 nM / 100 nM	100 nM
300 nM / 300 nM	100 nM
300 nM / 300 nM	200 nM

900 nM / 900 nM	200 nM

Table 8: Scheme for TaqMan primer and probe concentration optimization
The combination of primer and probe concentration in nM (nano Molar) with the best results was chosen for further studies.

3.11.5 Generation of calibration curves

Samples of quantitative real-time PCR needed to be calibrated in order to compare them. The best approach was the generation of standard curves for each target with their specific qPCR primers and probe. Standard curves from synthesized representative cDNA for both human GAPDH and DEK/CAN were generated. Another standard curve for mouse GAPDH was constructed. The specificity of the generated PCR products was confirmed by DNA gel electrophoresis.

3.11.6 Calculation of qPCR efficiency

In order to verify PCR efficiency and linearity of template amplification, serial dilutions of cDNA were tested by qPCR and the specific primers for each gene. These serial dilutions created a standard curve where, calculating the slope, the efficiency was determined. The used quantity of cDNA was linked to the CT value in a logarithmic function. The efficiency (E) was calculated with the following equation (Pfaffl 2001):

$$E = 10^{(-1/slope)}$$

3.11.7 Data analysis of qPCR

There are two main approaches to quantify qPCR results. There is the absolute quantification strategy as well as the relative quantification strategy. The absolute quantification strategy is based on a standard curve of plasmid DNA and defines the exact copy number of the target gene. The relative quantification strategy compares the target gene to a house keeping gene and leads to normalization of the gene expression results. It can be optimized by taking account of the estimated qPCR efficiency.

3.11.7.1 Relative quantification

In relative qPCR quantification, the gene expression analysis of a target gene is normalized to a second, non regulating and ubiquitary occurring refernce gene. It analyzes the relative changes in gene expression from qPCR experiments. In this study, the target gene was DEK/CAN which was normalized to the house-keeping gene GAPDH. All measurements were assayed in triplicates, using the mean CT for all further calculations. CT values were transferred into a worksheet for the calculation of fold changes according to the Comparative CT method. The amount of target, normalized to an endogenous GAPDH is given by $2^{-\Delta\Delta CT}$ (Livak und Schmittgen 2001).

ΔCT = CT target gene – CT reference gene

$\Delta\Delta CT$ = ΔCT treated sample – ΔCT control sample

Relative expression ratio = $2^{-\Delta\Delta CT}$

This Comparative CT method models allows the differentiation of single transcription differences between the control and the sample. The method presumes a 100 % efficiency of the PCR, which signifies a duplication of DNA amount in every PCR cycle. In order to assess that, the qPCR efficiency was calculated. With the known efficiency, the relative quantification can be corrected with the following equations. (Filion 2012; Meuer et al. 2001)

$$\text{Ratio} = \frac{(E_{\text{target}})^{\Delta CT_{\text{target}}\,(\text{control}-\text{sample})}}{(E_{\text{reference}})^{\Delta CT_{\text{reference}}\,(\text{control}-\text{sample})}}$$

$$\text{Ratio} = \frac{(E_{\text{target}})^{\Delta CT_{\text{target}}\,(\text{MEAN control}-\text{MEAN sample})}}{(E_{\text{reference}})^{\Delta CT_{\text{reference}}\,(\text{MEAN control}-\text{MEAN sample})}}$$

The relative expression ratio of a target gene can be calculated, regarding its qPCR efficiencies (E) or a static efficiency of 2, and the CT difference (CT Δ) of one unknown sample (sample) versus one control (ΔCT control - sample) (Livak und Schmittgen 2001). The relative calculation

procedure was conducted with a specifically designed Microsoft Excel worksheet, respecting the mean CT value of sample triplicates.

3.11.7.2 Absolute quantification

Absolute quantification allowed the calculation of the exact DNA copy number by analyzing linearized plasmid DNA, which contained the fusion transcript DEK/CAN. Standard curves were generated for qPCR by performing a serial dilution assay of plasmid DNA. Knowing the exact size of the plasmid in base pairs (bp), the number of grams per molecule, also known as copy number, can be determined. The following calculations were executed to define the copy number of the plasmid (Whelan et al. 2003):

$$\text{Weight in Dalton } (\text{g/mol}) = (\text{bp size plasmid} + \text{insert}) \text{ x } (330 \text{ Dalton x } 2 \text{ nucleotides/bp})$$

$$\text{Copy number} = \text{g/molecule } = \frac{\text{Weight in Dalton (g/mol)}}{\text{Avogadro's number } 6{,}02214199 \text{ x } 10^{23}}$$

Knowing the copy number and the concentration of the plasmid that is added to each PCR reaction, the precise number of molecules in that reaction was determined as follows:

$$\frac{\text{Concentration of plasmid (g/µl)}}{\text{copy number}} = \text{molecules/µl}$$

A series of dilutions was made for DNA amplification, generating a standard curve. The CT values were plotted against the logarithm of their initial copy number and led to the copy number of the unknown samples.

3.11.8 Specific gene validation

Numerous genes were chosen for further gene expression analysis and validation by TaqMan real-time quantitative PCR. They were chosen as a result of microarray data combined with broad research of literature. For each gene, a specific set of primers and probe was used. All samples were prepared in triplicates. The obtained data was analyzed by relative quantification as seen above.

3.12 Microarray analysis

Microarray technology is used to detect different levels of gene expression. It is possible to detect the expression levels of several thousand genes with only one experiment (Göhlmann und Talloen 2009). This technology was chosen to determine how an aberrant fusion protein such as DEK/CAN and PML/RARα, influences the level of gene expression in cells.

The Microarray was performed on a gene chip by Affymetrix, USA. The hybridization to the GeneChipMoGene, the washing steps and scanning of the microarray were carried out according to the Affymetrix protocol. The Spotfire software was used to design heatmaps (Spotfire Decision Site 9.1.2, TIBCO Spotfire, USA). The statistical analysis was completed considering the Student's t-distribution with $p \leq 0.05$ as statistically relevant result. GraphPad Prism 5.0 was used to provide the statistical calculations.

The following groups were evaluated in clusters:

DEK/CAN	-	Negative control
PML/RARα	-	Negative control
DEK/CAN and PML/RARα	-	Negative control

3.13 Electrophoretic separation of DNA

DNA electrophoresis was the ideal method to determine the product specificity after PCR by comparing it with the known DNA fragment size. The electric field was used to separate DNA fragments by size. Their velocity of migration depended on fragment size, agarose concentration of the gel and voltage. The electrophoresis was performed with 0,5 – 3 % agarose gels, depending

on the DNA size. Most commonly a 1 % agarose gel was used in this study. The agarose was mixed with 1 x TAE buffer in a glass falcon and dissolved completely by heat in the microwave. When cooled down, to approximately 50 °C, HD green as a fluorescent dye was added to the still liquid gel with a final concentration of 1 µg/ml. The gel was poured into a gel tray and cooled down. The samples were mixed with DNA loading buffer and the electrophoresis was performed in 1 x TAE buffer at 5 V/cm. Afterwards, the gel was placed into UV light (λ=320nm), which visualized the HD green-stained DNA fragments. Based on the DNA marker, DNA fragment length was possible to be determined.

3.14 Workflow summary

Gene expression assays on RNA level can be influenced by various factors. To eliminate any disturbances and aiming for clear results, the following optimized workflow was established in this study.

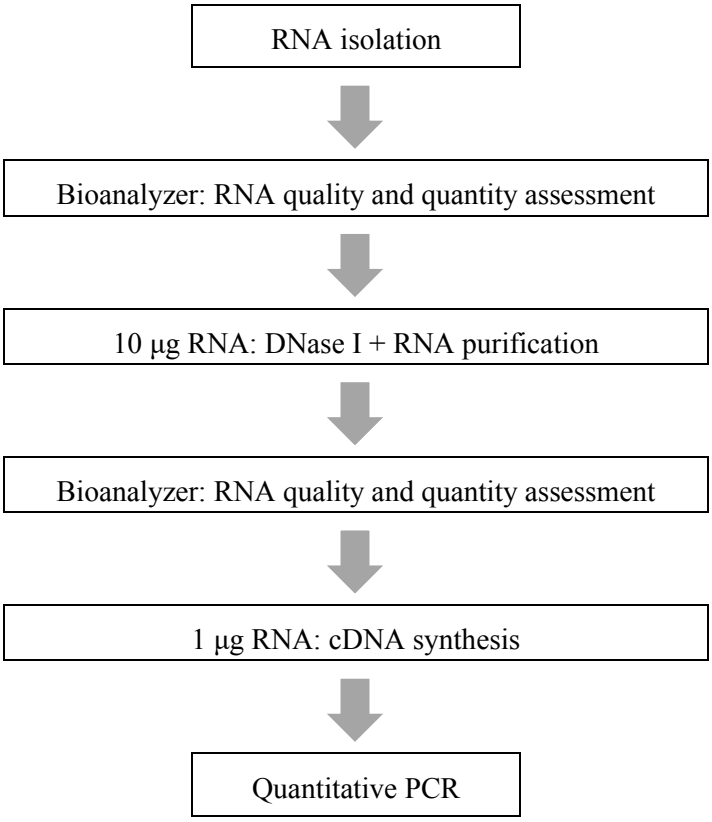

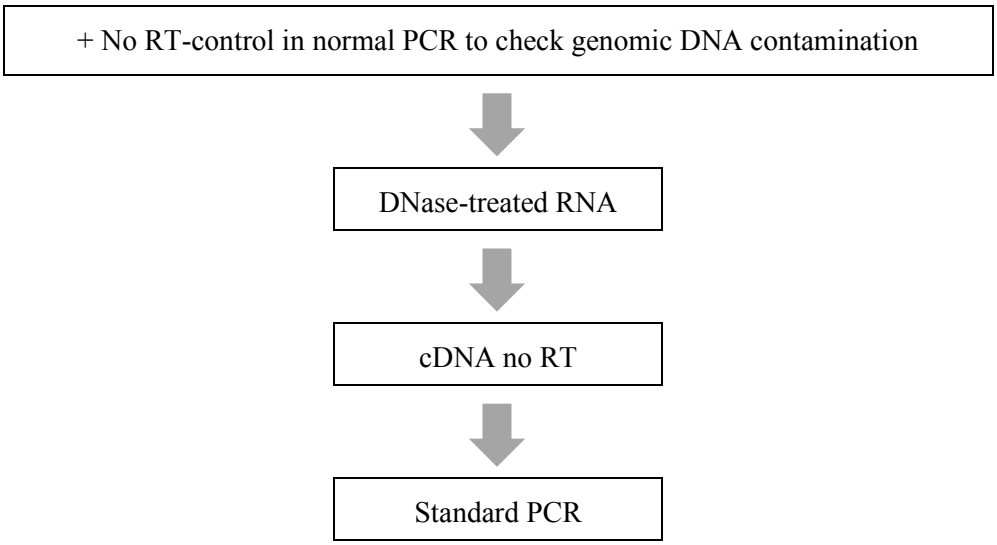
+ No RT-control in normal PCR to check genomic DNA contamination
DNase-treated RNA
cDNA no RT
Standard PCR

4 Results

4.1 The gene product DEK/CAN is detectable by standard PCR

The AML-associated fusion protein DEK/CAN originates from the aberrant chromosomal translocation, t(6;9) DEK/CAN. It is not physiologically present in healthy cells. An important step for further research was the establishment of a reliable method to detect the fusion protein in different cell models. The chosen method was PCR and real-time quantitative PCR which convince with their precise evaluation potential. PCR is one of the most valuable methods in molecular biology. It relies on the knowledge of DNA transcription, RNA translation and finally protein synthesis in the ribosomes. The transcribed messenger RNA reflects the gene expression in a cell as the basic module for protein synthesis (Kornberg 2007). In order to detect the gene sequences which are transcribed, one must analyze the RNA nucleotide sequence. RNA gets isolated from the sample cells and converted to cDNA by reverse transcription. This cDNA then serves as a template for the PCR reaction.

4.1.1 DNase treatment leads to a higher RNA Integrity

The isolated RNA, which was necessary for generating the template for further PCR reactions, was treated with or without DNase, to test its effect on the reduction of genomic DNA contamination. We compared the RNA quality in U937 wildtype (wt) and U937 Pinco-DC (Pinco-DEK/CAN) cells with the Bioanalyzer automated electrophoresis system. The RNA treated with DNase showed a higher RNA Integrity Number (RIN), compared to the non-DNase treated RNA and was therefore established in the workflow of RNA isolation and the subsequent steps of cDNA synthesis. The RIN stands for an algorithm which classifies RNA integrity. It consists of numbers from 1 to 10, selecting 1 to completely degraded RNA and 10 to fully intact RNA (Schroeder et al. 2006). A RIN above 5 is classified as good RNA integrity, a RIN above 8 is considered as perfect total RNA for further experiments (Fleige und Pfaffl 2006b). The mean RIN from DNase treated RNA of all the experiments in this work always remained between 8 to 10.

The Bioanalyzer electropherograms showed a higher degradation level of untreated RNA samples, as shown in Figure 8. The visual information of Bioanalyzer measurement corresponded to a

reduction of the fluorescence signal of the two ribosomal 18S and 28S bands of RNA, as well as elevated baseline signal intensities, among others. The RNA concentration was not relevantly reduced by DNase treatment.

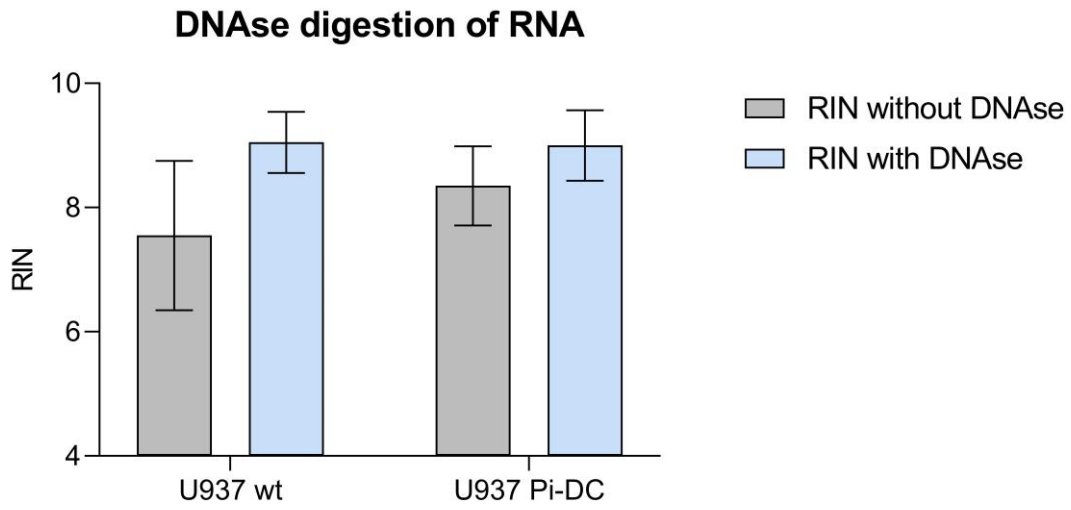

Figure 8: Influence of DNase digestion on RNA integrity
Isolated RNA from U937 Pi-DC (Pinco-DEK/CAN) and U937 wt (wildtype) cells were either treated with DNase digestion or without. The RNA Integrity Number (RIN), measured by Bioanalyzer electrophoresis, was higher in DNase-treated RNA. The shown RIN consists of the mean of triplicate measurements.

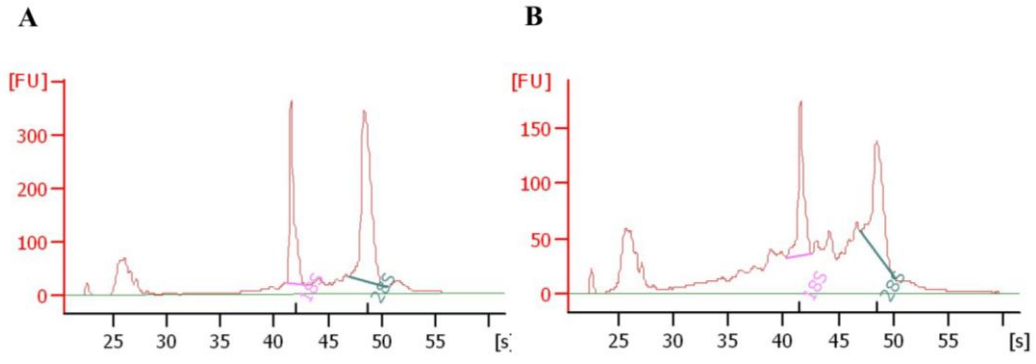

Figure 9: Electropherograms for RIN classification
The measurement shows RNA that was isolated from U937 wildtype (wt) cells. It was either treated with DNase (A) or without DNase (B). The RIN was higher in the DNase treated sample with the number 9,4 (A) and lower in the non-treated sample with the number 6,7 (B). The plotted curves show the 28S/18S rRNA-Ratio.

4.1.2 Specifity of primer and probe sequences

Specific primers and probes were designed to detect the sequence for the fusion protein DEK/CAN, as shown in Table 6. The gene of interest was amplified by standard PCR in Phoenix eco cells, transfected with the constructs Mock, an empty vector as a negative control, and a vector encoding the target gene DEK/CAN (Phoenix Paco-DC). A plasmid with the fusion transcript of interest Pinco-HA-DC served as a positive control. The visualization of the PCR product in gel electrophoresis confirmed the right size of the reference gene GAPDH amplificon with 157 base pairs and the DEK/CAN amplificon with 212 base pairs as shown in Figure 10. The negative control samples did not demonstrate a DNA band. An additional quality control was obtained by examining all primers and probes without Reverse Transcriptase (RT) in cDNA synthesis, to rule out contamination or non-specific products in the PCR reaction. The no RT samples did not show a DNA band. In conclusion, it was shown that the primer pairs were highly specific to the target genes and did not produce non-specific amplicons.

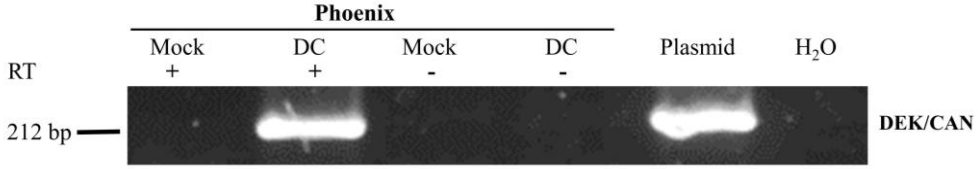

Figure 10: The DEK/CAN fusion product amplified by standard PCR
Gel electrophoresis shows the amplification of the DEK/CAN (DC) gene product in transfected Phoenix cells. No RT samples were used as negative control. The plasmid Pinco-HA-DC served as a positive control.

4.2 A real-time quantitative PCR (qPCR) system was established to detect and quantify the fusion protein DEK/CAN

The aim of this work was to detect the t(6;9) associated fusion protein DEK/CAN and characterize its genetic expression profile to get an insight into the mechanisms of DEK/CAN-induced leukemogenesis. Emphasis has been put on working with real-time quantitative PCR (qPCR) because of its ability to quantify the amplified PCR product by a direct measurement of a fluorescent dye which is linked to the PCR product. This molecular biological method was a

valuable technique to gain further understanding of the altered molecular mechanisms of DNA transcription, RNA translation and changes in gene expression in DEK/CAN-positive cells.

The chosen TaqMan primers and probes for DEK/CAN and the house-keeping-gene GAPDH were tested under different conditions and were optimized to obtain the maximum efficiency of the PCR reaction.

4.2.1 Primer and probe optimization

Real-time quantitative PCR was performed with various primer and probe combinations as shown in Table 3. The data was generated with a positive and negative control and was held in triplicates. The CT values consist of the mean of triplicate measurement for each subunit. The cDNA template was synthesized from purified RNA, acquired from Phoenix Eco cells, containing the transfected constructs Paco-empty and Paco-HA-DC, as well as a plasmid which contained the construct Pinco-HA-DC. DC stands for the fusion protein DEK/CAN.

GAPDH:

Primer conc	Probe conc	CT Phx Paco-empty	CT Phx Paco-HA-DC
100 nM / 100 nM	100 nM	17,66	19,1
300 nM / 300 nM	100 nM	18,24	18,73
300 nM / 300 nM	200 nM	17,49	18,69
900 nM / 900 nM	200 nM	18,09	19,02

DEK/CAN:

Primer conc	Probe conc	CT Phx Paco-empty	CT Phx Paco-HA-DC	Plasmid
100 nM / 100 nM	100 nM	N/A	20,25	9,04
300 nM / 300 nM	100 nM	N/A	20,13	7,57
300 nM / 300 nM	200 nM	N/A	20,22	8,15
900 nM / 900 nM	200 nM	N/A	19,58	7,69

Table 9: Primer and probe optimization for GAPDH and DEK/CAN
This table shows CT values derived from amplification plots with four different primer and probe concentrations and combinations for both GAPDH and DEK/CAN. Conc = concentration; N/A = non detects.

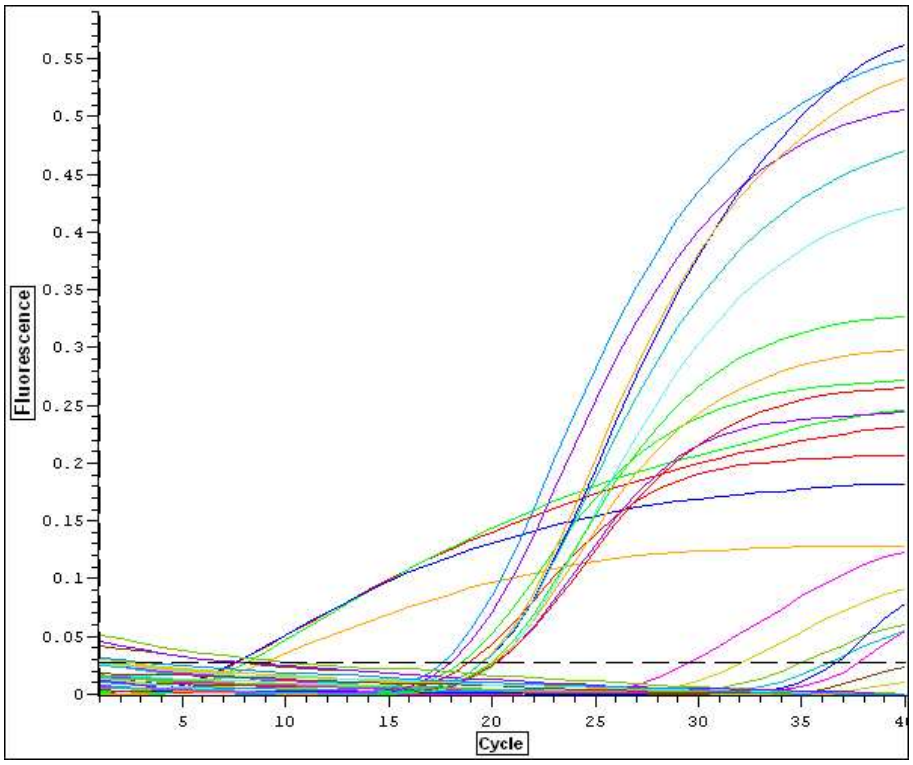

Figure 11: Amplification plots of primer concentration combinations for GAPDH and DEK/CAN
The amplification plots for the various primer and probe concentration combinations from the data of table 3 are visualized in this figure. The fluorescence of the TaqMan reaction **(Fluorescence)** is illustrated along with the number of cycles **(cycle)** that have been run in the qPCR reaction. The Cycle threshold (CT) value represents the point in time, in which the fluorescent signal crosses the threshold of the background fluorescence level and shows a stable measurement of the fluorescent signal.

The Primer and probe concentrations with the highest fluorescence and lowest CT value were chosen. This was accomplished for the combination of 300 nM primers and 200 nM probe for GAPDH and 300 nM primers and 100 nM probe for DEK/CAN. Further experiments were carried out with these optimized concentrations.

4.2.2 Generation of standard curves

The baseline for further calculations such as relative or absolute quantification as well as the calculation of qPCR efficiency was the creation of a standard curve for each target gene with their corresponding primers and probe. The synthesized cDNA was used from purified RNA from Phoenix Eco cells, containing an empty vector (Phoenix Paco-empty) and a vector for the target gene DEK/CAN (Phoenix Paco-DC). Additionally, the cDNA of the Plasmid Pinco-HA-DC was used as a positive control. Standard curves for human GAPDH and DEK/CAN were created by a

7-fold dilution series of the different cDNA templates. Another standard curve for mouse GAPDH was generated, using cDNA of purified RNA obtained from spleen cells of DEK/CAN-induced leukemic mice. The standard curves are shown in Figure 12, Figure 13 and Figure 14, presenting the CT value along with the cDNA dilution. Dilution 7 stands for the undiluted sample and 1 is the highest dilution.

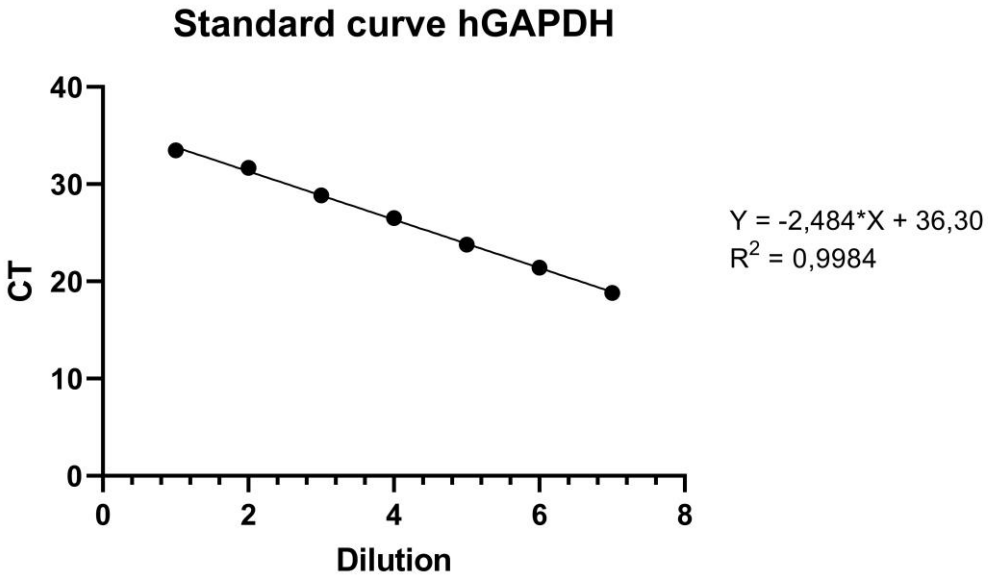

Figure 12: Standard curve for human GAPDH
This standard curve was constructed with 7-fold serial dilutions of Phoenix Paco-empty cDNA. The dilutions are shown along with their CT values. A reverse linear correlation is shown with a slope (Y) of – 2,484. The correlation coefficient (R^2) is 0,9984, indicating an accurate quantification of DNA product. Each point on the graph symbolizes a triplicate measurement of each subunit.

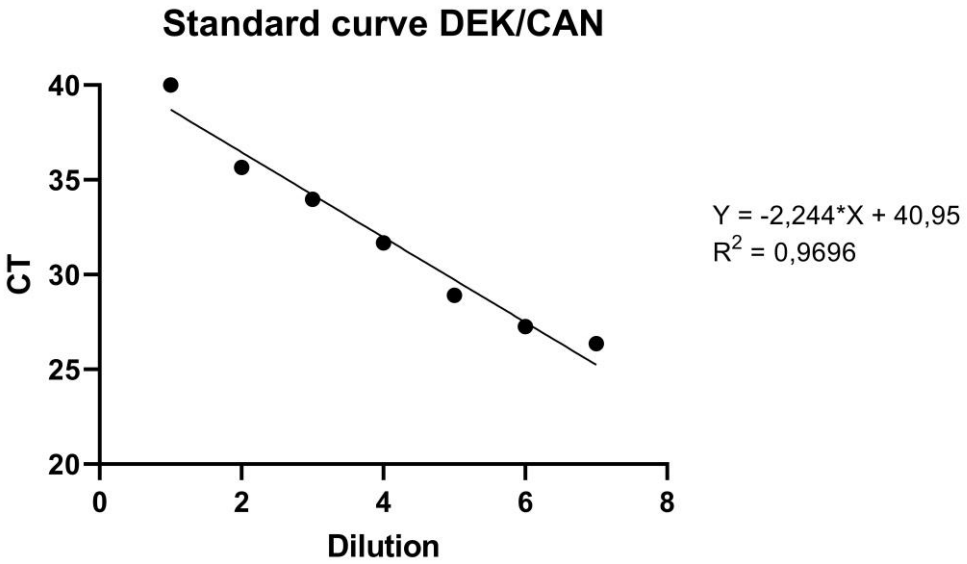

Figure 13: Standard curve for DEK/CAN
This standard curve was constructed with 7-fold serial dilutions of Phoenix Paco-DC cDNA. The dilutions are shown along with their CT values. Dilution 7 is the undiluted sample, dilution 1 is the highest diluted sample. A reverse linear correlation is shown with a slope (Y) of – 2,244. The correlation coefficient (R^2) is 0,9696, indicating an accurate quantification of DNA product. Each point on the graph symbolizes a triplicate measurement of each subunit.

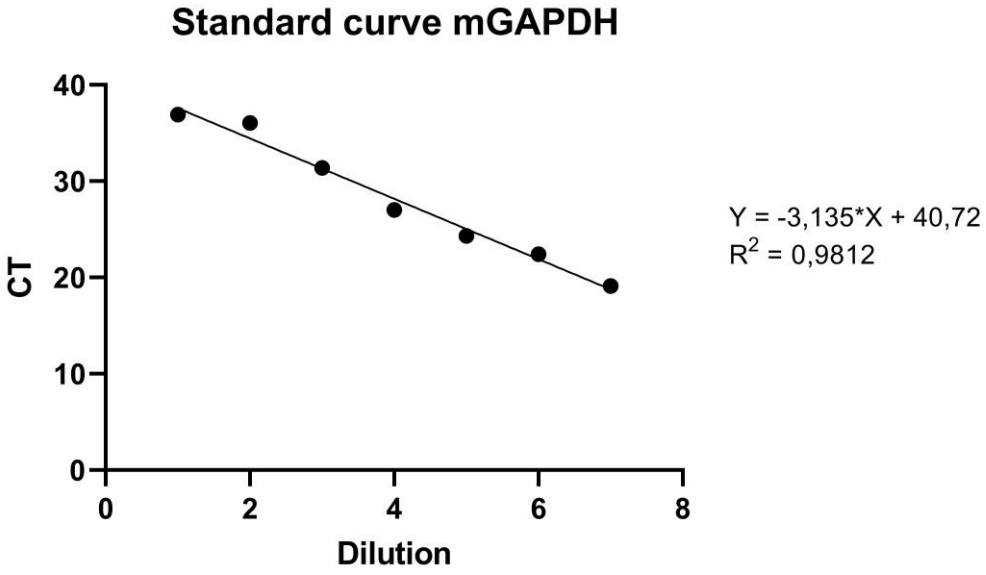

Figure 14: Standard curve for mouse GAPDH
This standard curve was constructed with 7-fold serial dilutions of Spleen Paco-empty cDNA. The dilutions are shown along with their CT values. Dilution 7 is the undiluted sample, dilution 1 is the highest diluted sample. A reverse linear correlation is shown with a slope (Y) of – 3,135. The correlation coefficient (R^2) is 0,9812, indicating an accurate quantification of DNA product. Each point on the graph symbolizes a triplicate measurement of each subunit.

The specificity of PCR products was confirmed by DNA gel electrophoresis and ethidium bromide staining (Figure 15, Gangisetty und Reddy 2009). The standard curves allowed the calculation of qPCR efficiency and relative quantification as described below.

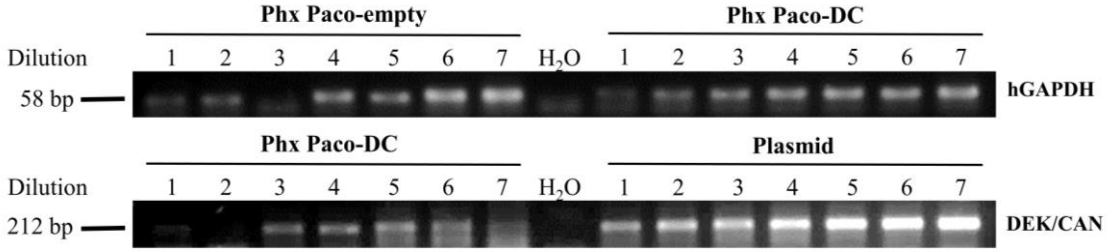

Figure 15: PCR products of human GAPDH and DEK/CAN in a dilution series
Gel electrophoresis of PCR products of human GAPDH and DEK/CAN in a 7-fold dilution series. Quantity of the PCR amplicon is indirectly shown by the intensity of the DNA band. The reference gene human GAPDH is represented by am amplificon with 58 bp and the fusion protein DEK/CAN by an amplificon with 212 bp.

4.2.3 Calculation of the efficiency of qPCR

Based on these shown standard curves for human GAPDH, mouse GAPDH and DEK/CAN gene amplification, the efficiency could be calculated by referring to the slope of each curve. Respecting the slope of each standard curve, the calculation succeeded as follows:

Human GAPDH

$E = 10^{(-1/slope)} = 10^{(-1/-2,484)} = 2,52683271$

DEK/CAN

$E = 10^{(-1/slope)} = 10^{(-1/-2,244)} = 2,79018371$

Mouse GAPDH

$E = 10^{(-1/slope)} = 10^{(-1/-3,135)} = 2,08439137$

An efficiency of 2 indicates an efficiency of 100 %, representing a doubling of PCR amplification product in each cycle. Assuming a doubling every cycle, the slope of the standard curve would be at – 3,3, leading to a 10-fold increase in DNA template every 3,3 cycles. In the shown calculations, all the efficiency measurements were above 100 %, which would theoretically not be possible. Previous studies have shown that the efficiency calculation may cause too good results, assuming an achieved efficiency of 100 % (Pfaffl 2001). For all further calculations, an 100 % efficiency with a slope of 2 was presumed.

4.2.4 Relative quantification

Relative quantification of a qPCR product required a non-regulated endogenous reference gene, which was normalized to the target gene expression. The reference gene GAPDH was chosen. The CT values of GAPDH were similar throughout the qPCR experiments, demonstrating a good quality and quantity of the extracted RNA.

The utilized calculations for relative quantification were applied for the experiments and will be presented in the following steps. cDNA was retrieved from purified RNA from Phoenix Paco-empty cells (control) and Phoenix Paco-HA-DC cells (sample). All samples were measured in triplicates, using the calculated mean value for further analysis. The qPCR optimization and efficiency calculation for these specific PCR reactions have been applied, as presented above.

		GAPDH	DC
Phx Paco-empty	Control	18,87	N/A = 40
Phx Paco-HA-DC	Sample	17,88	31,75

Table 10: Quantitative real-time PCR CT results of target gene (DC) and reference gene (GAPDH)
This table shows the results of qPCR in CT values of reference gene amplification (GAPDH) and target gene amplification (DC) in a control template (Phx Paco-empty) and in a sample (treated) template (Phx Paco-HA-DC). The CT values are the mean of sample triplicates. The non-detection of DEK/CAN in the negative control is interpreted as 40 because of 40 cycles of PCR reactions without crossing the threshold.

The calculation for the relative gene expression ratio, involving efficiency correction, was given by the following equation (Meuer et al. 2001).

$$\text{Ratio} = \frac{(E_{\text{target}})^{\Delta\ CT_{\text{target}}\ (\text{MEAN control}-\text{MEAN sample})}}{(E_{\text{reference}})^{\Delta\ CT_{\text{reference}}\ (\text{MEAN control}-\text{MEAN sample})}}$$

Referring to the Comparative CT method (Livak und Schmittgen 2001) and combining it with the efficiency correction, the gene expression ratio of the samples in Table 10 was calculated in the following steps:

$\Delta CT_{\text{reference}}$ = (CT GAPDH control - CT GAPDH sample)

= 18,87 - 17,88 = 0,99

$\Delta CT_{\text{target}}$ = (CT DC control - CT DC sample)

= 40 - 31,75 = 8,25

Fold change reference gene GAPDH = $(\text{efficiency})^{\Delta CT\ \text{reference}}$

$= (2)^{18,87-17,88} = (2)^{0,99} = 1,99$

Fold change target gene DC = $(\text{efficiency})^{\Delta CT\ \text{target}}$

$= (2)^{40-31,75} = (2)^{8,25} = 304,44$

$$\text{Relative expression ratio} = \frac{\text{Fold change target gene DC}}{\text{Fold change reference gene GAPDH}}$$

$$= \frac{304,44}{1,99} = 152,984925 \approx 153$$

When applying this calculated result to our gene of interest, it is shown that the target gene DEK/CAN is amplified with a fold change of 153 in samples containing the target gene, compared

to the control sample. To identify the exact copy number of DNA molecules, the absolute quantification was performed.

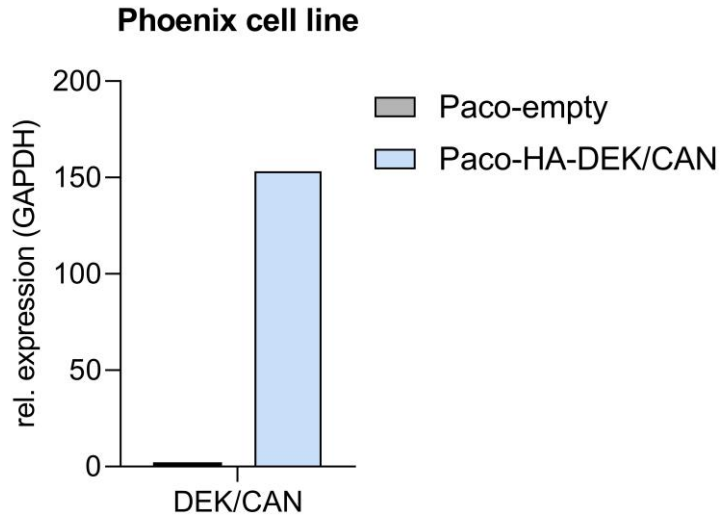

Figure 16: The fold change in gene expression of DEK/CAN in Phoenix cells
The relative expression ratio of the DEK/CAN expression is 153. The negative control is Phoenix Paco empty with the equation 1.

4.2.5 Absolute quantification

Absolute quantification was performed with a known size and concentration of a DNA template. In this case the linearized plasmid Pinco-HA-DC-GWB was used with its size of 18039 base pairs and a concentration of 0,041 µg/µl. A 10-fold dilution series was performed in triplicates of each dilution by TaqMan quantitative real-time PCR with the specific primers and probe for the target DEK/CAN. The dilution series with its measured CT values created a standard curve by linear regression through these points.

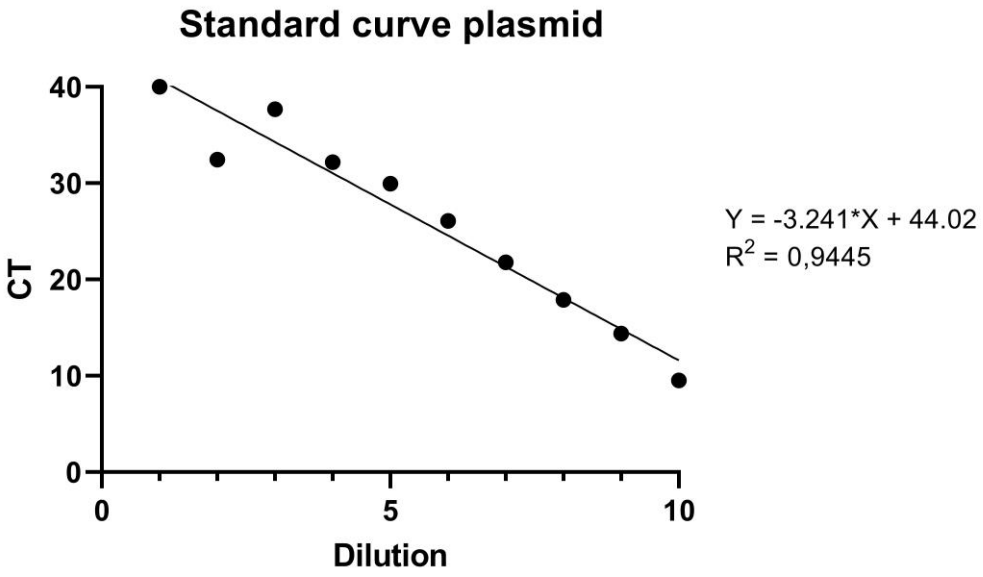

Figure 17: Standard curve for absolute quantification
This standard curve was created with a 10-fold serial dilution of the linearized plasmid Pinco-HA-DC-GWB. The dilutions are shown against their CT values. The dilutions ranged from 5 x 10^{-1} (dilution 1) to 5 x 10^{8} (dilution 10) copies/µl. Dilution 10 is the undiluted sample, dilution 1 is the highest diluted sample. A reverse linear correlation is shown with a slope (Y) of – 3,241. The correlation coefficient (R^2) is 0,9445, indicating an accurate quantification of DNA product. Each point on the graph symbolizes a triplicate measurement of each subunit.

The generated standard curve now served as normalization for absolute quantification by calculating the exact copy number of the DEK/CAN template.

In absolute quantification, the exact DNA copy number was computed by analyzing linearized plasmid DNA, which contained the fusion transcript DEK/CAN. A standard curve was created for qPCR by performing a serial dilution assay of the plasmid DNA. Knowing the exact size of the plasmid in base pairs led to the number of grams per molecule, also known as copy number. The following calculations were executed to determine the copy number of the plasmid (Whelan et al. 2003):

$$\text{Weight in Dalton } (\text{g/mol}) = (\text{Bp size plasmid} + \text{insert}) \text{ x } (330 \text{ Dalton x } 2 \text{ nucleotides/bp})$$

$$\text{Copy number} = \text{g/molecule} = \frac{\text{Weight in Dalton (g/mol)}}{\text{Avogadro's number } 6{,}02214199 \text{ x } 10^{23}}$$

Knowing the copy number and the concentration of the plasmid that is added to each PCR reaction, the precise number of molecules in that reaction was determined as follows:

Concentration of plasmid (g/µl) / copy number = molecules/µl

A series of dilutions was made for DNA amplification, generating a standard curve. The CT values were plotted against the logarithm of their initial template copy numbers and the copy number of the unknown samples can then be derived.

Plasmid: Pinco-HA-DC-GWB

Size: 18039 bp

Concentration: 0,041 µg/µl = 41 ng/µl

Weight in Dalton (g/mol) = (Bp size plasmid + insert) x (330 Dalton x 2 nucleotides/bp)

= 18039 bp x (330 Dalton x 2 nucleotides/bp)

= 11 905 740 g/mol

$$\text{Copy number} = \text{g/molecule} = \frac{\text{Weight in Dalton (g/mol)}}{\text{Avogadro's number } 6{,}02214199 \text{ x } 10^{23}}$$

$$= \frac{11905740 \text{ g/mol}}{\text{Avogadro's number } 6{,}02214199 \text{ x } 10^{23}}$$

$$= 1976994 \text{ x } 10^{-23}$$

$$= 19{,}76994 \text{ x } 10^{-18}$$

The copy number for this plasmid was 19,76994 x 10^{-18} g/molecule. Having calculated this number, the precise number of molecules in the reaction can be determined by knowing the concentration of the plasmid.

$$\frac{\text{Concentration of plasmid (g/µl)}}{\text{copy number}} = \text{molecules/µl}$$

$$\frac{4{,}1 \text{ x } 10^{-8} \text{ g/µl}}{19{,}76994 \text{ x } 10^{-18}} = 0{,}2 \text{ x } 10^{10} \text{ molecules/µl}$$

Each qPCR was performed with 5 µl of template in a 20-fold dilution of plasmid. Considering these changes, the copy number of the undiluted sample (dilution 10) was calculated as follows.

$$\frac{0{,}2 \text{ x } 10^{10} \text{ molecules/µl}}{20} = 0{,}01 \text{ x } 10^{10} \text{ molecules/µl}$$

$$0{,}01 \text{ x } 10^{10} \text{molecules/µl x } 5 = 5 \text{ x } 10^{8} \text{ molecules/µl}$$

The exact number of molecules in a µl of plasmid solution, containing the DEK/CAN template, was 5 x 10^8 molecules/µl in the undiluted sample (dilution 10). By generating a standard curve with serial dilutions, the copy number of an unknown sample can be derived. In this case, DEK/CAN was able to be detected at a minimum of 50 molecules/µl by qPCR. This represents a 10^{-7} dilution of our template DEK/CAN. The dilution from 10^{-6} to 10^{-7} demonstrates a good quality amplification of the gene template with reproducible CT values. Consequently, the reproducible sensitivity is 10^{-6} and the maximal sensitivity is 10^{-7}.

Molecules/µl	Dilution	CT value
5×10^{-1}	$1 = 10^{-9}$	N/A
5×10^{0}	$2 = 10^{-8}$	N/A
5×10^{1}	$3 = 10^{-7}$	37,68
5×10^{2}	$4 = 10^{-6}$	32,19
5×10^{3}	$5 = 10^{-5}$	29,96
5×10^{4}	$6 = 10^{-4}$	26,07
5×10^{5}	$7 = 10^{-3}$	21,77
5×10^{6}	$8 = 10^{-2}$	17,89
5×10^{7}	$9 = 10^{-1}$	14,38
5×10^{8}	$10 = 1$	9,53

Table 11: Absolute quantification of DEK/CAN by copy number calculations
Exact quantification of the fusion protein DEK/CAN in a 10-folg serial dilution assay. Dilution 10 is the undiluted sample, dilution 1 is the highest diluted sample. The fusion product DEK/CAN was detected in a range from 5×10^{8} to a minimum of 5×10^{1} molecules/µl by qPCR. The maximal detection of DEK/CAN was shown in the 10^{-7} dilution. N/A: non detectable.

4.2.6 Minimal residual disease diagnostics for DEK/CAN

Absolute quantification can be used as a diagnostic method in leukemic patients. The detection of the fusion protein DEK/CAN by qPCR can help to monitor the minimal residual disease (MRD) in an early stage during treatment and remission in t(6;9)-positive AML (Lindern et al. 1992). The developed qPCR method in this work was able to detect the quantity of the DEK/CAN fusion protein at a minimum of 50 molecules of the DEK/CAN transcript/µl. This represents an amplicon dilution and a maximal detection sensitivity of 10^{-7}. This diagnostic tool has a high relevance beside the standard diagnostic tools such as cytology and Fluorescence Activated Cell Sorting (FACS) because of its superior sensitivity. The molecular changes in AML relapse can be detected much earlier than showing the cytologic presence of leukemic blasts in the bone marrow. It should therefore always be used together with the standard diagnostics.

4.3 DEK/CAN is detectable in transfected Phoenix, FKH-1 and 32D cell lines by qPCR

The established workflow for qPCR was used to amplify the fusion product DEK/CAN in different cell lines. Detection of DEK/CAN worked in Phoenix cells with the retrovirally transduced vector Paco-HA-DC, the DEK/CAN expressing cell line FKH-1 as well as 32D cells, transfected with the vector Pinco-HA-DC. The quality of the PCR reaction was verified by DNA gel electrophoresis and ethidium bromide staining. PCR reaction without Reverse Transcriptase (RT) was used as an additional negative control, as shown Figure 19.

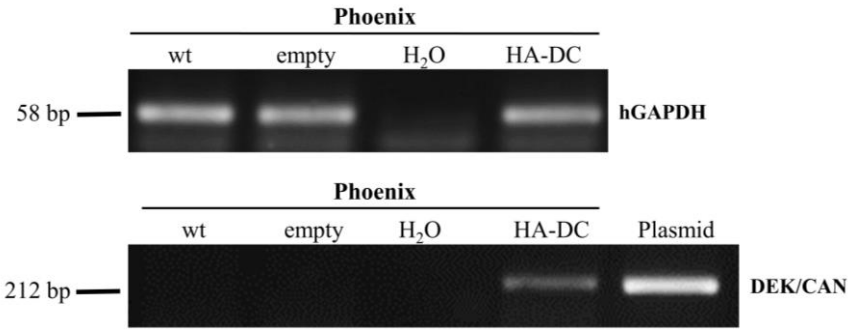

Figure 18: Gel electrophoresis of PCR products of human GAPDH and DEK/CAN
Quantitative real-time PCR with specific primers and probe amplificated the reference gene human GAPDH and the gene of interest DEK/CAN. The cDNA of Phoenix Eco cells wild type (wt) and Phoenix Eco transfected with the vectors Paco-empty and Paco-HA-DC were used. The plasmid Pinco-HA-DC-GWB was used as a positive control for DEK/CAN amplification. A single band was detected near the expected size for both amplificons, comparing it to the DNA marker indicating DNA size in base pairs. No band was detected in the PCR products of negative control samples without template DNA for DEK/CAN.

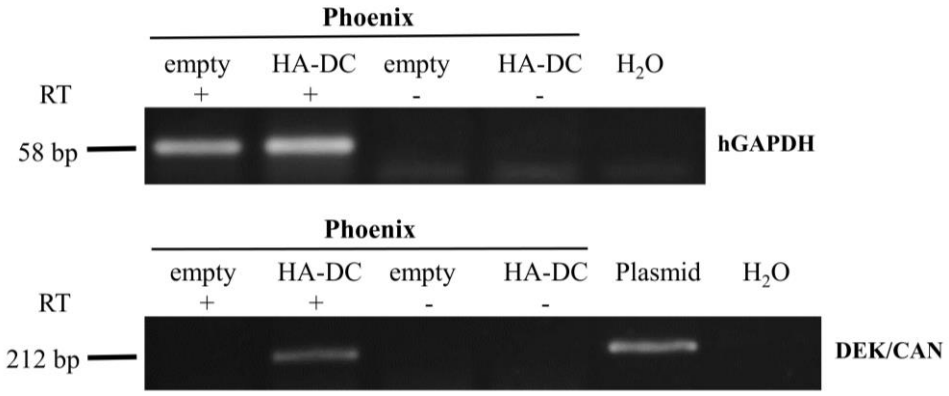

Figure 19: Gel electrophoresis of PCR products of human GAPDH and DEK/CAN with no RT control
Quantitative real-time PCR product from specific primers and probe for human GAPDH and DEK/CAN as shown in figure 2. Template of cDNA were obtained from Phoenix cells, transfected with the constructs Paco-empty and Paco-HA-DC. The plasmid Paco-HA-DC-GWB was used as a positive control for DEK/CAN amplification. In this plot, synthesis of cDNA without Reverse Transcriptase (RT) was used as a negative control. (+) indicates cDNA synthesis with RT and (-) indicates a cDNA synthesis without RT. No band were detected in the (-) RT samples.

The relative expression ratio of the DEK/CAN fusion product was calculated in DEK/CAN-positive Phoenix, 32D and FKH-1 cell lines. The human FKH-1 cell line shows a fold change of 1884 in DEK/CAN expression in comparison with the negative control. The fold change in DEK/CAN-transfected Phoenix cells was 302 and 1355130 in the DEK/CAN-transfected murine 32D cell line.

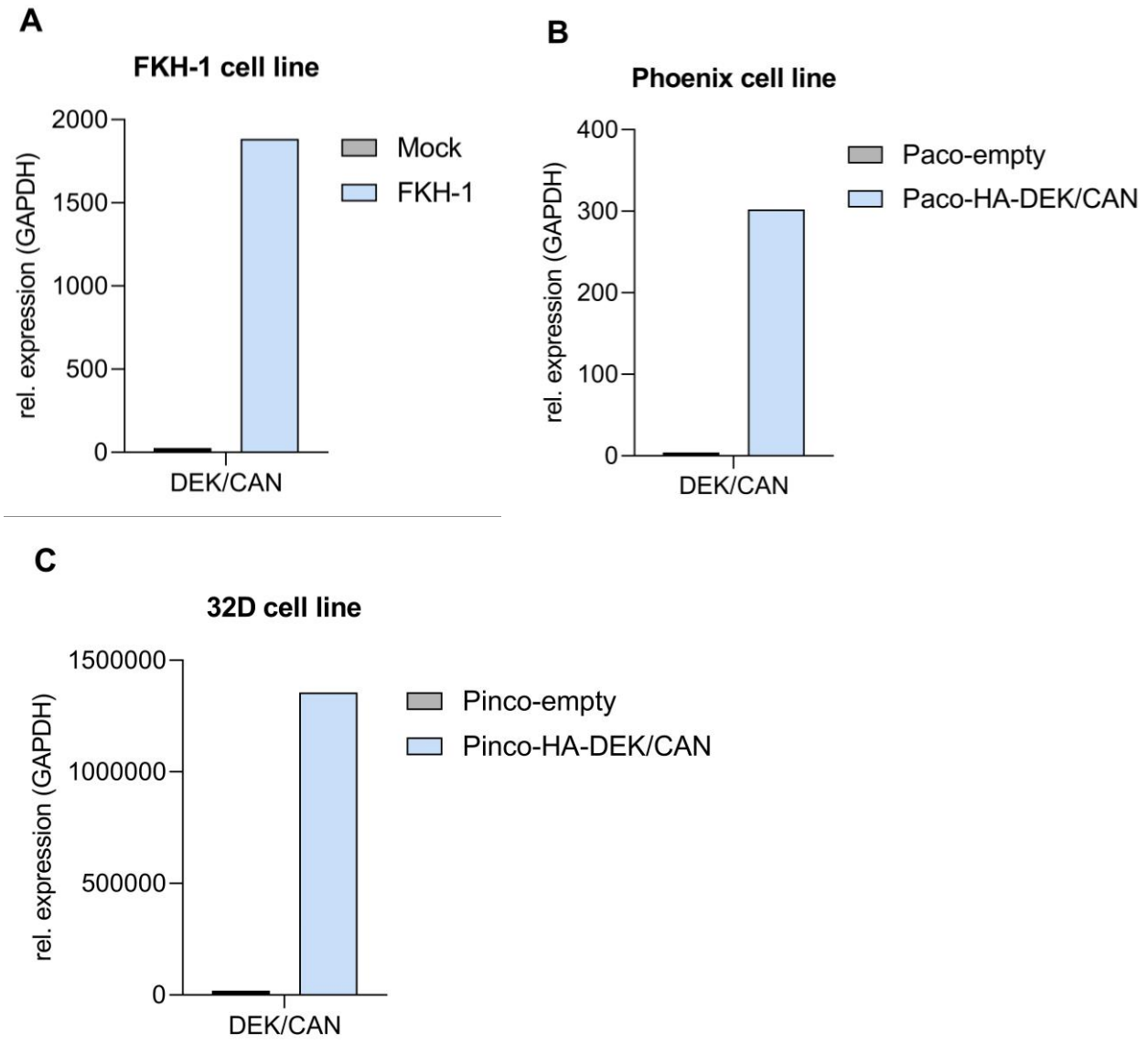

Figure 20: Relative expression ratio of the fusion product DEK/CAN in Phoenix, FKH-1 and 32 D cell lines
These figures show the relative expression ratio of the fusion product DEK/CAN by qPCR in different cell lines. **A** shows a fold change of 1884 in the human FKH-1 cell line. **B** shows a fold change of 302 in DEK/CAN-transfected Phoenix cells. **C** shows a fold change of 1355130 in the DEK/CAN-transfected murine 32D cell line.

Real-time quantitative PCR was also performed with spleen cells from CFU-S12 assays. Although the RNA integrity and the CT values for the house keeping gene GAPDH were ideal, DEK/CAN was not able to be amplified in the samples.

4.4 DEK/CAN´s influence on gene expression in hematopoietic cells

Now that the fusion protein DEK/CAN was able to be detected in different cell lines, further analysis was performed to understand the molecular mechanisms of DEK/CAN and its possible ways to induce and maintain AML. A gene expression profiling experiment was performed to examine the expression level of thousands of genes in the murine genome in DEK/CAN-positive cells. This led to the identification of genes, which show a change in their expression level in presence or in absence of DEK/CAN in the cells. The experiment was also performed with the fusion product PML/RARα, as a comparison of a well characterized leukemia-associated fusion protein.

Previous work has shown that DEK/CAN induces leukemogenesis in an early subset of hematopoietic stem cells (LT-HSCs) (Oancea et al. 2010). Therefore, we decided to use early hematopoietic Sca^{+}/Lin^{-} cells which were isolated from the bone marrow of C57BL/6 mice. These cells were then retrovirally transduced with an empty vector Pinco and with the constructs DEK/CAN and PML/RARα. After successful transfection, the RNA was isolated and the complementary DNA was synthesized. This cDNA served as the template for Bio-Chip Microarray gene expression analysis in the murine genome.

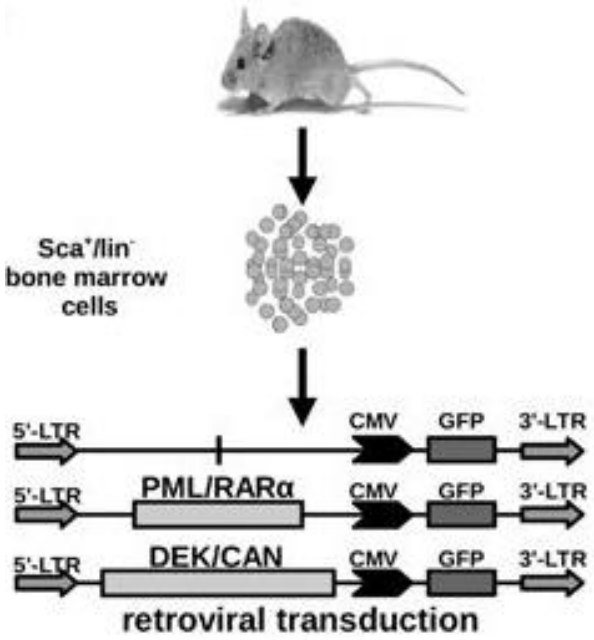

Figure 21: Sca+/Lin- bone marrow cells were transfected with the constructs PML/RARα and DEK/CAN
Sca+/Lin- cells were isolated from C57Bl/6 mice. The fusion products PML/RARα and DEK/CAN were retrovirally transduced in the murine bone marrow cells. An empty vector served as a negative control. All constructs had a GFP (green fluorescent protein) staining sequence (Oancea et al. 2010).

4.4.1 Bio-Chip Microarray analysis

The resulting data was analyzed relating to changes in gene expression, considering the student's t-distribution with $p \leq 0.05$ as a statistically relevant result. The data was collected in clusters, comparing genes that showed either an increase or decrease of their expression levels in presence or absence of DEK/CAN and PML/RARα. After extended research in literature data bases such as Pubmed and Affymetrix NetAffx™ Analysis Center, a further selection and subclassification of genes into certain functions of a cell, were made. The selection based on highly significant genes, involved in transcriptional regulations, cellular signaling pathways, apoptosis, cell proliferation, leukemogenesis, self-renewal and stem cell activity. The selected genes were evaluated considering either the single presence of DEK/CAN or PML/RARα as well as the relevant expression changes in presence of both fusion proteins compared to the empty vector. A selection of the identified genes is shown Figure 22.

An increased gene expression in both DEK/CAN and PML/RARα-positive cells was detected for the genes TRIM25, MBTD1, XPO1, HIF1α, ATF2, ZFP292, ZFP322A, PTP4A1, CCN1 and NDRG1. A decreased gene expression was seen in the genes SCNM1 and PTPRC. DEK/CAN alone, compared to a negative control, showed an increased gene expression for SMEK2, CASP8 and ARF4. PLM/RARα alone, compared to a negative control, showed an increased gene expression for the genes PLEK, CASP4, ASXL1, PLK1, PTP4A3, HDAC5 and MCL1. The genes PIM1 and CSFLR were downregulated. The maximum fold change in all samples ranged from 3,1 to -5,5.

The high expression of the transcription factors TRIM25 and HIF1α, with a fold change of 2,4 and 1,8, are mentionable. Additionally, the downregulation of PTPRC, which encodes the cluster of differentiation CD45, is an interesting observation, since it plays a big role in regulation signaling cascades as a tyrosine phosphatase. The gained results were now further selected and validated by qPCR.

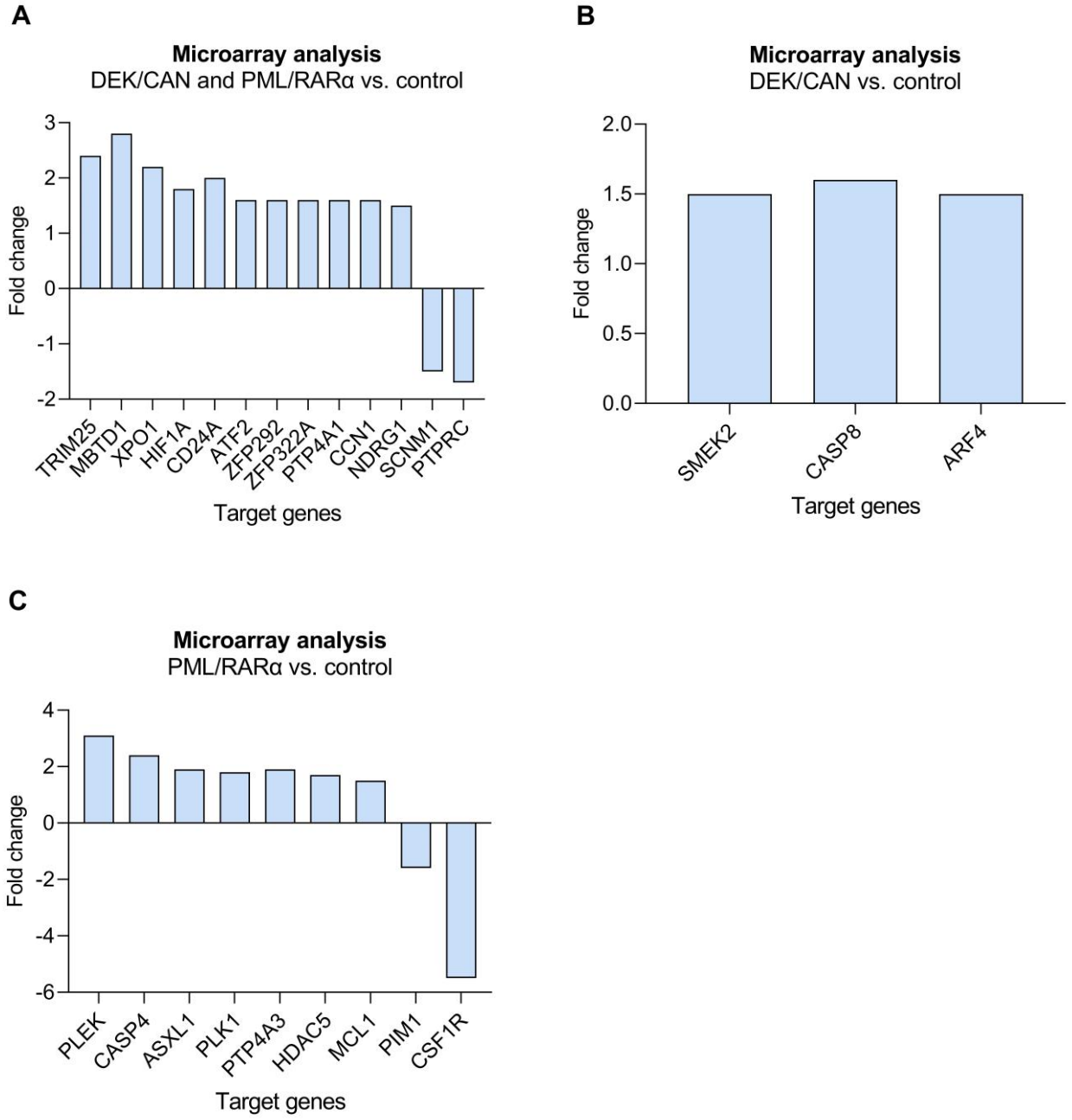

Figure 22: Relative gene expression ratio in DEK/CAN and PML/RARα transfected murine HSC
This figure demonstrates the altered gene expression profile, analyzed by a Bio-Chip microarray, in DEK/CAN and PML/RARα transfected Sca+ li- murine HSC. The fold change indicates the relative gene expression ratio of the selected genes. **A** shows the altered gene expression profile in both DEK/CAN and PML/RARα, whereas **B** shows the profile in only DEK/CAN and **C** in only PML/RARα-positive HSCs. The empty vector Pinco served as a negative control.

4.4.2 Validation of the Bio-Chip Microarray by real-time quantitative PCR

As shown in the previous chapters, we were able to detect the fusion product DEK/CAN by standard PCR and qPCR in different cell lines. The next step was validating the acquired data from the microarray by qPCR. Sixteen of the most significant and relevant genes were selected and analyzed by qPCR, relying on the established workflow as described above. The measurements were performed in triplicates with a positive and negative control. The validation was done with the murine, IL-3 dependent cell line 32D. We used 32D cells with a stable expression of the transfected vector Pinco-empty and the fusion transcripts Pinco-HA-DEK/CAN and Pinco-PML/RARα.

The expression level changes were normalized to the non-regulating house keeping gene GAPDH. This reduced the variance of potential biases and assured a good quality of the synthesized cDNA template. The results were analyzed, using the $2^{-\Delta\Delta CT}$ method (Livak und Schmittgen 2001) and the efficiency calculation as described above (Pfaffl 2001).

The results of the analysis revealed interesting changes in the gene expression profile in DEK/CAN- positive 32D cells shown Figure 23, matching the results of the microarray data. In presence of the DEK/CAN construct, an increased level of gene expression was observed for the genes TRIM25, XPO1, HIF1α, ATF2, CASP8, ASXL1, PTP4A3, PIM1, CSF1R and LMO2. A decrease of gene expression was observed for PTPRC, MBTD1, NDRG1, SMEK2, ARF4 and CASP4 in the same cells. There were some differences in the gene expression profile in presence of the PML/RARα construct. The genes PTPRC, MBTD1, NDRG1, SMEK2, ARF4 and CASP4 showed a contrary negative or positive expression level, compared to DEK/CAN-positive 32D cells.

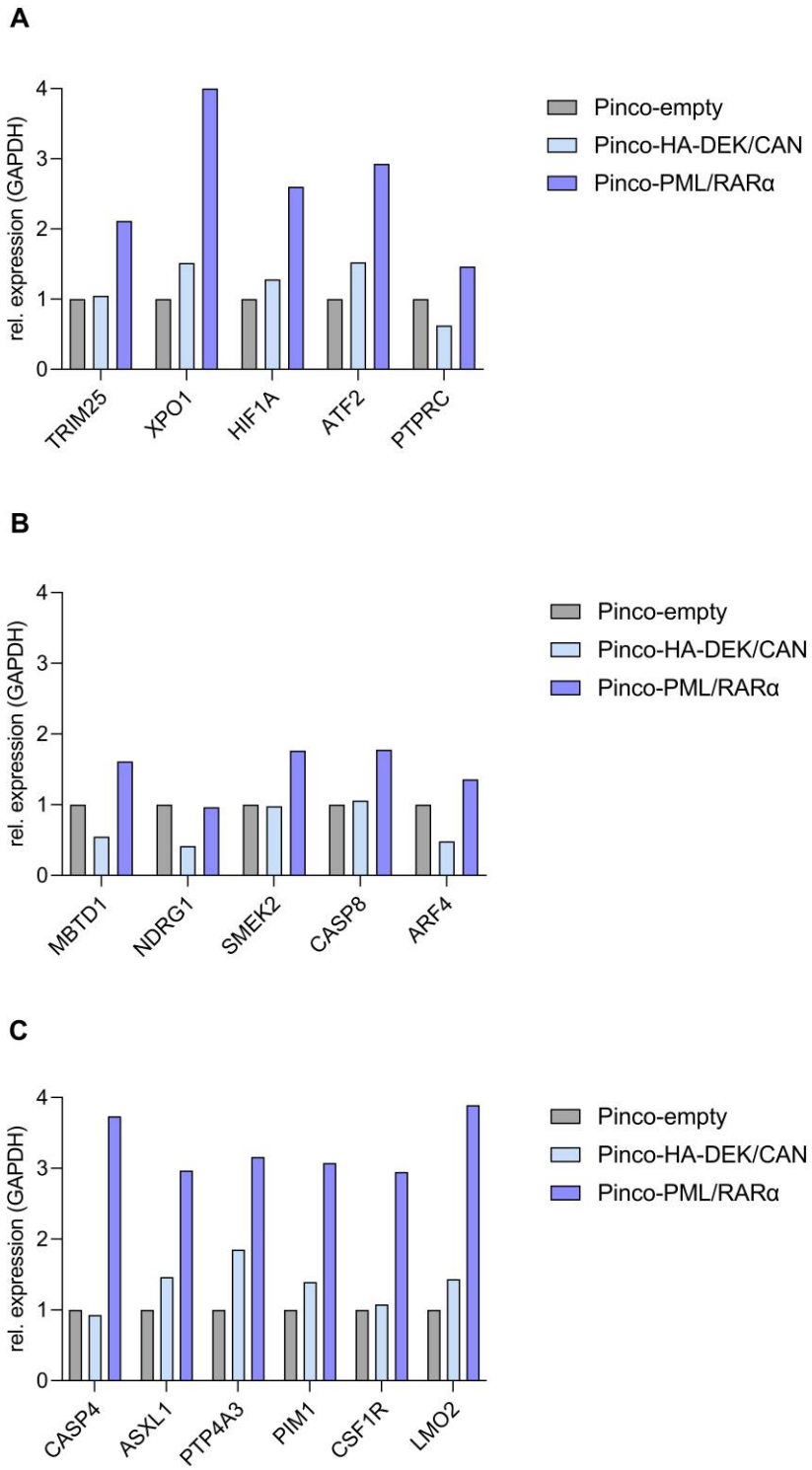

Figure 23: Gene expression analysis of selected genes in 32D cells with the constructs DEK/CAN and PML/RARα by qPCR

These figures show the relative expression ratio of 16 selected genes (**A** = genes 1-5, **B** = genes 6-10, **C** = genes 11-16) in 32D cells, which were transduced with an empty vector, the DEK/CAN construct and the PML/RARα construct. The relative expression ratio of the analyzed genes ranged from 0,4 to 4,0.

The genes have been subdivided in groups, dependent on their known function in a cell by literature research. The groups consisted of genes with catalytic activity such as phosphatases, proteases and hydrolases, molecular transducer activity, transporter activity and binding. The associated signaling pathways were NF-kB, Akt/mTOR, JAK/STAT and ERK1/2 pathway. Also, we identified genes involved in B- and T-cell activation.

DEK/CAN-positive 32D cells showed a higher gene expression of the genes TRIM25, HIF1α and ATF2, which function as transcription factors and might have an impact on the regulation of gene expression. The increased fold change was between 1,1 and 1,5, compared to the negative control. Mentionable is also the upregulation of XPO1, a nuclear export receptor and ASXL1, a well-characterized chromatin-binding protein.

This collection of altered gene expression in presence of the chromosomal translocation of DEK and CAN was further analyzed in relationship to cell signaling pathways. We focussed our interest on altered gene expression levels in genes, that are involved in the JAK/STAT signaling pathway.

The changes in gene expression, influenced by the fusion protein DEK/CAN and PML/RARα seen in the microarray, were consistent with the results of qPCR. The alternated gene expression levels function as an important baseline for further experiments to understand the mechanism of leukemogenesis induced by DEK/CAN.

4.4.2.1 DEK/CAN activates the JAK/STAT signaling pathway

Of special interest were the results of the JAK2 and STAT target genes PIM1 and LMO2 in the qPCR microarray validation. They were both upregulated with a fold change of 1,4 in DEK/CAN-positive 32D cells. Additionally, PTPRC, a tyrosine phosphatase (CD45), was downregulated with a fold change of 0,6, as shown Figure 24. These results equaled the previous microarray analysis. The three genes are involved in an activated JAK/STAT signaling pathway and may be a contributing mechanism in DEK/CAN-induced leukemogenesis.

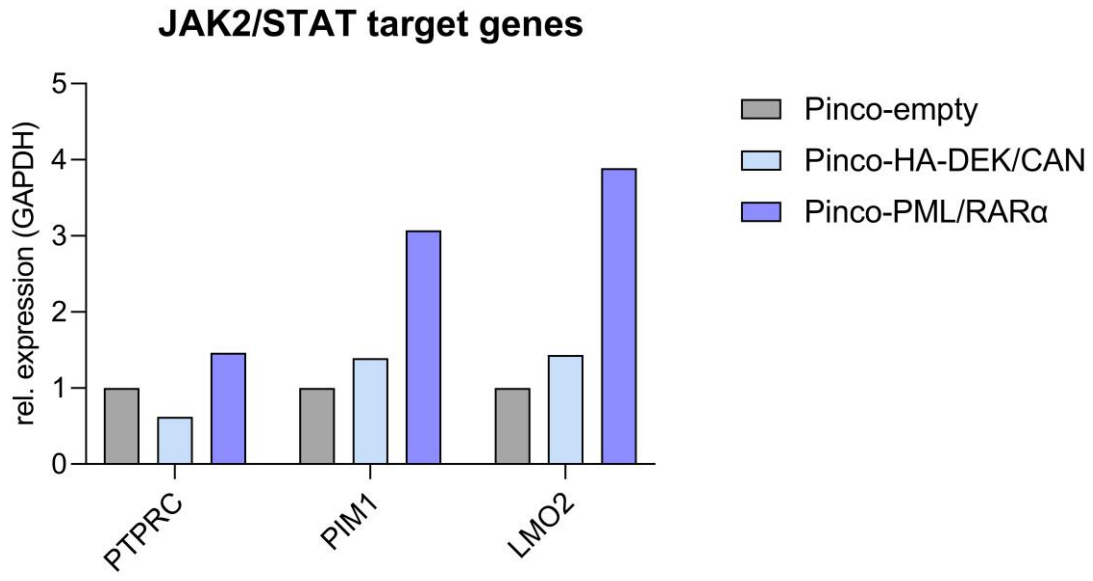

Figure 24: Gene expression analysis of PTPRC and the JAK2/STAT target genes PIM1 and LMO2 in 32D cells with the constructs DEK/CAN and PML/RARα by qPCR
Relative expression ratio of selected genes in 32D cells, which were transfected with an empty vector, the DEK/CAN construct and the PML/RARα construct. The relative expression ratio ranges from 0,6 to 3,8.

5 Discussion

The t(6;9) positive AML affects about 1 % of AML patients and classifies a high-risk group with an unfavourable outcome and poor prognosis (Slovak et al. 2006). Most affected patients are young adults with a median survival of only one year after being diagnosed. Conventional chemotherapy leads to complete remission in 50 % of cases, which leads to a higher necessity of an intensified treatment with allogeneic haematopoietic stem cell transplantation (Chi et al. 2008; Kayser et al. 2019).

This work aimed to establish a practicable workflow with real-time quantitative PCR (qPCR) to detect the fusion product DEK/CAN as a molecular marker for minimal residual disease. Additionally, the altered gene expression profile in DEK/CAN-positive cells was further analyzed by microarray gene expression analysis and its validation by qPCR.

5.1 Chosen Methods

A stable workflow to acquire high quality RNA was the headstone for all further experiments. RNA has a high risk of being damaged and degraded during its extraction and consequently loosing its validity. Therefore, we provided a very sensitive measurement of RNA integrity with the Bioanalyzer automated electrophoresis system. Also, we showed that RNA integrity is higher when treating the extracted RNA with DNase to prevent genomic contamination. Only RNA with a sufficiently high level of integrity (RIN > 8) was used for further cDNA synthesis. The produced cDNA served as a template for standard PCR and qPCR.

The results of qPCR were analyzed by using the model of relative and absolute quantification. By the formation of a standard curve with a dilution series, it was possible to estimate the qPCR amplification efficiency. The efficiency in this case, stands for the fraction of target molecules that get replicated in one PCR cycle (Svec et al. 2015) . In theory, a 100 % amplification efficiency is obtained when the PCR product doubles in each replication cycle. The amplification efficiency value gets affected by the PCR reaction conditions, such as time settings and temperature, as well as reagent concentrations and primer design. In our calculations we obtained a value higher that 100 %, which would theoretically not be possible.

Previous studies have shown that the efficiency calculation may result in too good results (Pfaffl 2001). A reason could be a high concentration of the target DNA with resulting base-line subtraction problems. Also, the PCR reaction reaches a plateau phase after an initial exponential amplification of the PCR product. In this plateau phase, primer and template can develop competitive effects and the gene amplification decreases. According to the actual literature, the maximum efficiency of 100 % for the qPCR can be assumed if the linearity of the standard curve is intact and the results are replicable. As this was the case in our experiment, we assumed an efficiency of 100%.

Although the standard curve is still method of choice for estimating the qPCR efficiency, these results may be a hint, that the efficiency calculation by Pfaffl is not ideal and overestimates the real efficiency. It is possible that a computed efficiency calculation by statistical analysis of the qPCR kinetics delivers a more exact approach (Tichopad et al. 2003; Panina et al. 2019).

5.2 Relevance of MRD diagnostics

The significance of the MRD workflow established here, lies in a high priority in AML diagnostics and follow up during treatment (Mo et al. 2017; Lindern et al. 1992). Before, during, or after treatment, patients can be closely monitored for MRD-positivity and any sign of relapse. With sensitive MRD diagnostics, a relapse might be detected in an early stage and certain interventions can be directed. For example, MRD-positive patients after allo-HSCT can be treated with donor lymphocyte infusions to induce the graft-versus-leukemia effect and regain MRD negativity (Mo et al. 2017).

Possible approaches for quantitative MRD detection are flow cytometric immunophenotyping by identifying aberrant immunophenotypes, PCR techniques using DNA or qPCR using RNA targets. The most sensitive method is qPCR of a RNA gene target or a RNA gene fusion product (van et al. 2003).

In this work, we presented our workflow to acquire high quality RNA and cDNA for the further established and optimized qPCR to detect the fusion protein DEK/CAN. Working with mRNA molecules of a chromosomal aberration bares the risk of RNA degradation because of its instability and genomic contamination. This is why the established high standard of RNA extraction and purification with DNase treatment and measurement with the Agilent Bioanalyzer is so important.

It might be more costly and time-consuming than standard treatment, but in the end worth the extra effort. Also, this method requires extra quality controls on a regular basis. The following method of relative and absolute quantification enabled the detection of the fusion product on a very low molecular level. The presented quantification method and the elaborate treatment requirements of RNA to gain high-quality RNA with a high integrity, should be a standard in all qPCR calculated MRD diagnostics, to avoid false negative results (Yokota und Kitamura 2000).

Especially the t(6;9)-positive AML benefits of this highly sensitive method because of its high risk of relapse and overall poor prognosis. Molecular monitoring in presence of the fusion protein DEK/CAN is necessary and part of the standard diagnostics at different time points during treatment of this specific subgroup of AML. MRD-positivity can be an important premonition of relapse and a chance to not loose time, but to change or begin treatment right away. The subsequent signs of relapse in standard diagnostics such as cytology or flow cytometry appear much later. It was shown that MRD negativity correlates with a better overall survival in the t(6;9)-positive AML (Garcon et al. 2005).

In the future, we might benefit from new diagnostic possibilities such as next generation sequencing or digital PCR as additional and possibly more precise methods to monitor the MRD in acute leukemia (Brüggemann et al. 2019; Drandi et al. 2018).

5.3 DEK/CAN and its influence on gene expression

The gene expression analysis of DEK/CAN-positive cells by microarray testing and further qPCR validation delivered an interesting dataset of altered gene expression. We focussed our interest on genes involved in transcriptional regulations, cellular signaling pathways, leukemogenesis, self-renewal and stem cell activity.

The DEK/CAN-positive 32D cells showed an altered gene expression of transcription factors, protein tyrosine phosphatases, caspases, hydrolases, chromatin-interacting proteins, and a nuclear transport protein. They indicated influences and importance in the NF-kB, Akt/mTOR, JAK/STAT and ERK1/2 signaling pathways, among others.

The genes TRIM25, HIF1α and ATF2, which encode transcription factors, showed an elevated gene expression in DEK/CAN- and PML/RARα-positive cells. As transcription factors with a direct DNA binding activity, an influence on the regulation of gene expression is likely.

The fusion protein PML/RARα is already known for its function as a transcription factor and leads to the question if DEK/CAN indicates similar ways of interacting with DNA. The gene RARα regulates the transcription of relevant genes concerning hematopoietic cell differentiation and can interact with DNA directly. This DNA-binding activity is preserved in the fusion protein PML/RARα (Gianni et al. 2017). The mentioned and upregulated transcription factors TRIM25 and HIF1α have also been reported to have an influence on myeloid hematopoietic or stem cell differentiation (Wu et al. 2020; Cui et al. 2021). Considering the fusion protein DEK/CAN, we mentioned that DEK alone functions as a transcription factor as well. The fusion of DEK and CAN might also show activity as an aberrant transcription factor with an influence on cell differentiation, similar to PML/RARα (Karam et al. 2014). A requirement for transcriptional function, is a localization in the nucleus. Our group was able to show the localization of DEK/CAN in the nucleus with a dotted pattern by Immunohistochemistry (unpublished data, Nathalie Guillen). This underlines the hypothesis, that DEK/CAN-positive cells show an altered transcription factor activity in the nucleus.

The nuclear export receptor XPO1 also showed a higher expression in DEK/CAN-positive cells with a fold change of 1,5. Since CAN is a member of the nuclear pore complex, an association with the XPO1-mediated nuclear transport and export activity is possible. It has been shown that CAN interacts with many nuclear transport receptors (NTRs), for example XPO1. The interaction of XPO1 and CAN remains in the fusion protein DEK/CAN and impairs the XPO1 function. Less mRNA and proteins are being transported to the cytoplasm and remain in the nucleus. It was shown that many proteins of the NF-κB pathway get exported less out of the nucleus and possibly have an influence on the differentiation block seen in leukemic hematopoietic cells (Saito et al. 2016).

Another interesting, upregulated gene was ASXL1. It is well known as a mutated ASXL1, often seen in AML and other hematologic diseases. It is usually associated with a poor prognosis in elderly AML, without clear knowledge of its influence on leukemogenesis (Lin et al. 2020). ASXL1 belongs to a gene family with epigenetic and gene transcription activity (Mossmann et al. 2018). Recent findings were able to show an activation of the Akt/mTOR pathway in mutant ASXL1 in hematopoietic stem cells (Fujino et al. 2021). The upregulated Akt/mTOR signaling by mutated ASXL1 lead to a dysfunction and depletion of HSC. The Akt/mTOR signaling pathway has previously been connected to an expression of the fusion product DEK/CAN. The fusion protein induced an overactivation of the mTOR signaling pathway in U937 cell lines and reacted

with reduced proliferation after treatment with the mTOR inhibitor Everolimus (Sandén et al. 2013). It was not shown directly, but seems possible, that an overexpression of wildtype ASXL1 contributes to a stimulation of the mTOR signaling pathway.

Additionally, we were able to identify a connection of different genes to an upregulation of the JAK/STAT signaling pathway, which corresponds to previous research in this field. The acquired data is a platform for further analysis to decrypt the mechanism of DEK/CAN-induced AML. Further emphasis is now placed on the gene products involved in the JAK/STAT signaling pathway, with altered expression in presence of DEK/CAN.

5.4 Downregulation of the tyrosine phosphatase PTPRC

PTPRC, the Protein Tyrosine Phosphatase Receptor Type C, also called CD45, is a tyrosine phosphatase with expression in nearly all hematopoietic cells. It is a transmembrane protein which regulates many different cellular processes as a signaling molecule.

Our experiments showed a downregulation of PTPRC gene expression in DEK/CAN-positive 32D cells. To interpret this finding, it is important to take a closer look at this specific phosphatase. In general, the regulation of tyrosine phosphorylation by kinases and phosphatases plays an important role in cell signaling (Tonks und Neel 1996).

CD45 can get stimulated by antigens, growth factors and cytokines. Activation occurs through direct antigen receptor interaction or through activation of kinases of the src (sarcoma) family. It was shown that CD45 regulates the antigen receptor signaling of T- and B-lymphocytes. A CD45 deficiency leads to a T- and B-cell dysfunction and subsequent immune deficiency (Byth et al. 1996; Rheinländer et al. 2018).

Why is it important in context with DEK/CAN-positive leukemia?

CD45 does not only activate, but also inhibit certain cellular processes. Previous work has shown a direct inhibition of JAKs and STATs and the comprised signaling pathway (Irie-Sasaki et al. 2001). An interleukin-3 (IL-3)- dependent bone-marrow-derived mast cell line (BMMC) from CD45+ and genetically inactivated CD45 (CD45-) mice was generated. The stimulation with IL-3 lead to a significantly higher proliferation of the CD45- cohort. Also, the CD45- cells showed an increased direct phosphorylation of JAK, STAT3 and STAT5. This activity was independent of the

src-family kinases, which are usually involved in cell signaling by CD45. The genetic inactivation of CD45 enhanced the STAT-associated DNA-binding activity and hyperactivated the JAK/STAT signaling pathway (Irie-Sasaki et al. 2001). This pathway is highly relevant in hematopoiesis and influences cell proliferation, differentiation, apoptosis and immunologic responses (Pencik et al. 2016). Alterations in this pathway have been reported in hematopoietic diseases such as myeloproliferative disorders and leukemia (James et al. 2005). Different forms of leukemia showed a hyperactivation of the JAK/STAT signaling pathway, supporting the postulation of being partly responsible for leukemogenesis. Point of action is a constitutive activation of STATs, reported in AML (Steelman et al. 2008; Brady et al. 2012). Our group was able to show that DEK/CAN-positive leukemia shows a remarkable high expression of STAT proteins, compared to non leukemic cells. In the DEK/CAN-positive cells, this STAT activation is accompanied by a constitutive activation of JAK2 and downregulation of CD45. These finding lead to the hypothesis, that the activation of JAK2 is due to a downregulation of CD45 (Oancea et al. 2010; Oancea et al. 2014).

Other reports showed a loss of CD45 expression with a resulting activation of the JAK/STAT pathway. Around 10% of ALL patients show a loss of CD45 expression on the cell surface or in some cases also a loss-of-function mutation in CD45 (Ratei et al. 1998; Porcu et al. 2012).

In this work we can report a decrease in gene expression of CD45 in DEK/CAN-positive early hematopoietic cells of the microarray experiment, as well as in transfected murine 32D cells validated by qPCR. This may be the starting point for an hyperactivated JAK/STAT signaling pathway and the induction and development of leukemic blasts.

5.5 Analysis of STAT5 and JAK2 target genes

We additionally examined a selection of target genes of STAT and JAK, to prove our previous data concerning the downregulation of CD45 as a reason for induced upstream JAK/STAT signaling.

The first gene we tested was PIM 1, the proviral integration site 1, a serine/threonine kinase with an association to hematopoietic malignancies and solid tumors as a proto-oncogene (Selten et al. 1986). PIM1 induces a growth-factor independent phosphorylation of proteins, involved in cell survival and proliferation. Interestingly, PIM1 is a direct transcriptional target of STAT5 (Yuan et al. 2014; Kim et al. 2005). PIM1 shows a higher gene expression in the microarray data as well as

in the validated qPCR data of PIM1. As a direct target gene of STAT5, it supports our hypothesis, that there is an independent STAT activation in the t(6;9)-positive AML, independent of any external cytokine induction. PIM1, activated by STAT5, showed a phosphorylation and activation of different signaling pathways such as the mammalian target of rapamycin (mTOR) pathway and target genes in ovarian cancer (Aziz et al. 2018).

We also analyzed LMO2, a target gene of JAK2, which showed increased expression levels in presence of the fusion protein DEK/CAN. LMO2, LIM domain 2, is a protein responsible of erythropoiesis and stem cell differentiation. It has been discovered as an oncogene in T cell acute lymphoblastic leukemia (Ferrando et al. 2002; McCormack et al. 2010). Further studies described LMO2 as one of the most important target gene of JAK2 by regulating its gene expression. Activating mutations of the JAK2 gene were associated with a high LMO2 gene expression and cytokine independent constitutive activation of the JAK/STAT pathway (Dawson et al. 2009). These findings add to the former described hyperactivation of JAK2 in DEK/CAN-positive AML and additionally supports our hypothesis of independent activation of the JAK/STAT-signaling pathway as an important driver of leukemogenesis (Oancea et al. 2010; Oancea et al. 2014).

CSF1R, the Colony Stimulating Factor 1 Receptor, is mostly associated with regulation of proliferation, differentiation and function of macrophages (Yu et al. 2012). It is a tyrosine kinase transmembrane receptor which gets stimulated by the ligands CSF-1 and Interleukin 34 (Lin et al. 2008). Alterations in the CSF1R gene have been associated with neoplastic development and progression in various entities. (Xun et al. 2019). It has been reported that CSF1R stimulates STAT activation (Roberts et al. 2017). This adds to our hypothesis of activated JAK/STAT signaling in DEK/CAN-positive AML.

5.6 Inhibition of the JAK/STAT-signaling pathway might be a therapeutic strategy for DEK/CAN-positive AML

DEK/CAN-positive leukemia belongs to the adverse risk group considering the 2017 ELN risk stratification with a poor prognosis and frequent necessity of allo-SCT to get a chance of achieving complete remission. Regarding the results of this work, which give evidence of an upregulation of the JAK/STAT signaling pathway in t(6;9)-positive AML, the current standard treatment options should be reconsidered. The ongoing goal in hematology and oncology of identifying specific

mutations or genetic aberrations and target them directly could also play an important role in this group of AML. The addition of targeted therapy to the standard therapy might have a big impact on the overall survival rate and improve the prognosis in the t(6;9)-positive AML.

Since we identified the activation of STAT5 and JAK2 target genes, which might drive cell proliferation, we should discuss the use of pan-JAK inhibitors. They are mostly used in myeloproliferative neoplasms (MPN) because of the high incidence of JAK mutations and a constitutive JAK/STAT pathway activation. The JAK1 and 2 inhibitor Ruxolitinib showed its benefit in treatment of myelofibrosis and has been approved for the treatment of this disease (Kvasnicka et al. 2018). There are ongoing studies, evaluating a positive effect of the drug in relapsed or refractory AML in clinical trials (Pemmaraju et al. 2015). Especially the affected patients of the t(6;9)-positive AML might benefit of a JAK-inhibitor by a better outcome and overall survival.

There also have been findings that the common drug Methotrexate (MTX) is a suppressor of the JAK/STAT signaling pathway (Thomas et al. 2015). This would be another valuable approach of treating the disease on an additional, more specific level.

Previous work of our group has also shown a sensitivity in DEK/CAN-positive AML towards arsenic trioxide (ATO) (Oancea et al. 2014). This effect is known and well-established in the PML/RARα-positive AML (Ghavamzadeh et al. 2011). Interestingly, research has shown an inhibition of protein tyrosine kinases (PTK), which phosphorylate and activate STATs, by ATO. STAT activation and leukemic cell proliferation was reduced by ATO treatment (Wetzler et al. 2006). Our group was able to detect apoptosis in DEK/CAN-positive murine leukemic cells with high expression of STATs in vitro and in vivo by ATO treatment. This was seen in a similar extent as the PML/RARα-positive leukemic cells. ATO might be another treatment option in leukemic cells with activated STATs (Oancea et al. 2014).

5.7 Outlook

Acute myeloid leukemia is a disease that has been characterized thoroughly in the last decade. Next generation sequencing enabled a wide molecular characterisation of AML with correlation to prognosis and treatment response within clinical studies. The identification of genetic aberrations has led to new therapy options such as protein kinase inhibitors, epigenetic modulators and new

cytotoxic agents. The scope is to step away from classic chemotherapy treatment only and aim for an additional targeted therapy, respecting the molecular profile of each specific AML (Döhner et al. 2017).

Patients with DEK/CAN-positive AML would also benefit from new therapeutic options due to its very limited prognosis and adverse risk profile. The shown influence and activation of the JAK/STAT signaling pathway could lead the way to new treatment options including additional pan-JAK inhibitors or arsenic trioxide (ATO), beside standard chemotherapy and allo-HSCT.

Considering the current state of research, further emphasis should be placed on experiments in human samples of patients with DEK/CAN-positive AML. The increasingly advanced and complex techniques of genetic analysis should be utilized to gain a more profound insight in DEK/CAN-positive leukemogenesis. Techniques, such as multi-omic single cell approaches including genomics, transcriptomics, proteomics and epigenetics will lead to a more detailed understanding of molecular processes in leukemic cells and could help to find new therapeutic targets in DEK/CAN-positive AML (Mimitou et al. 2021).

If the presented findings of this work are reproducible in human patient samples, or if additional drug targets can be identified, further steps towards in vitro and in vivo drug testing along with clinical trails should be considered.

6 Schriftliche Erklärung

Ich erkläre ehrenwörtlich, dass ich die dem Fachbereich Medizin der Johann Wolfgang Goethe-Universität Frankfurt am Main zur Promotionsprüfung eingereichte Dissertation mit dem Titel

Minimal residual disease detection of the fusion protein DEK/CAN in t(6;9)(p23;q34) positive Acute Myeloid Leukemia and identification of target genes and key pathways for leukemogenesis

im Zentrum der Inneren Medizin, Medizinische Klinik 2, Abteilung Hämatologie des Universitätsklinikums Frankfurt am Main bei Prof. Dr. Hubert Serve unter Betreuung und Anleitung von PD Dr. Martin Ruthdardt mit Unterstützung durch Dr. Claudia Oancea ohne sonstige Hilfe selbst durchgeführt und bei der Abfassung der Arbeit keine anderen als die in der Dissertation angeführten Hilfsmittel benutzt habe. Darüber hinaus versichere ich, nicht die Hilfe einer kommerziellen Promotionsvermittlung in Anspruch genommen zu haben.

Ich habe bisher an keiner in- oder ausländischen Universität ein Gesuch um Zulassung zur Promotion eingereicht. Die vorliegende Arbeit wurde bisher nicht als Dissertation eingereicht.

Frankfurt am Main, 29. April 2022

Selina Ferrara

7 References

Ageberg, Malin; Gullberg, Urban; Lindmark, Anders (2006): The involvement of cellular proliferation status in the expression of the human proto-oncogene DEK. In: *Haematologica* 91 (2), S. 268–269.

Alber, Frank; Dokudovskaya, Svetlana; Veenhoff, Liesbeth M.; Zhang, Wenzhu; Kipper, Julia; Devos, Damien et al. (2007): The molecular architecture of the nuclear pore complex. In: *Nature* 450 (7170), S. 695–701. DOI: 10.1038/nature06405.

Arber, Daniel A.; Orazi, Attilio; Hasserjian, Robert; Thiele, Jürgen; Borowitz, Michael J.; Le Beau, Michelle M. et al. (2016): The 2016 revision to the World Health Organization classification of myeloid neoplasms and acute leukemia. In: *Blood* 127 (20), S. 2391–2405. DOI: 10.1182/blood-2016-03-643544.

Asada, Shuhei; Fujino, Takeshi; Goyama, Susumu; Kitamura, Toshio (2019): The role of ASXL1 in hematopoiesis and myeloid malignancies. In: *Cellular and molecular life sciences : CMLS* 76 (13), S. 2511–2523. DOI: 10.1007/s00018-019-03084-7.

Avvisati, G.; Cate, J. W. ten; Mandelli, F. (1992): Acute promyelocytic leukaemia. In: *British journal of haematology* 81 (3), S. 315–320.

Aziz, Aziz Ur Rehman; Farid, Sumbal; Qin, Kairong; Wang, Hanqin; Liu, Bo (2018): PIM Kinases and Their Relevance to the PI3K/AKT/mTOR Pathway in the Regulation of Ovarian Cancer. In: *Biomolecules* 8 (1). DOI: 10.3390/biom8010007.

Bennett, J. M.; Catovsky, D.; Daniel, M. T.; Flandrin, G.; Galton, D. A.; Gralnick, H. R.; Sultan, C. (1976): Proposals for the classification of the acute leukaemias. French-American-British (FAB) co-operative group. In: *British journal of haematology* 33 (4), S. 451–458.

Böhm, Friederike; Kappes, Ferdinand; Scholten, Ingo; Richter, Nicole; Matsuo, Hiroshi; Knippers, Rolf; Waldmann, Tanja (2005): The SAF-box domain of chromatin protein DEK. In: *Nucleic acids research* 33 (3), S. 1101–1110. DOI: 10.1093/nar/gki258.

Bonnet, D.; Dick, J. E. (1997): Human acute myeloid leukemia is organized as a hierarchy that originates from a primitive hematopoietic cell. In: *Nature medicine* 3 (7), S. 730–737.

Brady, Anna; Gibson, Sarah; Rybicki, Lisa; Hsi, Eric; Sauntharajah, Yogen; Sekeres, Mikkael A. et al. (2012): Expression of phosphorylated signal transducer and activator of transcription 5 is

associated with an increased risk of death in acute myeloid leukemia. In: *European journal of haematology* 89 (4), S. 288–293. DOI: 10.1111/j.1600-0609.2012.01825.x.

Brown, C. M. S.; Larsen, S. R.; Iland, H. J.; Joshua, D. E.; Gibson, J. (2012): Leukaemias into the 21st century: part 1: the acute leukaemias. In: *Internal medicine journal* 42 (11), S. 1179–1186. DOI: 10.1111/j.1445-5994.2012.02938.x.

Brüggemann, Monika; Kotrová, Michaela; Knecht, Henrik; Bartram, Jack; Boudjogrha, Myriam; Bystry, Vojtech et al. (2019): Standardized next-generation sequencing of immunoglobulin and T-cell receptor gene recombinations for MRD marker identification in acute lymphoblastic leukaemia; a EuroClonality-NGS validation study. In: *Leukemia* 33 (9), S. 2241–2253. DOI: 10.1038/s41375-019-0496-7.

Bullinger, Lars; Döhner, Konstanze; Döhner, Hartmut (2017): Genomics of Acute Myeloid Leukemia Diagnosis and Pathways. In: *Journal of clinical oncology : official journal of the American Society of Clinical Oncology* 35 (9), S. 934–946. DOI: 10.1200/JCO.2016.71.2208.

Byth, K. F.; Conroy, L. A.; Howlett, S.; Smith, A. J.; May, J.; Alexander, D. R.; Holmes, N. (1996): CD45-null transgenic mice reveal a positive regulatory role for CD45 in early thymocyte development, in the selection of CD4+CD8+ thymocytes, and B cell maturation. In: *The Journal of experimental medicine* 183 (4), S. 1707–1718. DOI: 10.1084/jem.183.4.1707.

Caligiuri, M. A.; Strout, M. P.; Gilliland, D. G. (1997): Molecular biology of acute myeloid leukemia. In: *Seminars in oncology* 24 (1), S. 32–44.

Capitano, Maegan L.; Broxmeyer, Hal E. (2017): A role for intracellular and extracellular DEK in regulating hematopoiesis. In: *Current opinion in hematology* 24 (4), S. 300–306. DOI: 10.1097/MOH.0000000000000344.

Capitano, Maegan L.; Mor-Vaknin, Nirit; Saha, Anjan K.; Cooper, Scott; Legendre, Maureen; Guo, Haihong et al. (2019): Secreted nuclear protein DEK regulates hematopoiesis through CXCR2 signaling. In: *The Journal of clinical investigation* 129 (6), S. 2555–2570. DOI: 10.1172/JCI127460.

Charbord, P.; Tavian, M.; Humeau, L.; Péault, B. (1996): Early ontogeny of the human marrow from long bones: an immunohistochemical study of hematopoiesis and its microenvironment. In: *Blood* 87 (10), S. 4109–4119.

Chatel, Guillaume; Fahrenkrog, Birthe (2012): Dynamics and diverse functions of nuclear pore complex proteins. In: *Nucleus (Austin, Tex.)* 3 (2), S. 162–171. DOI: 10.4161/nucl.19674.

Chi, Yiqing; Lindgren, Valerie; Quigley, Sean; Gaitonde, Sujata (2008): Acute myelogenous leukemia with t(6;9)(p23;q34) and marrow basophilia: an overview. In: *Archives of pathology & laboratory medicine* 132 (11), S. 1835–1837. DOI: 10.1043/1543-2165-132.11.1835.

Cleary, Joanne; Sitwala, Kajal V.; Khodadoust, Michael S.; Kwok, Roland P. S.; Mor-Vaknin, Nirit; Cebrat, Marek et al. (2005): p300/CBP-associated factor drives DEK into interchromatin granule clusters. In: *The Journal of biological chemistry* 280 (36), S. 31760–31767. DOI: 10.1074/jbc.M500884200.

Cline, M. J.; Golde, D. W. (1977): Mobilization of hematopoietic stem cells (CFU-C) into the peripheral blood of man by endotoxin. In: *Experimental hematology* 5 (3), S. 186–190.

Coombs, C. C.; Tavakkoli, M.; Tallman, M. S. (2015): Acute promyelocytic leukemia: where did we start, where are we now, and the future. In: *Blood cancer journal* 5, e304. DOI: 10.1038/bcj.2015.25.

Copeland, N. G.; Gilbert, D. J.; Schindler, C.; Zhong, Z.; Wen, Z.; Darnell, J. E. et al. (1995): Distribution of the mammalian Stat gene family in mouse chromosomes. In: *Genomics* 29 (1), S. 225–228.

Cui, Peng; Zhang, Ping; Yuan, Lin; Wang, Li; Guo, Xin; Cui, Guanghui et al. (2021): HIF-1α Affects the Neural Stem Cell Differentiation of Human Induced Pluripotent Stem Cells via MFN2-Mediated Wnt/β-Catenin Signaling. In: *Frontiers in cell and developmental biology* 9, S. 671704. DOI: 10.3389/fcell.2021.671704.

Dawson, Mark A.; Bannister, Andrew J.; Göttgens, Berthold; Foster, Samuel D.; Bartke, Till; Green, Anthony R.; Kouzarides, Tony (2009): JAK2 phosphorylates histone H3Y41 and excludes HP1alpha from chromatin. In: *Nature* 461 (7265), S. 819–822. DOI: 10.1038/nature08448.

DiNardo, Courtney D.; Pratz, Keith; Pullarkat, Vinod; Jonas, Brian A.; Arellano, Martha; Becker, Pamela S. et al. (2019): Venetoclax combined with decitabine or azacitidine in treatment-naive, elderly patients with acute myeloid leukemia. In: *Blood* 133 (1), S. 7–17. DOI: 10.1182/blood-2018-08-868752.

DiNardo, Courtney D.; Rausch, Caitlin R.; Benton, Christopher; Kadia, Tapan; Jain, Nitin; Pemmaraju, Naveen et al. (2018): Clinical experience with the BCL2-inhibitor venetoclax in combination therapy for relapsed and refractory acute myeloid leukemia and related myeloid malignancies. In: *American journal of hematology* 93 (3), S. 401–407. DOI: 10.1002/ajh.25000.

Döhner, Hartmut; Estey, Elihu; Grimwade, David; Amadori, Sergio; Appelbaum, Frederick R.; Büchner, Thomas et al. (2017): Diagnosis and management of AML in adults: 2017 ELN recommendations from an international expert panel. In: *Blood* 129 (4), S. 424–447. DOI: 10.1182/blood-2016-08-733196.

Döhner, Hartmut; Estey, Elihu H.; Amadori, Sergio; Appelbaum, Frederick R.; Büchner, Thomas; Burnett, Alan K. et al. (2010): Diagnosis and management of acute myeloid leukemia in adults: recommendations from an international expert panel, on behalf of the European LeukemiaNet. In: *Blood* 115 (3), S. 453–474. DOI: 10.1182/blood-2009-07-235358.

Dong, X.; Michelis, M. A.; Wang, J.; Bose, R.; DeLange, T.; Reeves, W. H. (1998): Autoantibodies to DEK oncoprotein in a patient with systemic lupus erythematosus and sarcoidosis. In: *Arthritis and rheumatism* 41 (8), S. 1505–1510. DOI: 10.1002/1529-0131(199808)41:8<1505::AID-ART23>3.0.CO;2-N.

Drandi, Daniela; Ferrero, Simone; Ladetto, Marco (2018): Droplet Digital PCR for Minimal Residual Disease Detection in Mature Lymphoproliferative Disorders. In: *Methods in molecular biology (Clifton, N.J.)* 1768, S. 229–256. DOI: 10.1007/978-1-4939-7778-9_14.

Dührsen, U. (1988): In vitro growth patterns and autocrine production of hemopoietic colony stimulating factors: analysis of leukemic populations arising in irradiated mice from cells of an injected factor-dependent continuous cell line. In: *Leukemia* 2 (6), S. 334–342.

Erickson, P.; Gao, J.; Chang, K. S.; Look, T.; Whisenant, E.; Raimondi, S. et al. (1992): Identification of breakpoints in t(8;21) acute myelogenous leukemia and isolation of a fusion transcript, AML1/ETO, with similarity to Drosophila segmentation gene, runt. In: *Blood* 80 (7), S. 1825–1831.

Falini, Brunangelo; Mecucci, Cristina; Tiacci, Enrico; Alcalay, Myriam; Rosati, Roberto; Pasqualucci, Laura et al. (2005): Cytoplasmic nucleophosmin in acute myelogenous leukemia with a normal karyotype. In: *The New England journal of medicine* 352 (3), S. 254–266. DOI: 10.1056/NEJMoa041974.

Ferrando, Adolfo A.; Neuberg, Donna S.; Staunton, Jane; Loh, Mignon L.; Huard, Christine; Raimondi, Susana C. et al. (2002): Gene expression signatures define novel oncogenic pathways in T cell acute lymphoblastic leukemia. In: *Cancer cell* 1 (1), S. 75–87. DOI: 10.1016/S1535-6108(02)00018-1.

Filion, Martin (Hg.) (2012): Quantitative real-time PCR in applied microbiology. Norfolk: Caister Acad. Press.

Fleige, Simone; Pfaffl, Michael W. (2006a): RNA integrity and the effect on the real-time qRT-PCR performance. In: *Molecular aspects of medicine* 27 (2-3), S. 126–139. DOI: 10.1016/j.mam.2005.12.003.

Fleige, Simone; Pfaffl, Michael W. (2006b): RNA integrity and the effect on the real-time qRT-PCR performance. In: *Molecular aspects of medicine* 27 (2-3), S. 126–139. DOI: 10.1016/j.mam.2005.12.003.

Fujino, Takeshi; Goyama, Susumu; Sugiura, Yuki; Inoue, Daichi; Asada, Shuhei; Yamasaki, Satoshi et al. (2021): Mutant ASXL1 induces age-related expansion of phenotypic hematopoietic stem cells through activation of Akt/mTOR pathway. In: *Nature communications* 12 (1), S. 1826. DOI: 10.1038/s41467-021-22053-y.

Fukuda, M.; Asano, S.; Nakamura, T.; Adachi, M.; Yoshida, M.; Yanagida, M.; Nishida, E. (1997): CRM1 is responsible for intracellular transport mediated by the nuclear export signal. In: *Nature* 390 (6657), S. 308–311. DOI: 10.1038/36894.

Gaidzik, V. I.; Teleanu, V.; Papaemmanuil, E.; Weber, D.; Paschka, P.; Hahn, J. et al. (2016): RUNX1 mutations in acute myeloid leukemia are associated with distinct clinico-pathologic and genetic features. In: *Leukemia* 30 (11), S. 2282. DOI: 10.1038/leu.2016.207.

Gangisetty, Omkaram; Reddy, Doodipala Samba (2009): The optimization of TaqMan real-time RT-PCR assay for transcriptional profiling of GABA-A receptor subunit plasticity. In: *Journal of neuroscience methods* 181 (1), S. 58–66. DOI: 10.1016/j.jneumeth.2009.04.016.

Garcon, L.; Libura, M.; Delabesse, E.; Valensi, F.; Asnafi, V.; Berger, C. et al. (2005): DEK-CAN molecular monitoring of myeloid malignancies could aid therapeutic stratification. In: *Leukemia* 19 (8), S. 1338–1344. DOI: 10.1038/sj.leu.2403835.

Ghavamzadeh, Ardeshir; Alimoghaddam, Kamran; Rostami, Shahrbano; Ghaffari, Seyed Hamidolah; Jahani, Mohamad; Iravani, Massoud et al. (2011): Phase II study of single-agent arsenic trioxide for the front-line therapy of acute promyelocytic leukemia. In: *Journal of clinical oncology : official journal of the American Society of Clinical Oncology* 29 (20), S. 2753–2757. DOI: 10.1200/JCO.2010.32.2107.

Gianni, Maurizio; Fratelli, Maddalena; Bolis, Marco; Kurosaki, Mami; Zanetti, Adriana; Paroni, Gabriela et al. (2017): RARα2 and PML-RAR similarities in the control of basal and retinoic acid induced myeloid maturation of acute myeloid leukemia cells. In: *Oncotarget* 8 (23), S. 37041–37060. DOI: 10.18632/oncotarget.10556.

Göhlmann, Hinrich; Talloen, Willem (2009): Gene expression studies using affymetrix microarrays. Boca Raton: Taylor & Francis (Mathematical and computational biology series). Online verfügbar unter http://site.ebrary.com/lib/alltitles/docDetail.action?docID=10419894.

Graux, C.; Cools, J.; Melotte, C.; Quentmeier, H.; Ferrando, A.; Levine, R. et al. (2004): Fusion of NUP214 to ABL1 on amplified episomes in T-cell acute lymphoblastic leukemia. In: *Nature genetics* 36 (10), S. 1084–1089. DOI: 10.1038/ng1425.

Greenlund, A. C.; Farrar, M. A.; Viviano, B. L.; Schreiber, R. D. (1994): Ligand-induced IFN gamma receptor tyrosine phosphorylation couples the receptor to its signal transduction system (p91). In: *The EMBO journal* 13 (7), S. 1591–1600.

Haan, S.; Kortylewski, M.; Behrmann, I.; Müller-Esterl, W.; Heinrich, P. C.; Schaper, F. (2000): Cytoplasmic STAT proteins associate prior to activation. In: *The Biochemical journal* 345 Pt 3, S. 417–421.

Hanahan, D.; Weinberg, R. A. (2000): The hallmarks of cancer. In: *Cell* 100 (1), S. 57–70.

Heim, M. H.; Kerr, I. M.; Stark, G. R.; Darnell, J. E. (1995): Contribution of STAT SH2 groups to specific interferon signaling by the Jak-STAT pathway. In: *Science (New York, N.Y.)* 267 (5202), S. 1347–1349.

Holland, P. M.; Abramson, R. D.; Watson, R.; Gelfand, D. H. (1991): Detection of specific polymerase chain reaction product by utilizing the 5'----3' exonuclease activity of Thermus aquaticus DNA polymerase. In: *Proceedings of the National Academy of Sciences of the United States of America* 88 (16), S. 7276–7280.

Horvath, C. M. (2000): STAT proteins and transcriptional responses to extracellular signals. In: *Trends in biochemical sciences* 25 (10), S. 496–502.

Howlader, N.; Noone, AM.; Krapcho, M.; Miller, D.; Bishop, K.; Kosary, CL. et al. (2014a): SEER Cancer Statistics Review 1975-2014. Based on November 2016 SEER data submission, posted to the SEER web site, April 2017. Unter Mitarbeit von N. Howlader, AM. Noone, M. Krapcho, D. Miller, K. Bishop, CL. Kosary et al. Hg. v. National Cancer Institute. National Cancer Institute. Bethesda. Online verfügbar unter https://seer.cancer.gov/csr/1975_2014/.

Howlader, N.; Noone, AM.; Krapcho, M.; Miller, D.; Bishop, K.; Kosary, CL. et al. (2014b): SEER Cancer Statistics Review 1975-2014. Based on November 2016 SEER data submission, posted to the SEER web site, April 2017. Unter Mitarbeit von N. Howlader, AM. Noone, M. Krapcho, D. Miller, K. Bishop, CL. Kosary et al. Hg. v. National Cancer Institute. National Cancer Institute. Bethesda. Online verfügbar unter https://seer.cancer.gov/csr/1975_2014/.

Huang, Z.; Fasco, M. J.; Kaminsky, L. S. (1996): Optimization of Dnase I removal of contaminating DNA from RNA for use in quantitative RNA-PCR. In: *BioTechniques* 20 (6), 1012-4, 1016, 1018-20.

Irie-Sasaki, J.; Sasaki, T.; Matsumoto, W.; Opavsky, A.; Cheng, M.; Welstead, G. et al. (2001): CD45 is a JAK phosphatase and negatively regulates cytokine receptor signalling. In: *Nature* 409 (6818), S. 349–354. DOI: 10.1038/35053086.

Ishikawa, Yuichi; Kiyoi, Hitoshi; Tsujimura, Akane; Miyawaki, Shuichi; Miyazaki, Yasushi; Kuriyama, Kazutaka et al. (2009): Comprehensive analysis of cooperative gene mutations between class I and class II in de novo acute myeloid leukemia. In: *European journal of haematology* 83 (2), S. 90–98. DOI: 10.1111/j.1600-0609.2009.01261.x.

Jagannathan-Bogdan, Madhumita; Zon, Leonard I. (2013): Hematopoiesis. In: *Development (Cambridge, England)* 140 (12), S. 2463–2467. DOI: 10.1242/dev.083147.

James, Chloé; Ugo, Valérie; Le Couédic, Jean-Pierre; Staerk, Judith; Delhommeau, François; Lacout, Catherine et al. (2005): A unique clonal JAK2 mutation leading to constitutive signalling causes polycythaemia vera. In: *Nature* 434 (7037), S. 1144–1148. DOI: 10.1038/nature03546.

Juliusson, Gunnar; Lazarevic, Vladimir; Hörstedt, Ann-Sofi; Hagberg, Oskar; Höglund, Martin (2012): Acute myeloid leukemia in the real world: why population-based registries are needed. In: *Blood* 119 (17), S. 3890–3899. DOI: 10.1182/blood-2011-12-379008.

Kampen, Kim R. (2012): The discovery and early understanding of leukemia. In: *Leukemia research* 36 (1), S. 6–13. DOI: 10.1016/j.leukres.2011.09.028.

Kappes, F.; Burger, K.; Baack, M.; Fackelmayer, F. O.; Gruss, C. (2001): Subcellular localization of the human proto-oncogene protein DEK. In: *The Journal of biological chemistry* 276 (28), S. 26317–26323. DOI: 10.1074/jbc.M100162200.

Kappes, F.; Fahrer, J.; Khodadoust, M. S.; Tabbert, A.; Strasser, C.; Mor-Vaknin, N. et al. (2008): DEK is a poly(ADP-ribose) acceptor in apoptosis and mediates resistance to genotoxic stress. In: *Molecular and cellular biology* 28 (10), S. 3245–3257. DOI: 10.1128/MCB.01921-07.

Kappes, Ferdinand; Damoc, Catalina; Knippers, Rolf; Przybylski, Michael; Pinna, Lorenzo A.; Gruss, Claudia (2004): Phosphorylation by protein kinase CK2 changes the DNA binding properties of the human chromatin protein DEK. In: *Molecular and cellular biology* 24 (13), S. 6011–6020. DOI: 10.1128/MCB.24.13.6011-6020.2004.

Karam, Maroun; Thenoz, Morgan; Capraro, Valérie; Robin, Jean-Philippe; Pinatel, Christiane; Lancon, Agnès et al. (2014): Chromatin redistribution of the DEK oncoprotein represses hTERT transcription in leukemias. In: *Neoplasia (New York, N.Y.)* 16 (1), S. 21–30. DOI: 10.1593/neo.131658.

Kavanaugh, Gina M.; Wise-Draper, Trisha M.; Morreale, Richard J.; Morrison, Monique A.; Gole, Boris; Schwemberger, Sandy et al. (2011): The human DEK oncogene regulates DNA damage response signaling and repair. In: *Nucleic acids research* 39 (17), S. 7465–7476. DOI: 10.1093/nar/gkr454.

Kayser, Sabine; Hills, Robert K.; Luskin, Marlise R.; Brunner, Andrew M.; Terré, Christine; Westermann, Jörg et al. (2019): Allogeneic hematopoietic cell transplantation improves outcome of adults with t(6;9) acute myeloid leukemia - results from an international collaborative study. In: *Haematologica*. DOI: 10.3324/haematol.2018.208678.

Keersmaecker, K. de; Versele, M.; Cools, J.; Superti-Furga, G.; Hantschel, O. (2008): Intrinsic differences between the catalytic properties of the oncogenic NUP214-ABL1 and BCR-ABL1 fusion protein kinases. In: *Leukemia* 22 (12), S. 2208–2216. DOI: 10.1038/leu.2008.242.

Kern, Wolfgang; Danhauser-Riedl, Susanne; Ratei, Richard; Schnittger, Susanne; Schoch, Claudia; Kolb, Hans-Jochem et al. (2003): Detection of minimal residual disease in unselected patients with acute myeloid leukemia using multiparameter flow cytometry for definition of

leukemia-associated immunophenotypes and determination of their frequencies in normal bone marrow. In: *Haematologica* 88 (6), S. 646–653.

Khodadoust, Michael S.; Verhaegen, Monique; Kappes, Ferdinand; Riveiro-Falkenbach, Erica; Cigudosa, Juan C.; Kim, David S. L. et al. (2009): Melanoma proliferation and chemoresistance controlled by the DEK oncogene. In: *Cancer research* 69 (16), S. 6405–6413. DOI: 10.1158/0008-5472.CAN-09-1063.

Kim, Kyu-Tae; Baird, Kristin; Ahn, Joon-Young; Meltzer, Paul; Lilly, Michael; Levis, Mark; Small, Donald (2005): Pim-1 is up-regulated by constitutively activated FLT3 and plays a role in FLT3-mediated cell survival. In: *Blood* 105 (4), S. 1759–1767. DOI: 10.1182/blood-2004-05-2006.

Kornberg, Roger D. (2007): The molecular basis of eukaryotic transcription. In: *Proceedings of the National Academy of Sciences of the United States of America* 104 (32), S. 12955–12961. DOI: 10.1073/pnas.0704138104.

Kouchkovsky, I. de; Abdul-Hay, M. (2016): 'Acute myeloid leukemia: a comprehensive review and 2016 update'. In: *Blood cancer journal* 6 (7), e441. DOI: 10.1038/bcj.2016.50.

Kraemer, D.; Wozniak, R. W.; Blobel, G.; Radu, A. (1994): The human CAN protein, a putative oncogene product associated with myeloid leukemogenesis, is a nuclear pore complex protein that faces the cytoplasm. In: *Proceedings of the National Academy of Sciences of the United States of America* 91 (4), S. 1519–1523. DOI: 10.1073/pnas.91.4.1519.

Kramer, M. F.; Coen, D. M. (2001): Enzymatic amplification of DNA by PCR: standard procedures and optimization. In: *Current protocols in molecular biology* Chapter 15, Unit 15.1. DOI: 10.1002/0471142727.mb1501s56.

Kronenwett, R.; Martin, S.; Haas, R. (2000): The role of cytokines and adhesion molecules for mobilization of peripheral blood stem cells. In: *Stem cells (Dayton, Ohio)* 18 (5), S. 320–330. DOI: 10.1634/stemcells.18-5-320.

Kumar, C. Chandra (2011): Genetic abnormalities and challenges in the treatment of acute myeloid leukemia. In: *Genes & cancer* 2 (2), S. 95–107. DOI: 10.1177/1947601911408076.

Kvasnicka, Hans Michael; Thiele, Jürgen; Bueso-Ramos, Carlos E.; Sun, William; Cortes, Jorge; Kantarjian, Hagop M.; Verstovsek, Srdan (2018): Long-term effects of ruxolitinib versus best

available therapy on bone marrow fibrosis in patients with myelofibrosis. In: *Journal of hematology & oncology* 11 (1), S. 42. DOI: 10.1186/s13045-018-0585-5.

Le Yu; Huang, Xiaobin; Zhang, Wenfa; Zhao, Huakan; Wu, Gang; Lv, Fenglin et al. (2016): Critical role of DEK and its regulation in tumorigenesis and metastasis of hepatocellular carcinoma. In: *Oncotarget* 7 (18), S. 26844–26855. DOI: 10.18632/oncotarget.8565.

Levy, David E.; Darnell, J. E. (2002): Stats: transcriptional control and biological impact. In: *Nature reviews. Molecular cell biology* 3 (9), S. 651–662. DOI: 10.1038/nrm909.

Lewin, B. (1991): Oncogenic conversion by regulatory changes in transcription factors. In: *Cell* 64 (2), S. 303–312.

Ley, Timothy J.; Miller, Christopher; Ding, Li; Raphael, Benjamin J.; Mungall, Andrew J.; Robertson, A. Gordon et al. (2013a): Genomic and epigenomic landscapes of adult de novo acute myeloid leukemia. In: *The New England journal of medicine* 368 (22), S. 2059–2074. DOI: 10.1056/NEJMoa1301689.

Ley, Timothy J.; Miller, Christopher; Ding, Li; Raphael, Benjamin J.; Mungall, Andrew J.; Robertson, A. Gordon et al. (2013b): Genomic and epigenomic landscapes of adult de novo acute myeloid leukemia. In: *The New England journal of medicine* 368 (22), S. 2059–2074. DOI: 10.1056/NEJMoa1301689.

Licht, J. D. (2001): AML1 and the AML1-ETO fusion protein in the pathogenesis of t(8;21) AML. In: *Oncogene* 20 (40), S. 5660–5679. DOI: 10.1038/sj.onc.1204593.

Licht, Jonathan D. (2006): Reconstructing a disease: What essential features of the retinoic acid receptor fusion oncoproteins generate acute promyelocytic leukemia? In: *Cancer cell* 9 (2), S. 73–74. DOI: 10.1016/j.ccr.2006.01.024.

Lim, Roderick Y. H.; Huang, Ning-Ping; Köser, Joachim; Deng, Jie; Lau, K. H. Aaron; Schwarz-Herion, Kyrill et al. (2006): Flexible phenylalanine-glycine nucleoporins as entropic barriers to nucleocytoplasmic transport. In: *Proceedings of the National Academy of Sciences of the United States of America* 103 (25), S. 9512–9517. DOI: 10.1073/pnas.0603521103.

Lin, Haishan; Lee, Ernestine; Hestir, Kevin; Leo, Cindy; Huang, Minmei; Bosch, Elizabeth et al. (2008): Discovery of a cytokine and its receptor by functional screening of the extracellular proteome. In: *Science (New York, N.Y.)* 320 (5877), S. 807–811. DOI: 10.1126/science.1154370.

Lin, Yun; Wang, Yaping; Zheng, Yi; Wang, Zechuan; Wang, Yanni; Wang, Shaoyuan (2020): Clinical characteristics and prognostic study of adult acute myeloid leukemia patients with ASXL1 mutations. In: *Hematology (Amsterdam, Netherlands)* 25 (1), S. 446–456. DOI: 10.1080/16078454.2020.1847801.

Lindern, M. von; Fornerod, M.; van Baal, S.; Jaegle, M.; Wit, T. de; Buijs, A.; Grosveld, G. (1992): The translocation (6;9), associated with a specific subtype of acute myeloid leukemia, results in the fusion of two genes, dek and can, and the expression of a chimeric, leukemia-specific dek-can mRNA. In: *Molecular and cellular biology* 12 (4), S. 1687–1697.

Liu, Heping; Wang, Hong; Shi, Zhiyang; Wang, Hua; Yang, Chaoyong; Silke, Spering et al. (2006): TaqMan probe array for quantitative detection of DNA targets. In: *Nucleic acids research* 34 (1), e4. DOI: 10.1093/nar/gnj006.

Liu, Shuangping; Wang, Xiaoyan; Sun, Fengdan; Kong, Jienan; Li, Zhuhu; Lin, Zhenhua (2012): DEK overexpression is correlated with the clinical features of breast cancer. In: *Pathology international* 62 (3), S. 176–181. DOI: 10.1111/j.1440-1827.2011.02775.x.

Livak, K. J.; Schmittgen, T. D. (2001): Analysis of relative gene expression data using real-time quantitative PCR and the 2(-Delta Delta C(T)) Method. In: *Methods (San Diego, Calif.)* 25 (4), S. 402–408. DOI: 10.1006/meth.2001.1262.

Look, A. T. (1997): Oncogenic transcription factors in the human acute leukemias. In: *Science (New York, N.Y.)* 278 (5340), S. 1059–1064.

Löwenberg, B.; Downing, J. R.; Burnett, A. (1999): Acute myeloid leukemia. In: *The New England journal of medicine* 341 (14), S. 1051–1062. DOI: 10.1056/NEJM199909303411407.

Martens, Joost H. A.; Brinkman, Arie B.; Simmer, Femke; Francoijs, Kees-Jan; Nebbioso, Angela; Ferrara, Felicetto et al. (2010): PML-RARalpha/RXR Alters the Epigenetic Landscape in Acute Promyelocytic Leukemia. In: *Cancer cell* 17 (2), S. 173–185. DOI: 10.1016/j.ccr.2009.12.042.

McCormack, Matthew P.; Young, Lauren F.; Vasudevan, Sumitha; Graaf, Carolyn A. de; Codrington, Rosalind; Rabbitts, Terence H. et al. (2010): The Lmo2 oncogene initiates leukemia in mice by inducing thymocyte self-renewal. In: *Science (New York, N.Y.)* 327 (5967), S. 879–883. DOI: 10.1126/science.1182378.

Mendes, Adélia; Fahrenkrog, Birthe (2019): NUP214 in Leukemia: It's More than Transport. In: *Cells* 8 (1). DOI: 10.3390/cells8010076.

Meuer, Stefan; Wittwer, Carl; Nakagawara, Kan-ichi (Hg.) (2001): Rapid cycle real-time PCR. Methods and applications ; with 209 tables. Berlin: Springer.

Mimitou, Eleni P.; Lareau, Caleb A.; Chen, Kelvin Y.; Zorzetto-Fernandes, Andre L.; Hao, Yuhan; Takeshima, Yusuke et al. (2021): Scalable, multimodal profiling of chromatin accessibility, gene expression and protein levels in single cells. In: *Nature biotechnology* 39 (10), S. 1246–1258. DOI: 10.1038/s41587-021-00927-2.

Mo, Xiao-Dong; Lv, Meng; Huang, Xiao-Jun (2017): Preventing relapse after haematopoietic stem cell transplantation for acute leukaemia: the role of post-transplantation minimal residual disease (MRD) monitoring and MRD-directed intervention. In: *British journal of haematology* 179 (2), S. 184–197. DOI: 10.1111/bjh.14778.

Mondesir, Johanna; Willekens, Christophe; Touat, Mehdi; Botton, Stéphane de (2016): IDH1 and IDH2 mutations as novel therapeutic targets: current perspectives. In: *Journal of blood medicine* 7, S. 171–180. DOI: 10.2147/JBM.S70716.

Morrison, Sean J.; Scadden, David T. (2014): The bone marrow niche for haematopoietic stem cells. In: *Nature* 505 (7483), S. 327–334. DOI: 10.1038/nature12984.

Mossmann, Dirk; Park, Sujin; Hall, Michael N. (2018): mTOR signalling and cellular metabolism are mutual determinants in cancer. In: *Nature reviews. Cancer* 18 (12), S. 744–757. DOI: 10.1038/s41568-018-0074-8.

Nennecke, A.; Wienecke, A.; Kraywinkel, K. (2014): Inzidenz und Überleben bei Leukämien in Deutschland nach aktuellen standardisierten Kategorien. In: *Bundesgesundheitsblatt, Gesundheitsforschung, Gesundheitsschutz* 57 (1), S. 93–102. DOI: 10.1007/s00103-013-1869-0.

Newell, Laura F.; Cook, Rachel J. (2021): Advances in acute myeloid leukemia. In: *BMJ (Clinical research ed.)* 375, n2026. DOI: 10.1136/bmj.n2026.

Oancea, C.; Ruster, B.; Henschler, R.; Puccetti, E.; Ruthardt, M. (2010): The t(6;9) associated DEK/CAN fusion protein targets a population of long-term repopulating hematopoietic stem cells for leukemogenic transformation. In: *Leukemia* 24 (11), S. 1910–1919. DOI: 10.1038/leu.2010.180.

Oancea, Claudia; Ruster, Brigitte; Brill, Boris; Roos, Jessica; Heinssmann, Maria; Bug, Gesine et al. (2014): STAT activation status differentiates leukemogenic from non-leukemogenic stem cells in AML and is suppressed by arsenic in t(6;9)-positive AML. In: *Genes & cancer* 5 (11-12), S. 378–392. DOI: 10.18632/genesandcancer.39.

Ostergaard, Mette; Stentoft, Jesper; Hokland, Peter (2004): A real-time quantitative RT-PCR assay for monitoring DEK-CAN fusion transcripts arising from translocation t(6;9) in acute myeloid leukemia. In: *Leukemia research* 28 (11), S. 1213–1215. DOI: 10.1016/j.leukres.2004.03.011.

Oyarzo, Mauricio P.; Lin, Pei; Glassman, Armand; Bueso-Ramos, Carlos E.; Luthra, Rajyalakshmi; Medeiros, L. Jeffrey (2004): Acute myeloid leukemia with t(6;9)(p23;q34) is associated with dysplasia and a high frequency of flt3 gene mutations. In: *American journal of clinical pathology* 122 (3), S. 348–358. DOI: 10.1309/5DGB-59KQ-A527-PD47.

Panina, Yulia; Germond, Arno; David, Brit G.; Watanabe, Tomonobu M. (2019): Pairwise efficiency: a new mathematical approach to qPCR data analysis increases the precision of the calibration curve assay. In: *BMC bioinformatics* 20 (1), S. 295. DOI: 10.1186/s12859-019-2911-5.

Papaemmanuil, Elli; Gerstung, Moritz; Bullinger, Lars; Gaidzik, Verena I.; Paschka, Peter; Roberts, Nicola D. et al. (2016): Genomic Classification and Prognosis in Acute Myeloid Leukemia. In: *The New England journal of medicine* 374 (23), S. 2209–2221. DOI: 10.1056/NEJMoa1516192.

Passegué, Emmanuelle; Jamieson, Catriona H. M.; Ailles, Laurie E.; Weissman, Irving L. (2003): Normal and leukemic hematopoiesis: are leukemias a stem cell disorder or a reacquisition of stem cell characteristics? In: *Proceedings of the National Academy of Sciences of the United States of America* 100 Suppl 1, S. 11842–11849. DOI: 10.1073/pnas.2034201100.

Patel, Jay P.; Gönen, Mithat; Figueroa, Maria E.; Fernandez, Hugo; Sun, Zhuoxin; Racevskis, Janis et al. (2012): Prognostic relevance of integrated genetic profiling in acute myeloid leukemia. In: *The New England journal of medicine* 366 (12), S. 1079–1089. DOI: 10.1056/NEJMoa1112304.

Pearson, M. G.; Vardiman, J. W.; Le Beau, M. M.; Rowley, J. D.; Schwartz, S.; Kerman, S. L. et al. (1985): Increased numbers of marrow basophils may be associated with a t(6;9) in ANLL. In: *American journal of hematology* 18 (4), S. 393–403. DOI: 10.1002/ajh.2830180409.

Pemmaraju, Naveen; Kantarjian, Hagop; Kadia, Tapan; Cortes, Jorge; Borthakur, Gautam; Newberry, Kate et al. (2015): A phase I/II study of the Janus kinase (JAK)1 and 2 inhibitor

ruxolitinib in patients with relapsed or refractory acute myeloid leukemia. In: *Clinical lymphoma, myeloma & leukemia* 15 (3), S. 171–176. DOI: 10.1016/j.clml.2014.08.003.

Pencik, Jan; Pham, Ha Thi Thanh; Schmoellerl, Johannes; Javaheri, Tahereh; Schlederer, Michaela; Culig, Zoran et al. (2016): JAK-STAT signaling in cancer: From cytokines to non-coding genome. In: *Cytokine* 87, S. 26–36. DOI: 10.1016/j.cyto.2016.06.017.

Perl, Alexander E.; Martinelli, Giovanni; Cortes, Jorge E.; Neubauer, Andreas; Berman, Ellin; Paolini, Stefania et al. (2019): Gilteritinib or Chemotherapy for Relapsed or Refractory FLT3-Mutated AML. In: *The New England journal of medicine* 381 (18), S. 1728–1740. DOI: 10.1056/NEJMoa1902688.

Pfaffl, M. W. (2001): A new mathematical model for relative quantification in real-time RT-PCR. In: *Nucleic acids research* 29 (9), e45.

Porcu, Michaël; Kleppe, Maria; Gianfelici, Valentina; Geerdens, Ellen; Keersmaecker, Kim de; Tartaglia, Marco et al. (2012): Mutation of the receptor tyrosine phosphatase PTPRC (CD45) in T-cell acute lymphoblastic leukemia. In: *Blood* 119 (19), S. 4476–4479. DOI: 10.1182/blood-2011-09-379958.

Ratei, R.; Sperling, C.; Karawajew, L.; Schott, G.; Schrappe, M.; Harbott, J. et al. (1998): Immunophenotype and clinical characteristics of CD45-negative and CD45-positive childhood acute lymphoblastic leukemia. In: *Annals of hematology* 77 (3), S. 107–114. DOI: 10.1007/s002770050424.

Ravandi, Farhad; Walter, Roland B.; Freeman, Sylvie D. (2018): Evaluating measurable residual disease in acute myeloid leukemia. In: *Blood Advances* 2 (11), S. 1356–1366. DOI: 10.1182/bloodadvances.2018016378.

Reya, T.; Morrison, S. J.; Clarke, M. F.; Weissman, I. L. (2001): Stem cells, cancer, and cancer stem cells. In: *Nature* 414 (6859), S. 105–111. DOI: 10.1038/35102167.

Rheinländer, Andreas; Schraven, Burkhart; Bommhardt, Ursula (2018): CD45 in human physiology and clinical medicine. In: *Immunology letters* 196, S. 22–32. DOI: 10.1016/j.imlet.2018.01.009.

Richman, C. M.; Weiner, R. S.; Yankee, R. A. (1976): Increase in circulating stem cells following chemotherapy in man. In: *Blood* 47 (6), S. 1031–1039.

Roberts, Kathryn G.; Yang, Yung-Li; Payne-Turner, Debbie; Lin, Wenwei; Files, Jacob K.; Dickerson, Kirsten et al. (2017): Oncogenic role and therapeutic targeting of ABL-class and JAK-STAT activating kinase alterations in Ph-like ALL. In: *Blood Advances* 1 (20), S. 1657–1671. DOI: 10.1182/bloodadvances.2017011296.

Rout, M. P.; Aitchison, J. D.; Suprapto, A.; Hjertaas, K.; Zhao, Y.; Chait, B. T. (2000): The yeast nuclear pore complex: composition, architecture, and transport mechanism. In: *The Journal of cell biology* 148 (4), S. 635–651. DOI: 10.1083/jcb.148.4.635.

Saito, Shoko; Cigdem, Sadik; Okuwaki, Mitsuru; Nagata, Kyosuke (2016): Leukemia-Associated Nup214 Fusion Proteins Disturb the XPO1-Mediated Nuclear-Cytoplasmic Transport Pathway and Thereby the NF-κB Signaling Pathway. In: *Molecular and cellular biology* 36 (13), S. 1820–1835. DOI: 10.1128/MCB.00158-16.

Sandén, Carl; Ageberg, Malin; Petersson, Jessica; Lennartsson, Andreas; Gullberg, Urban (2013): Forced expression of the DEK-NUP214 fusion protein promotes proliferation dependent on upregulation of mTOR. In: *BMC cancer* 13, S. 440. DOI: 10.1186/1471-2407-13-440.

Schmitt, M.; Hoffmann, J-M; Lorenz, K.; Publicover, A.; Schmitt, A.; Nagler, A. (2016): Mobilization of autologous and allogeneic peripheral blood stem cells for transplantation in haematological malignancies using biosimilar G-CSF. In: *Vox sanguinis* 111 (2), S. 178–186. DOI: 10.1111/vox.12397.

Schofield, R. (1978): The relationship between the spleen colony-forming cell and the haemopoietic stem cell. In: *Blood cells* 4 (1-2), S. 7–25.

Schroeder, Andreas; Mueller, Odilo; Stocker, Susanne; Salowsky, Ruediger; Leiber, Michael; Gassmann, Marcus et al. (2006): The RIN: an RNA integrity number for assigning integrity values to RNA measurements. In: *BMC molecular biology* 7, S. 3. DOI: 10.1186/1471-2199-7-3.

Schwartzberg, L. S.; Birch, R.; Hazelton, B.; Tauer, K. W.; Lee, P.; Altemose, R. et al. (1992): Peripheral blood stem cell mobilization by chemotherapy with and without recombinant human granulocyte colony-stimulating factor. In: *Journal of hematotherapy* 1 (4), S. 317–327. DOI: 10.1089/scd.1.1992.1.317.

Selten, G.; Cuypers, H. T.; Boelens, W.; Robanus-Maandag, E.; Verbeek, J.; Domen, J. et al. (1986): The primary structure of the putative oncogene pim-1 shows extensive homology with protein kinases. In: *Cell* 46 (4), S. 603–611. DOI: 10.1016/0092-8674(86)90886-x.

Shallis, Rory M.; Wang, Rong; Davidoff, Amy; Ma, Xiaomei; Zeidan, Amer M. (2019): Epidemiology of acute myeloid leukemia: Recent progress and enduring challenges. In: *Blood reviews* 36, S. 70–87. DOI: 10.1016/j.blre.2019.04.005.

Shephard, Elizabeth A.; Neal, Richard D.; Rose, Peter W.; Walter, Fiona M.; Hamilton, Willie (2016): Symptoms of adult chronic and acute leukaemia before diagnosis: large primary care case-control studies using electronic records. In: *The British journal of general practice : the journal of the Royal College of General Practitioners* 66 (644), e182-8. DOI: 10.3399/bjgp16X683989.

Sheridan, W. P.; Begley, C. G.; Juttner, C. A.; Szer, J.; To, L. B.; Maher, D. et al. (1992): Effect of peripheral-blood progenitor cells mobilised by filgrastim (G-CSF) on platelet recovery after high-dose chemotherapy. In: *Lancet (London, England)* 339 (8794), S. 640–644.

Sierakowska, H.; Williams, K. R.; Szer, I. S.; Szer, W. (1993): The putative oncoprotein DEK, part of a chimera protein associated with acute myeloid leukaemia, is an autoantigen in juvenile rheumatoid arthritis. In: *Clinical and experimental immunology* 94 (3), S. 435–439.

Slovak, M. L.; Gundacker, H.; Bloomfield, C. D.; Dewald, G.; Appelbaum, F. R.; Larson, R. A. et al. (2006): A retrospective study of 69 patients with t(6;9)(p23;q34) AML emphasizes the need for a prospective, multicenter initiative for rare 'poor prognosis' myeloid malignancies. In: *Leukemia* 20 (7), S. 1295–1297. DOI: 10.1038/sj.leu.2404233.

Soekarman, D.; Lindern, M. von; Daenen, S.; Jong, B. de; Fonatsch, C.; Heinze, B. et al. (1992): The translocation (6;9) (p23;q34) shows consistent rearrangement of two genes and defines a myeloproliferative disorder with specific clinical features. In: *Blood* 79 (11), S. 2990–2997.

Steelman, L. S.; Abrams, S. L.; Whelan, J.; Bertrand, F. E.; Ludwig, D. E.; Bäsecke, J. et al. (2008): Contributions of the Raf/MEK/ERK, PI3K/PTEN/Akt/mTOR and Jak/STAT pathways to leukemia. In: *Leukemia* 22 (4), S. 686–707. DOI: 10.1038/leu.2008.26.

Stein, Eytan M.; DiNardo, Courtney D.; Fathi, Amir T.; Pollyea, Daniel A.; Stone, Richard M.; Altman, Jessica K. et al. (2019): Molecular remission and response patterns in patients with mutant-IDH2 acute myeloid leukemia treated with enasidenib. In: *Blood* 133 (7), S. 676–687. DOI: 10.1182/blood-2018-08-869008.

Svec, David; Tichopad, Ales; Novosadova, Vendula; Pfaffl, Michael W.; Kubista, Mikael (2015): How good is a PCR efficiency estimate: Recommendations for precise and robust qPCR efficiency

assessments. In: *Biomolecular Detection and Quantification* 3, S. 9–16. DOI: 10.1016/j.bdq.2015.01.005.

Thé, H. de; Lavau, C.; Marchio, A.; Chomienne, C.; Degos, L.; Dejean, A. (1991): The PML-RAR alpha fusion mRNA generated by the t(15;17) translocation in acute promyelocytic leukemia encodes a functionally altered RAR. In: *Cell* 66 (4), S. 675–684.

Thiede, Christian; Steudel, Christine; Mohr, Brigitte; Schaich, Markus; Schäkel, Ulrike; Platzbecker, Uwe et al. (2002): Analysis of FLT3-activating mutations in 979 patients with acute myelogenous leukemia: association with FAB subtypes and identification of subgroups with poor prognosis. In: *Blood* 99 (12), S. 4326–4335. DOI: 10.1182/blood.v99.12.4326.

Thomas, Sally; Fisher, Katherine H.; Snowden, John A.; Danson, Sarah J.; Brown, Stephen; Zeidler, Martin P. (2015): Methotrexate Is a JAK/STAT Pathway Inhibitor. In: *PloS one* 10 (7), e0130078. DOI: 10.1371/journal.pone.0130078.

Tichopad, Ales; Dilger, Michael; Schwarz, Gerhard; Pfaffl, Michael W. (2003): Standardized determination of real-time PCR efficiency from a single reaction set-up. In: *Nucleic acids research* 31 (20), e122.

TILL, J. E.; MCCULLOCH, E. A. (1961): A direct measurement of the radiation sensitivity of normal mouse bone marrow cells. In: *Radiation research* 14, S. 213–222.

Tonks, N. K.; Neel, B. G. (1996): From form to function: signaling by protein tyrosine phosphatases. In: *Cell* 87 (3), S. 365–368. DOI: 10.1016/s0092-8674(00)81357-4.

van, der Velden VH; Hochhaus, A.; Cazzaniga, G.; Szczepanski, T.; Gabert, J.; van, Dongen J. J. (2003): Detection of minimal residual disease in hematologic malignancies by real-time quantitative PCR: principles, approaches, and laboratory aspects. In: *Leukemia* 17 (6). DOI: 10.1038/sj.leu.2402922.

van Deursen, J.; Boer, J.; Kasper, L.; Grosveld, G. (1996): G2 arrest and impaired nucleocytoplasmic transport in mouse embryos lacking the proto-oncogene CAN/Nup214. In: *The EMBO journal* 15 (20), S. 5574–5583. DOI: 10.1002/j.1460-2075.1996.tb00942.x.

Vardiman, James W.; Thiele, Jüergen; Arber, Daniel A.; Brunning, Richard D.; Borowitz, Michael J.; Porwit, Anna et al. (2009): The 2008 revision of the World Health Organization (WHO)

classification of myeloid neoplasms and acute leukemia: rationale and important changes. In: *Blood* 114 (5), S. 937–951. DOI: 10.1182/blood-2009-03-209262.

Velazquez, Laura; Fellous, Marc; Stark, George R.; Pellegrini, Sandra (2011): Pillars article: A protein tyrosine kinase in the interferon α/β signaling pathway. Cell. 1992. 70: 313-322. In: *Journal of immunology (Baltimore, Md. : 1950)* 187 (11), S. 5479–5488.

Wang, Jean C. Y.; Dick, John E. (2005): Cancer stem cells: lessons from leukemia. In: *Trends in cell biology* 15 (9), S. 494–501. DOI: 10.1016/j.tcb.2005.07.004.

Weissman, Irving L.; Shizuru, Judith A. (2008): The origins of the identification and isolation of hematopoietic stem cells, and their capability to induce donor-specific transplantation tolerance and treat autoimmune diseases. In: *Blood* 112 (9), S. 3543–3553. DOI: 10.1182/blood-2008-08-078220.

Wetzler, Meir; Brady, Michael T.; Tracy, Erin; Li, Zhang-Rong; Donohue, Kathleen A.; O'Loughlin, Kieran L. et al. (2006): Arsenic trioxide affects signal transducer and activator of transcription proteins through alteration of protein tyrosine kinase phosphorylation. In: *Clinical cancer research : an official journal of the American Association for Cancer Research* 12 (22), S. 6817–6825. DOI: 10.1158/1078-0432.CCR-06-1354.

Whelan, Joseph A.; Russell, Nick B.; Whelan, Michael A. (2003): A method for the absolute quantification of cDNA using real-time PCR. In: *Journal of immunological methods* 278 (1-2), S. 261–269.

Wilks, A. F.; Harpur, A. G.; Kurban, R. R.; Ralph, S. J.; Zürcher, G.; Ziemiecki, A. (1991): Two novel protein-tyrosine kinases, each with a second phosphotransferase-related catalytic domain, define a new class of protein kinase. In: *Molecular and cellular biology* 11 (4), S. 2057–2065.

Wu, Song-Fang; Xia, Li; Shi, Xiao-Dong; Dai, Yu-Jun; Zhang, Wei-Na; Zhao, Jun-Mei et al. (2020): RIG-I regulates myeloid differentiation by promoting TRIM25-mediated ISGylation. In: *Proceedings of the National Academy of Sciences of the United States of America* 117 (25), S. 14395–14404. DOI: 10.1073/pnas.1918596117.

Xu, Dan; Qu, Cheng-Kui (2008): Protein tyrosine phosphatases in the JAK/STAT pathway. In: *Frontiers in bioscience : a journal and virtual library* 13, S. 4925–4932.

Xun, Qiuju; Wang, Zhen; Hu, Xianglong; Ding, Ke; Lu, Xiaoyun (2019): Small-Molecule CSF1R Inhibitors as Anticancer Agents. In: *Current medicinal chemistry*. DOI: 10.2174/1573394715666190618121649.

Yokota, H.; Kitamura, K. (2000): The genetic diagnosis of hematopoietic malignancy by polymerase chain reaction method. In: *Rinsho byori. The Japanese journal of clinical pathology* 48 (8), S. 708–715.

Yu, Wenfeng; Chen, Jian; Xiong, Ying; Pixley, Fiona J.; Yeung, Yee-Guide; Stanley, E. Richard (2012): Macrophage proliferation is regulated through CSF-1 receptor tyrosines 544, 559, and 807. In: *The Journal of biological chemistry* 287 (17), S. 13694–13704. DOI: 10.1074/jbc.M112.355610.

Yuan, L. L.; Green, A. S.; Bertoli, S.; Grimal, F.; Mansat-De Mas, V.; Dozier, C. et al. (2014): Pim kinases phosphorylate Chk1 and regulate its functions in acute myeloid leukemia. In: *Leukemia* 28 (2), S. 293–301. DOI: 10.1038/leu.2013.168.

Zheng, Xiaomin; Beissert, Tim; Kukoc-Zivojnov, Natasa; Puccetti, Elena; Altschmied, Joachim; Strolz, Corinna et al. (2004): Gamma-catenin contributes to leukemogenesis induced by AML-associated translocation products by increasing the self-renewal of very primitive progenitor cells. In: *Blood* 103 (9), S. 3535–3543. DOI: 10.1182/blood-2003-09-3335.